THE UNIVERSITY OF CALGARY

Molecular Mechanisms of the CD36-*Plasmodium falciparum* Interaction in Cytoadherence

by

Bryan Yipp

A THESIS

SUBMITTED TO THE FACULTY OF GRADUATE STUDIES

IN PARTIAL FULFILMENT OF THE REQUIREMENTS FOR THE

DEGREE OF MASTER OF SCIENCE

DEPARTMENT OF MEDICAL SCIENCE

CALGARY, ALBERTA

JUNE, 2002

Your file Votre référence
ISBN: 0-494-03840-3
Our file Notre référence
ISBN: 0-494-03840-3

ABSTRACT

The central pathological process in severe *P. falciparum* malaria is the cytoadherence of infected erythrocytes (IRBC) to microvascular endothelial receptors including CD36, ICAM-1, VCAM-1 and P-selectin. The molecular mechanisms of IRBC firm adhesion to CD36 are incompletely understood, particularily in vivo. Using a human/SCID mouse chimeric model of cytoadherence, we found that P-selectin and ICAM-1 enhance firm adhesion to CD36 through rolling-increased and decreased mechanisms. As well, a recombinant peptide (y179) based on the parasite protein PfEMP1 was found to inhibit and reverse firm adhesion of multiple clinical parasite isolates in vitro and in vivo. Finally, a novel model of firm adhesion involving both outside-in and inside-out signaling mechansims was demonstrated. The PfEMP1-CD36 interaction induced a Src-family kinase signal (outside-in) that is linked to an ecto-alkaline phosphatase capable of enhancing subsequent firm adhesion (inside-out). Optimal firm adhesion is dependent on both Src-family kinase activation and ecto-alkaline phosphatase activity.

ACKNOWLEDGEMENTS

I would like to thank the following people and laboratories:

Dr. May Ho, Dr. Paul Kubes, Dr. Donna-Marie McCafferty and Dr. Kamala Patel for their supervision and guidance

Dr. Allan Murray for help with the human/SCID mouse model

Dr. Paul Kubes and members of his laboratory for help with the in vivo experiments and for the use of the intravital microscopy facilities

Dr. Steve Robbins and Mary Resek for their help with the cell signaling project and for the use of their laboratory and reagents

Dr. Dror Baruch for providing the y179 peptide and helpful discussions

Dr. Joseph Smith for participating as an external examiner

TABLE OF CONTENTS

LIST OF FIGURES

LIST OF ABBREVIATIONS

Ab	antibody
AP	alkaline phosphatase
BSA	bovine serum albumin
CIDR	cysteine-rich interdomain region
CR	consensus repeats
CSF	cerebralspinal fluid
CSA	chondroitin sulfate A
DBL	Duffy binding like
EBM	endothelial basal medium
ECL	enhanced chemiluminescense
EDTA	ethylenediaminetetra acetic acid
EGF	epidermal growth factor
ERK	extracellular signal-related kinase
FITC	fluorescein isothiocyanate
GPI	glycophosphatidylinositol
HA	hyaluronic acid
HBSS	Hank's balanced salt solution
HDL	high-density lipoprotein
HDMEC	human dermal microvascular endothelial cells
HRF	histamine releasing factor
HRP	horseradish peroxidase
HUVEC	human umbilical vein endothelial cells

ICAM-1	intercellular adhesion molecule-1
IRBC	infected red blood cell
Ig	immunoglobulin
IL	interleukin
JNK	Jun amino terminal kinases
KAHRP	knob-associated histidine-rich protein
LFA-1	lymphocyte function-associated antigen-1
LPS	lipopolysaccharide
M199	medium 199
mAb	monoclonal antibody
MC	Malayan Camp
MAPK	mitogen activated protein kinase
Ni-NTA	nickel-nitriltriacetic acid-agarose
NO	nitric oxide
NTS	N-terminal segment
OSM	oncostatin-M
oxLDL	oxidized low-density lipoprotein
PBS	phosphate-buffered saline
PKA	protein kinase A
PKC	protein kinase C
PfEMP	*Plasmodium falciparum* erythrocyte membrane protein
PTP	protein tyrosine phosphatase
SAPK	stress-activated protein kinases

SCID	severe combined immunodeficient
SH	src-homology
SOV	sodium orthovanadate
TBS	tris buffered saline
TCTP	translationally controlled tumor protein
TNF	tumor necrosis factor
TSP-1	thrombospondin-1
VAP-1	vascular adhesion protein-1
VCAM-1	vascular cell adhesion molecule-1
VLA-4	very late antigen-4
vWF	von Willebrand factor

CHAPTER 1

INTRODUCTION AND LITERATURE REVIEW

1.1 Introduction

Plasmodium falciparum malaria is an acute febrile illness characterized by fever, chills, headache, anemia, and splenomegaly that respond promptly to antimalarial therapy (1). In a small percentage of patients, the infection is complicated by multiple organ dysfunction. Death most commonly results from cerebral malaria, severe anemia, metabolic acidosis or pulmonary edema (2, 3). Although the underlying mechanisms leading to severe falciparum malaria and death are still not completely understood, there is little doubt that the pathogenicity of *P. falciparum* is dependent largely on its unique ability to adhere to the host endothelium, a characteristic not shared with the other three species of human malaria parasites (4).

On infected erythrocytes (IRBC), cytoadherence is mediated by the parasite protein *Plasmodium falciparum* erythrocyte membrane protein 1 (PfEMP1) (5-7), a large variant surface expressed protein that has the capacity to interact with a number of adhesion molecules via different structural domains (8). On vascular endothelium, cytoadherence is mediated by a number of adhesion molecules in a synergistic fashion under flow conditions in vitro (9), mimicking the adhesive events in the leukocyte recruitment cascade. IRBC can tether and roll on intercellular adhesion molecule 1(ICAM-1), vascular cell adhesion molecule 1 (VCAM-1), and P-selectin (9-11). These low affinity interactions do not by themselves lead to the arrest of the interacting cells. However, they do enhance the subsequent adhesion of nearly all clinical parasite isolates tested to CD36. Whether this cascade of adhesive events involving multiple adhesion molecules

occurs in vivo in a human microvasulature has not been well documented. It is also not known if the adhesion of IRBC on CD36 represents a true ligand-receptor interaction that can lead to intracellular signaling, with resultant modification of the adhesion process.

The overall objective of this thesis was to investigate the molecular interaction between PfEMP1 and CD36. In particular, the accessory roles of ICAM-1, VCAM-1 and P-selectin on IRBC adhesion to CD36 was examined in a novel human/SCID mouse model that allows for the direct visualization of the adhesive interactions of IRBC in a human microvasculature in vivo. The potential to inhibit and/or reverse cytoadherence by a recombinant protein based on the CD36 binding domain of PfEMP1 was evaluated. Furthermore, experiments were conducted to determine if the IRBC-CD36 interaction activates intracellular signaling pathways in endothelial cells, and the functional consequences of the activation.

1.2 Pathophysiology of severe *P. falciparum* malaria

The most common and consistent pathological feature of severe falciparum malaria is the sequestration of IRBC in the capillaries and post-capillary venules of vital organs (Figure 1.1). Although most of the pathological studies have been performed on the brain, IRBC sequestration can be seen in all vital organs such as the heart, liver, lung, kidney and spleen. (4, 12-16). The degree and organ distribution of parasite sequestration tends to reflect the clinical features of the preceding clinical illness. For example, sequestration is

the highest in the brain compared to that in other organs in patients who died of cerebral malaria. Within the brain, a positive correlation has been demonstrated between quantitative measures of sequestration and the degree of coma (4, 17). At the microvascular level, there is considerable heterogeneity among the individual vessels. The majority of vessels are packed with IRBC containing parasites that are fully developed, while others contain the immature ring stages of the parasite. This synchronous clustering suggests that once the IRBC have adhered, detachment does not occur. There is remarkably little inflammatory infiltration, and although occasional fibrin strands can be seen, platelets are also conspicuously absent.

The sequestration of IRBC in microvessels is postulated to cause impairment of microcirculatory blood flow, resulting in local tissue hypoxia and metabolic abnormality. There is clinical evidence to support this pathological mechanism (18). In Thai adults with cerebral malaria, cerebral blood flow was reduced relative to arterial oxygen tension. There was a concomitant increase in the production of cerebral lactate, indicating a lack of aerobic cellular respiration and a move towards anaerobic glycolysis. Lactate levels in the cerebralspinal fluid (CSF) were consistently high in patients with cerebral malaria, and were higher in fatal cases compared to patients who survived (19).

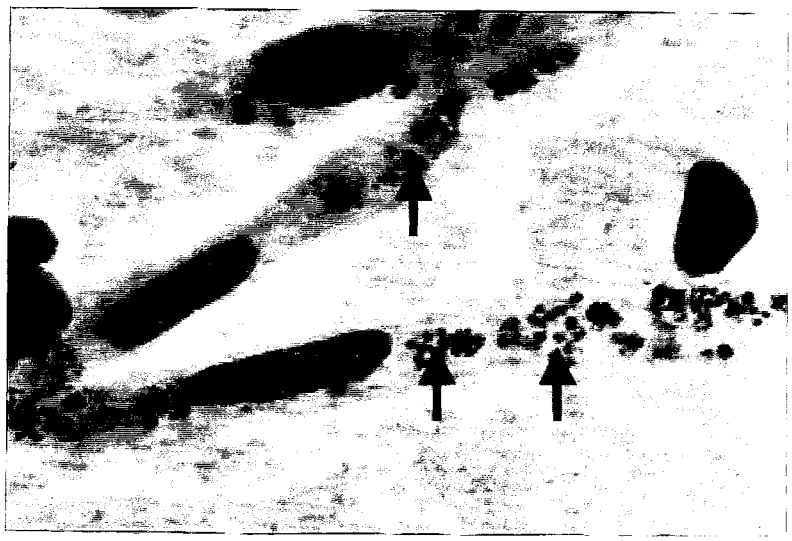

Figure 1.1 Cytoadherence of IRBC in cerebral microvessels. Cerebral vessels are congested with infected erythrocytes containing schizonts (arrows) in a case of fatal cerebral malaria (Ho, unpublished data).

A related pathogenic process in severe falciparum malaria is the production of pro-inflammatory cytokines. Plasma concentrations of tumor necrosis factor-α (TNF-α), IL-1β and IL-6 are increased in patients with severe falciparum malaria, and the highest levels of these cytokines are associated with mortality (20). The deleterious effect of TNF-α is probably not due to a direct effect of the cytokine on the host, as it is also markedly elevated in the non-lethal *P.vivax* malaria (21). Pro-inflammatory cytokines are known to upregulate or induce the expression of endothelial adhesion molecules. By so doing, they may contribute to the pathogenesis of severe falciparum malaria by enhancing adhesion and subsequent microcirculatory obstruction.

1.2.1 Cytoadherence

The term cytoadherence was coined to describe the unique ability of *P. falciparum* to adhere to capillary and postcapillary venular endothelium during the second half of its 48-hour life cycle (4, 12). Although the transit of IRBC can be delayed in microvessels due to a loss of deformability, it has been widely postulated that parasites actively adhere to microvascular endothelium in order to evade clearance by the spleen. The stage and host cell specificity of the adhesion process indicate that the interactions involve specific parasite ligands and endothelial receptors. The molecular basis of the interactions has been intensively studied both in an effort to understand the pathogenesis of the infection, and for the rational development of anti-adhesive therapies.

1.2.2.1 Parasite cytoadherent proteins

Several parasite-derived proteins are exported to the surface of the IRBC during the second half of the parasite life cycle, coincident with the ability of the IRBC to adhere to endothelium (Figure 1.2)(22, 23). These proteins form electron dense protrusions on the cell surface known as knobs that serve to concentrate parasite ligands at discrete sites, and are essential for firm adhesion under flow conditions by facilitating the initial attachment of IRBC to the endothelium (24, 25). To date, five parasite proteins are known to be involved in either formation of the knob complex or directly mediating adhesion. PfEMP1, 2 and 3 along with the knob-associated histidine rich protein (KAHRP) are found within the knob structure (26). The fifth protein thought to be necessary for adhesion is the gene product of *clag9* (27). However the identity, location and role of this protein are still undetermined. PfEMP1 is the only known protein that extends beyond the cell surface to mediate cytoadherence directly. However, its export and positioning within the knob depend on the other proteins. KAHRP is a major component of knobs and is critical for cytoadherence under flow conditions (25). This protein interacts with both the cytoskeleton of the red cell membrane and the cytoplasmic tail of PfEMP1 (24, 28, 29). PfEMP3 is also critical for adhesion, as mutagenesis of this protein disrupts PfEMP1 export to the knob structure, thereby inhibiting adhesion (30). PfEMP2, also known as mature parasite-infected erythrocyte surface antigen (MESA), is involved in binding to the host cytoskeletal protein 4.1 (31), but the importance of this interaction is not established.

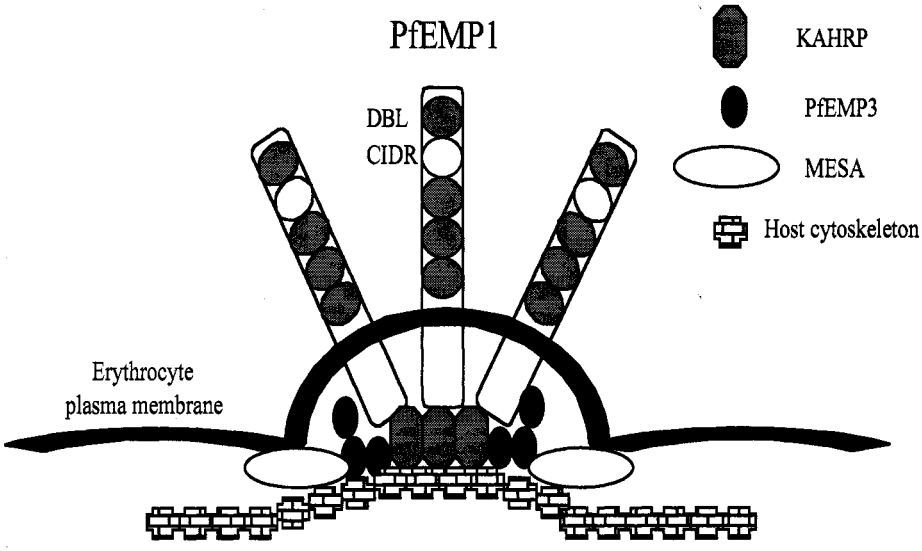

Figure 1.2 Schematic diagram of the knob-associated IRBC proteins. Knobs are formed by parasite proteins that are transported to the host plasma membrane where they associate with the host cytoskeleton. PfEMP1- *Plasmodium falciparum* erythrocyte membrane protein; MESA- Mature parasite-infected erythrocyte surface antigen; KAHRP- Knob-associated histidine-rich protein; DBL- Duffy binding-like domain; CIDR- Cysteine-rich interdomain. This figure was modified from Coppel, 1998 (26).

Recent data have shown that KAHRP, PfEMP1 and PfEMP3 associate within the host cytosol in parasite derived structures known as Maurer's clefts. These structures are responsible for assembling the knob complex and exporting it to the erythrocyte plasma membrane (32).

1.2.1.2 *P. falciparum* erythrocyte membrane protein 1 (PfEMP1)

PfEMP1 is the best-studied parasite cytoadherent ligand. It was originally identified as a large (200-350kDa), antigenically diverse protein family expressed only on IRBC containing mature parasites (22, 23). In depth molecular analysis of this protein followed when the PfEMP1 gene was cloned and found to be encoded by a large diverse gene family named *var* (5-7). This family consists of between 50-150 members distributed throughout the *P. falciparum* genome, and many of them are transcribed in the early stages of the parasite cycle. However, each IRBC only expresses one *var* gene product when the parasite reaches maturity, while the remaining genes are inactivated by an as yet unknown silencing mechanism (33).

Although the protein sequences of the *var* gene products are diverse, four common structural extracellular domains have been identified: an N-terminal segment (NTS), Duffy binding like domain (DBL), cysteine-rich interdomain region (CIDR), and C2 domains (Figure 1.3A) (5-7). Further analysis has demonstrated that the DBL and CIDR domains can be grouped into classes based on relatedness. Five types of DBL domains (designated α, β, γ, δ, and ε) and three types of CIDR domains (designated α, β and γ) have been described

(34). Individual PfEMP1 molecules contain between 2-7 DBL domains and 1-2 CIDR domains.

A number of host receptors are known to bind directly to PfEMP1 and the domains required for adhesion have been mapped. CD36 binding occurs within the CIDR1α domain (6, 35, 36) that is almost always found with a DBL1α domain and forms a semi-conserved head structure (37). IRBC bind chondroitin sulfate A (CSA) (38, 39) through DBLγ (40). CSA-binding PfEMP1 contains a CIDR1 but is unable to bind CD36 because of a triple amino acid substitution resulting in a conformational change (41). ICAM-1 binding has been mapped to the DBL2β-C2 tandem domain (42). P-selectin also binds directly to PfEMP1, but the molecular domain(s) involved in the interaction have not been determined (43).

Malayan Camp (MC) is a laboratory-adapted parasite clone for which the PfEMP1 gene and protein have been the best characterized. The *MCvar-1* gene contains 4 DBL domains and 2 CIDR domains located between DBL1-2 and DBL2-3. The critical region involved in binding CD36 was localized to a 179 amino acid sequence within CIDR1 (35) (Figure 1.3B). This 179 amino acid peptide (y179) can inhibit and reverse the adhesion of the homologous strain (MC) as well as a few heterologous lab-adapted clones to purified CD36 in a flow chamber in vitro (44).

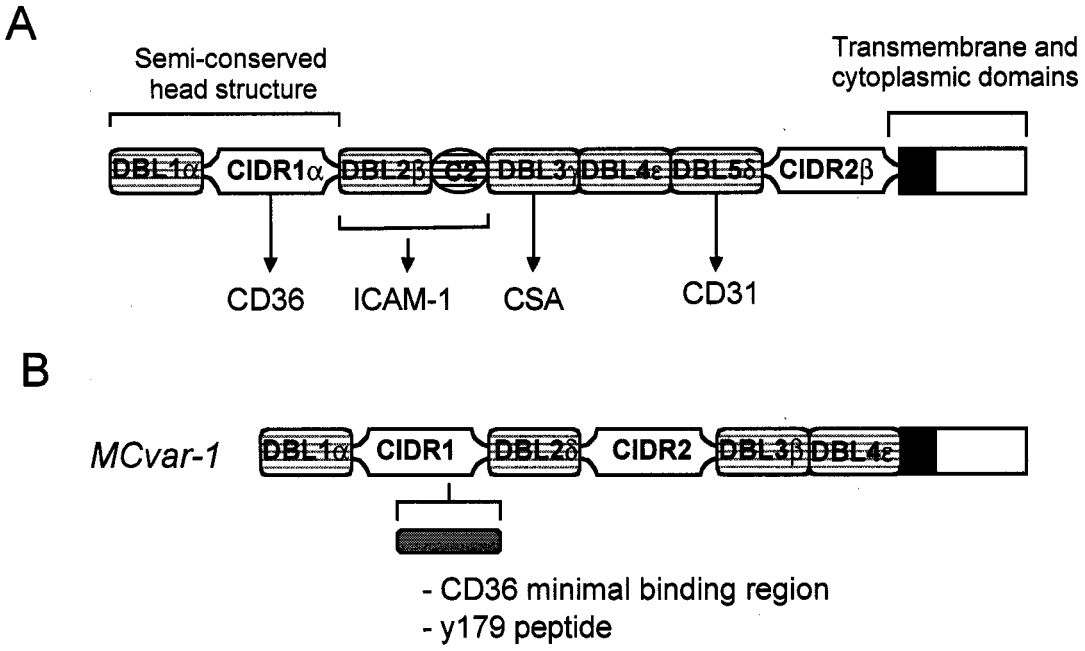

Figure 1.3 Structural domains of PfEMP1. A) Structural and functional binding domains of a prototypical PfEMP1. B) Structure of *MCvar1*PfEMP1 for which the minimal CD36 binding site has been mapped. DBL-Duffy binding-like; CIDR-Cysteine-rich interdomain. These figures were modified from Gamain (45) and Smith (8).

1.2.1.3 Host endothelial cells

In addition to the different virulence factors associated with the parasite, progression of disease from uncomplicated to severe falciparum malaria may be highly dependent on the host endothelial cell. During inflammation, endothelial cells are a gateway for directing where and when leukocytes are required in a tissue by upregulating adhesion molecule expression and chemokine production. The state of endothelial activation during a malaria infection may also direct the course and progression of the disease. Many host receptors have been implicated in mediating cytoadherence, including CD36 (46), CD31 (47), ICAM1 (48), VCAM1 (49), thrombospondin-1 (TSP-1) (50), E-selectin (49), P-selectin (11) and CSA (38). This section will introduce the important extracellular and intracellular molecules involved in cytoadhesion of IRBC to human endothelium under physiological flow conditions.

1.2.1.4 Endothelial receptors

CD36 is a multifunctional scavenger receptor found on microvascular endothelial cells (51, 52), erythroblasts (53), adipose tissue (54), platelets (55) dendritic cells (56, 57) and macrophages (58). Its natural ligands include collagen, TSP-1, oxidized low-density lipoprotein (oxLDL), high-density lipoprotein (HDL) and apoptotic cells. This 471 amino acid, 88-kDa transmembrane glycoprotein exists in a unique conformation with two hydrophobic membrane-spanning domains and a single hydrophobic region

thought to sit within, but not through, the outer leaflet of the plasma membrane. This structure results in two cytoplasmic tails and two extracellular protein loops (Figure 1.4). CD36 serves many physiological roles such as the uptake of apoptotic bodies (59), fatty acid transport (54), apoptosis of endothelial cells to prevent neovascularization (60) and may have significant roles in the pathogenesis of atherosclerosis (61), diabetes (62-64) and cardiomyopathy (65, 66), .

The TSP-1-CD36 interaction has been the most extensively studied. Initially, CD36 was identified as a platelet receptor for TSP-1 and implicated in platelet aggregation and monocyte-platelet interactions (67, 68). Peptide mapping has shown that TSP-1 may bind CD36 in two distinct regions. Initial binding to CD36 is between amino acid 139-155 and results in a conformational change in TSP-1 exposing a high affinity site that now binds CD36 between amino acids 98-110 (69, 70). It was subsequently determined that the phosphorylation state of the CD36 ectodomain on platelets is also critical for TSP-1 binding (71). Under normal conditions CD36 constitutively possesses a PKC-dependent phosphorylated amino acid, threonine-92, that is located in the ectodomain near the secondary TSP-1 binding site. Phosphorylated CD36 is the low affinity receptor for TSP-1 and preferentially binds collagen. Upon initial TSP-1 binding platelets become activated and degranulate. Several acid phosphatases are released into the surrounding environment specifically dephosphorylating the ectodomain of CD36. Dephosphorylated CD36 preferentially binds TSP-1 with high affinity.

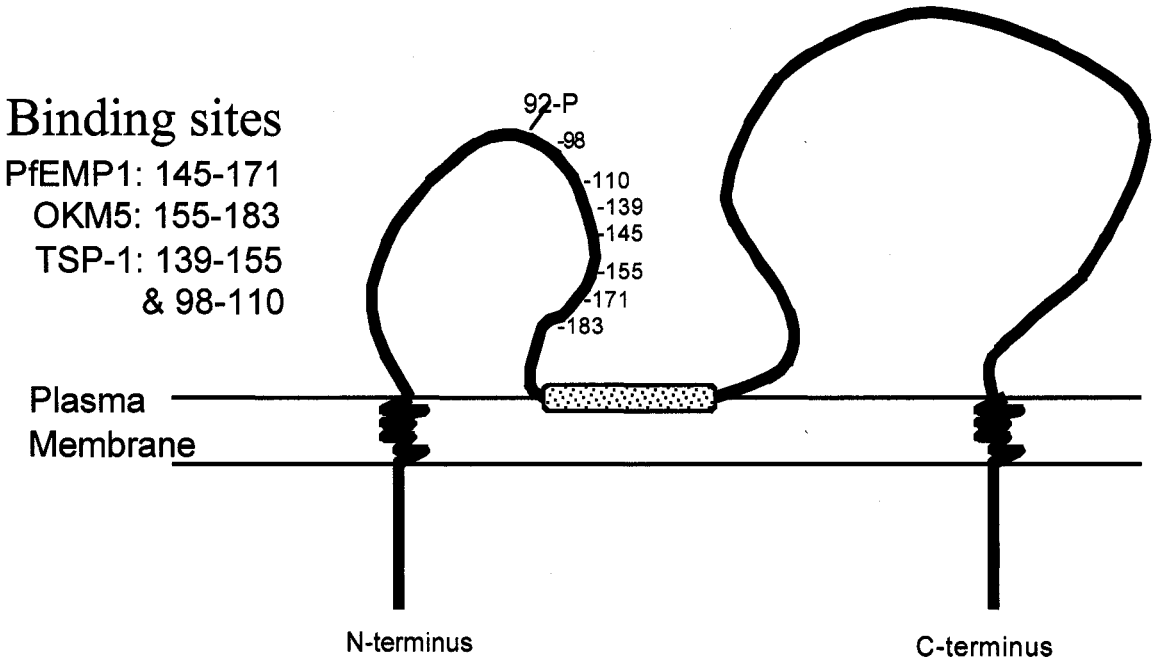

Figure 1.4 CD36 membrane topology and binding sites. This unique structure contains two cytoplasmic tails and two extracellular loops separated by a hydrophobic section that sits within the outer leaflet of the plasma membrane. Threonine-92 is ecto-phosphorylated in platelet CD36.

Further analysis of the interaction of TSP-1 with CD36 on endothelium has provided new insights into CD36-dependent cell signaling pathways. TSP-1 inhibits neovascularization by inducing receptor-mediated apoptosis in microvascular endothelial cells and this effect was determined to be specific and dependent on CD36. TSP-1-CD36 interaction results in activation of the src-kinase family member Fyn and the p38 mitogen activated protein kinases (MAPK) (60). This signaling pathway is critical for the anti-angiogenic effects of TSP-1 on microvascular endothelial cells. The study provided elegant evidence for a src-family kinase mediated CD36 cell signal with significant biological consequences. However, it is not the only evidence for CD36 cell signaling. Src-kinase signaling molecules have been found physically associated with the intracellular tails of both platelet and endothelial CD36 (72, 73) and antibody crosslinking CD36 on monocytes induces activation of both extracellular signal-related kinases (ERK)1/2 and p38 MAPK signaling pathways (74).

Almost all clinical parasite isolates studied adhere primarily to CD36 (10, 39, 75, 76) even though the amino acid sequence of CIDR domains of individual PfEMP1 molecules is quite diverse (8). The adhesion of diverse parasite isolates can also be inhibited by the same inhibitory anti-CD36 mAb, OKM5, suggesting that all parasites use a similar epitope on CD36 for firm adhesion. The OKM5 mAb binding site has been mapped to a region between residues 155-183, which is known to be the immunodominant region (77). A more detailed analysis was performed for IRBC binding by using peptide mapping and showed that the binding site for IRBC was between residues 145-171 (78).

The role of CD36 in the pathogenesis of severe falciparum malaria remains controversial. Results from studies to determine a correlation between CD36 mediated adhesion and disease severity have been variable, and appear to depend on the assay method and the geographical origin of the parasites. The tissue distribution of CD36 further complicates the issue as CD36 expression in the brain and kidney microvessels is minimal, but is highly expressed in the liver, lung, muscle, spleen and dermal microvessels (79). As well, CD36 is not upregulated in cerebral microvasculature in human cerebral malaria patients (80). These findings suggest that CD36 may be the major cytoadherence receptor outside of the brain. Recent genetic studies in African and Asian populations have shown that there is a high frequency of a point mutation in the CD36 gene that might result in the loss of expression of CD36. There is correlation of this genotype with protection against respiratory distress, severe anemia or hypoglycemia, but not cerebral malaria (81). On the other hand, an earlier study demonstrated a significant association of CD36 mutations with susceptibility to severe malaria, particularly cerebral malaria (82).

ICAM-1, or CD54, is a 90-kDa glycoprotein belonging to the immunoglobulin superfamily of adhesion molecules. It is a 453 residue transmembrane protein containing 5 extracellular immunoglobulin-like domains. ICAM-1 is an inducible protein expressed on the surface of activated endothelium and is a critical molecule in the leukocyte recruitment cascade responsible for mediating firm adhesion of leukocytes during inflammation. Although ICAM-1 is constitutively expressed on endothelium, its expression is significantly increased

in the presence of pro-inflammatory cytokines or bacterial lipid moieties such as lipopolysaccharide (LPS). TNF-α for example will increase ICAM-1 expression as early as 4h and the effect and can persist for up to 72h (9, 83, 84). ICAM-1 is an endothelial receptor for two different β2-integrins (CD18) found on the leukocyte cell surface. CD11a/CD18 (LFA-1) is found on lymphocytes and neutrophils while CD11b/CD18 (Mac-1) is mostly found on neutrophils.

ICAM-1 was first identified as a receptor for IRBC by selecting adherent parasites on human umbilical vein endothelial cells (HUVEC), which does not express CD36. The selected parasites specifically adhered to ICAM-1 transfected COS cells (48). PfEMP-1 was subsequently shown to mediate the adhesion of IRBC to ICAM-1 through a tandem domain comprised of the DBLβ and C2 domains, distinct from the CIDR CD36 binding domain (42). In contrast to adhesion to CD36, only 5-10% of clinical isolates firmly adhere to ICAM-1, and for isolates that adhere to both CD36 and ICAM-1, there is a 10-fold difference in the degree of adhesion to ICAM-1 compared to CD36 (10, 75, 76, 85). It has been proposed that the ICAM-1 binding trait might be associated with cerebral malaria as ICAM-1 expression is increased in the brain microvasculature of human cerebral malaria and co-localizes with sites of parasite sequestration (13, 42, 79). A genetic polymorphism in the ICAM-1 gene has suggested a role for ICAM-1 in the pathogenesis of severe malaria, however these findings could not be confirmed. A high frequency polymorphism, encoding methionine at position 29 in the N-terminal domain of ICAM-1 (ICAM-1^{kilifi}), has been reported in a malaria-endemic population in Kenya and The Gambia. Individuals homozygous

for this polymorphism in Kenya developed higher rate of cerebral malaria (86). However, the increased susceptibility to cerebral malaria was not observed in The Gambia (87) or Thailand (88). In addition, in flow chamber experiments, an ICAM-1 binding parasite line adhered less to purified ICAM-1^{kilifi} than to wild-type ICAM-1, although the number of rolling IRBC on ICAM-1^{kilifi} was greater (89). These results suggest a weaker and not stronger interaction with the mutant molecule.

VCAM-1 is also a member of the immunoglobulin superfamily of adhesion molecules and consists of 6 or 7 immunoglobulin domains. In contrast to ICAM-1, VCAM-1 is not constitutively expressed on endothelium. TNF-α induced expression of VCAM-1 is slower than ICAM-1, the molecule being expressed on human dermal microvascular endothelial cells (HDMEC) by 5h but did not reach a peak until 16h to 24h post-stimulation (9). VCAM-1 is the endothelial receptor for the α4-integrins, α4β1 (Very late antigen-4, VLA-4) and α4β7 (90, 91). The α4-integrin is normally only found on mononuclear cells and eosinophils (92) and the α4-integrin/VCAM-1 interaction mediates tethering and rolling of T cells and eosinophils and supports firm adhesion of monocytes (90, 93-95). Although mature circulating neutrophils do not normally express α4-integrin, chemically activated neutrophils will roll and adhere to VCAM-1 (96). More recently it was shown that neutrophils from septic patients express the α4-integin and can roll and adhere on VCAM-1. The α4-integrin-VCAM-1 interaction may represent an alternative neutrophil adhesion pathway that contributes to inappropriate leukocyte recruitment in sepsis (97). IRBC can adhere minimally to purified

VCAM-1 under static conditions but under flow conditions it only mediates tethering and rolling of IRBC (10, 49, 85). TNF-α induced VCAM-1 on HDMEC enhances adhesion to CD36, but does not support adhesion on its own or in the absence of functional CD36 (9).

The selectins are a family of multifunctional calcium-dependent transmembrane adhesion molecules that recognize fucosylated, sialylated and sulfated carbohydrate ligands. P-selectin is a 140-kDa protein expressed on platelets and endothelium and is composed of three major extracellular structural domains (98). All selectins have an N-terminal lectin like domain, followed by an epidermal growth factor-like domain (EGF) followed by a variable number of consensus repeat (CR) domains. P-selectin contains 9 CR domains, the most of the three selectins, giving it an extended structure capable of protruding beyond the extracellular glycocalyx (99). Preformed P-selectin pools are stored in both α-granules in resting platelets and Weibel-Palade bodies in endothelial cells and can be rapidly redistributed to the cell surface upon stimulation (100, 101). The major function of endothelial P-selectin is to capture leukocytes from the rapidly flowing blood by mediating the initial tethering and rolling of leukocytes (102). This initial step in the leukocyte recruitment cascade is critical for subsequent firm adhesion (103). Since P-selectin can be rapidly expressed on the cell surface within minutes it is able to mediate early inflammatory responses (104). Endothelial cells can also transcribe new P-selectin mRNA and synthesize new protein in response to the cytokines IL-4 and oncostatin M (OSM). In this case,

cell surface expression of P-selectin does not reach a peak for 24-48h (105, 106).

IRBC roll on purified P-selectin under flow conditions, and rolling has been shown to be Ca^{2+}-dependent suggesting an interaction with the lectin-like domain of P-selectin (11). IRBC rolling and adhesion are increased on oncostatin M-stimulated HDMEC and the increase is dependent on the upregulation of P-selectin (9). Further investigation has revealed that PfEMP-1 is the ligand responsible for IRBC interaction with P-selectin (43), but the domains on PfEMP1 mediating the interaction have not been identified.

1.2.1.5 Cytoadherence under flow in vitro and in vivo

There are no appropriate animal models for studying cytoadherence. As a result, the molecular interactions of IRBC with host endothelial cells has been studied under physiologically relevant shear stresses using endothelial monolayers in vitro (parallel plate flow chamber) and an intact human dermal microvascular bed in vivo (human/SCID mouse chimera). These models allow for the direct visualization of adhesive interactions in real time. Using the flow chamber assay, our lab has previously shown that IRBC can tether and roll on CD36, ICAM-1, P-selectin and VCAM-1, but not E-selectin. (10). These experiments were performed using stable transfectants to characterize the different types of interaction mediated by a single molecule. The strength of the rolling interaction with each receptor molecules varies, as reflected in the

difference in rolling velocity. Firm adhesion is almost exclusively to CD36, and IRBC can bypass the rolling event and adhere directly to CD36 after tethering.

The interactions of IRBC with multiple adhesion receptors expressed on the same substratum were investigated using cytokine stimulated HDMEC monolayers in the parallel plate flow chamber. TNFα induced the expression of both ICAM-1 and VCAM-1 resulting in an increase in the proportion of rolling IRBC that became firmly adherent to CD36. In contrast, OSM induced P-selectin expression resulted in an increase in both the number of rolling and adherent IRBC (9), indicating that P-selectin actually increases the recruitment of IRBC from the centerline blood flow to the endothelium. These findings demonstrated that IRBC are capable of exploiting multiple adhesion molecules synergistically, analogous to the leukocyte recruitment cascade (Figure 1.5).

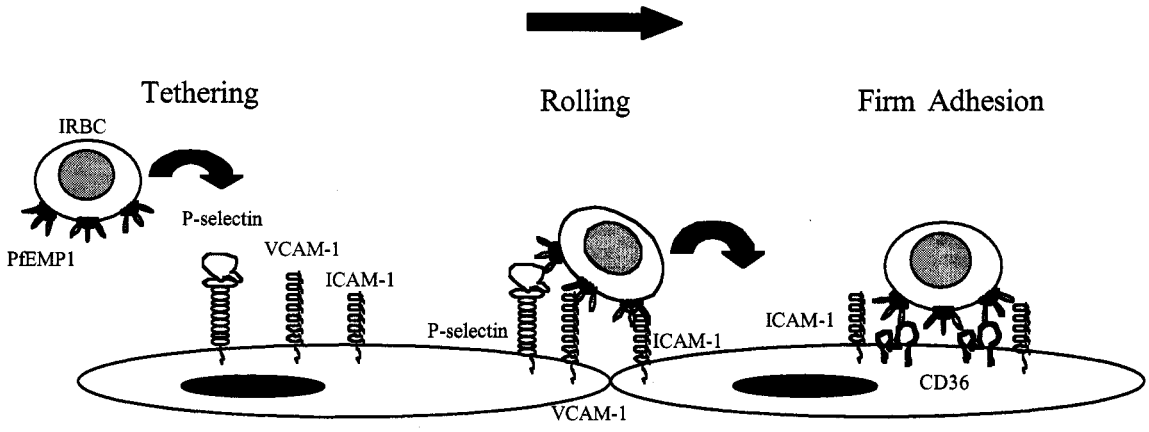

Figure 1.5 Schematic model of the cytoadherence cascade under flow conditions. IRBC are observed to have three distinct interactions with microvascular endothelium: tethering, rolling and firm adhesion.

Although the parallel plate flow chamber system in vitro has been very useful for identifying synergistic interactions of IRBC with multiple adhesion molecules in the cytoadherence cascade, it has limitations. In particular, it is difficult to accurately reproduce in vivo shear forces using the flow chamber apparatus. In addition, IRBC suspensions are infused at 1% hematocrit to optimize visualization. This certainly does not reflect the *in vivo* situation where cytoadherence occurs at much higher hematocrit and in the presence of other cellular elements. Finally, endothelium maintained in static culture may have phenotypic differences from endothelium maintained in a natural state in terms of its environment, surrounding cells, tissue architecture and constant shear force. Indeed it has been shown that cultured endothelium responds much differently if grown under shear flow as opposed to static conditions (107-112).

To address these issues, our lab has adapted a human/SCID mouse model in which human skin is grafted on to the back of SCID mice. The skin graft retains the human microvascular bed of the superficial dermis, and the graft blood supply is restored by spontaneous anastomosis of the mouse and human microvessels at the base of the graft (113). At the time of experimentation the human skin flap is exposed and human microvasculature can be visualized using intravital microscopy. This model provided the first direct evidence that IRBC roll and adhere to CD36 in vivo (114). The role of the accessory molecules ICAM-1, VCAM-1 and P-selectin in vivo has not been determined.

1.3 Cell signaling pathways

The leukocyte recruitment cascade involves multiple endothelial adhesion molecules that protrude from the membrane to serve as specific attachment points for leukocyte ligands. Much of the initial research in this field focused on the extracellular domains of the adhesion molecules and the extracellular events that mediate tethering, rolling and adhesion. It is now well recognized that adhesion molecules may also serve as receptor signaling molecules capable of transducing an outside-in signal cascade leading to cellular changes. For example, each member of the selectin family can transduce an outside-in cell signal. L-selectin initiates a MAPK signaling cascade in T lymphocytes (115) and neutrophils (116) resulting in leukocyte activation, enhanced cellular adhesion (117), neutrophil shape change and degranulation (118). E-selectin, found on the endothelium, specifically induces increases in intracellular calcium and the formation of stress fibers in endothelial cells following leukocyte interaction (119). Further investigation has revealed that the cytoplasmic tail of E-selectin associates with cytoskeletal elements (120, 121). Leukocyte adhesion or crosslinking E-selectin leads to cytoplasmic binding of SHP2 (122) resulting in a signaling complex formation and activation of ERK 1/2 (123). Evidence also exists for VCAM-1 (119), ICAM-1 (124) and P-selectin (119, 125) mediated outside-in signaling due to cellular interaction. These studies provide strong evidence that molecules capable of mediating adhesion are also cell-signaling molecules. It is not known if IRBC interaction with any adhesion molecule during cytoadherence elicits a cell signal.

1.3.1 Src-family kinases

Src-family kinases are non-receptor tyrosine kinases consisting of nine members: Src, Blk, Fgr, Fyn, Hck, Lck, Lyn, Yes and Yrk. These molecules play critical roles in receptor signaling and cellular communication. Each member contains conserved protein domains as well as unique amino acid sequence regions. In general Src-family kinases contain the following domains from the N- to C-terminus; Src-homology (SH) 4, a unique region, SH3, SH2, SH1 and the C-terminal tail (Figure 1.6). Plasma membrane localization is determined by the N-terminus and SH4 domain due to myristoylation and palmitoylation sites (126-128). The SH3 and SH2 domains are involved in negative regulation and cytoskeletal localization although SH2 plays a more significant role in negative regulation(129-131). The SH1 domain contains the catalytic kinase activity and also contains the autophosphorylation site involved in positive regulation. Under normal circumstances the Src-family kinases are maintained in an inactive state. In the inactive state Tyr 530 located in the C-terminus is phosphorylated and interacts intramolecularly with the src SH2 domain thereby by looping back onto itself covering the catalytic domain and inactivating the SH1 tyrosine kinase enzyme (131). Dephosphorylation of Tyr 530 by protein tyrosine phosphatases (PTP) opens up the complex and allows access of the SH1 kinase domain to potential substrates (132). Src-family kinase activation can also occur from interaction with src-binding proteins that disrupt the intramolecular inhibitory loop. Tyrosine phosphorylated intracellular growth factor receptor tails can compete for the SH2 domain breaking the intramolecular inhibitory loop causing Src-family

kinase activation. The intracellular tails of CD36 physically associate with Fyn, Lyn and Yes in human platelets while Fyn, Src and Yes bind to the CD36 tails in human microvascular endothelial cells (72) A recent report has demonstrated that the anti-angiogenic affect of TSP-1 on HDMEC is due to specific TSP-1-CD36 interaction and is dependent on a cell signaling pathway initiated by the src-kinase Fyn (60).

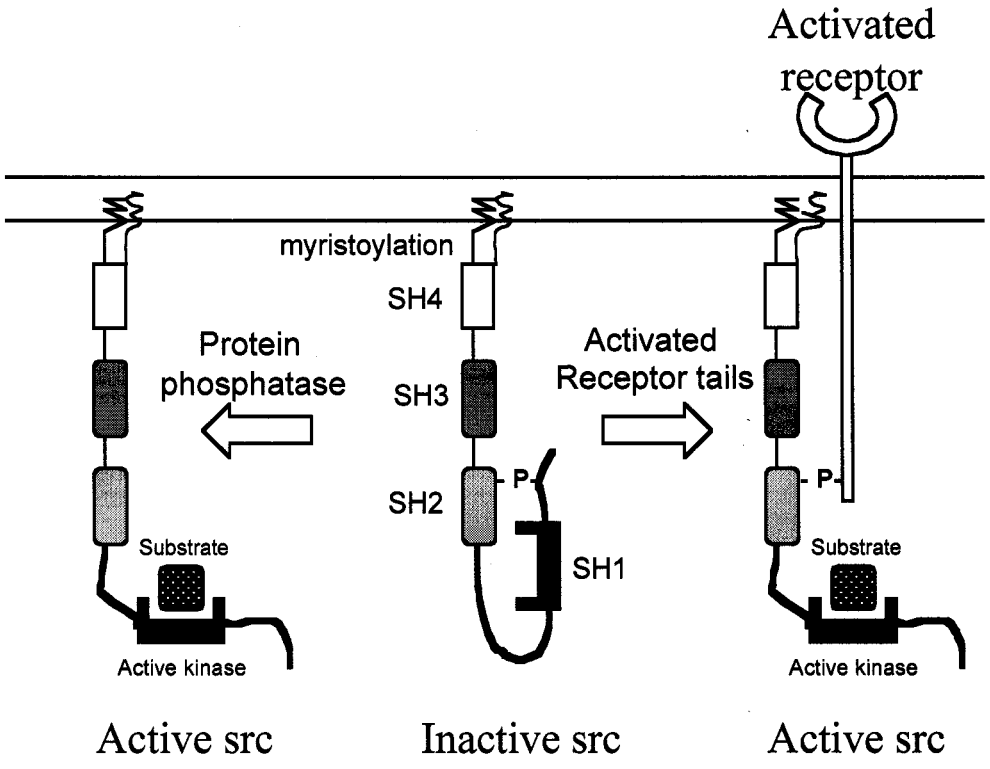

Figure 1.6 Schematic model of membrane bound Src-family kinase activation. Src-family kinases are held in an inactive state through an intramolecular interaction that closes the SH1 (kinase enzyme) domain. Activation can occur by removing the phosphate in the C-terminus via a protein phosphatase or through a phosphorylated protein competing for the SH2 negative regulatory binding site.

1.3.2 Mitogen-activated protein kinase (MAPK) signaling pathways

The MAPK family of signaling molecules consists of three major groups and three progressive tiers of activation forming an intricate cascade of molecules with diverse cellular function. Together these pathways form a cell signal network that mediates cellular responses to a wide range of stimuli. The three major groups include ERK 1/2, Jun amino-terminal kinases / stress-activated protein kinases (JNK/SAPK) and p38 pathways. Each tier of a cascade is modulated by an upstream group of kinases, which are in turn modulated by an upstream kinase. For instance, ERK 1/2 is dually phosphorylated on both a tyrosine and a threonine residue (133), thereby activating it, by an upstream kinase, MAPK-kinase, which in turn is phosphorylated by an upstream kinase, MAPKK-kinase, which in some cases may be activated by another kinase MAPKKK-kinase (Figure 1.7). A general scheme for the ERK 1/2 pathway begins with the activation of a growth factor receptor, followed by sequential activation of Raf (MAPKK-kinase) (134, 135), MEK 1/2 (MAPK-kinase) (136, 137) and finally ERK 1/2 (MAPK). Molecules targeted for activation by ERK 1/2 are diverse and include both nuclear substrates, Myc, c-Fos and Elk-1(138-140), and cytoplasmic substrates like phospholipase A_2 (141) and paxillin (142). The ERK 1/2 and the p38 MAPK pathways have been shown to be activated in monocytes following CD36 crosslinking with mAb (74) and the p38 MAPK pathway is activated downstream of TSP-1-CD36 interaction in HDMEC (60).

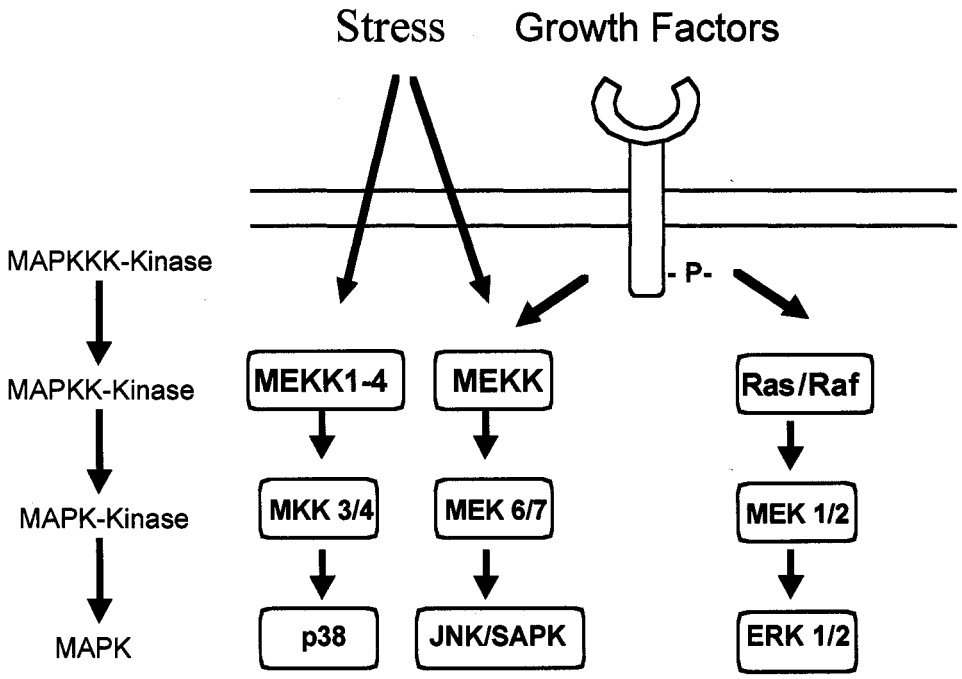

Figure 1.7 Schematic model of the three major MAPK family pathways.

1.3.3 Ecto-domain alkaline phosphatase

Alkaline phosphatases (AP) are expressed in many tissues, including the placenta, liver, brain, heart and kidney and are found on the outer surface of endothelium as glycophosphatidylinositol (GPI)-linked proteins. The physiological function of GPI-AP remains unclear. Increased ecto-AP activity is associated with some forms of cancers (143) and appears to be involved in insulin transport in the brain (144), cell differentiation (145), wound repair (146) and caveolae internalization (147). Although extracellular substrates for AP have been difficult to determine, it has been proposed that ectodomains of transmembrane proteins may be potential targets. As well ecto-protein-kinase / phosphatase systems are known to exist (148), but have not been well defined. In T cells the αβTCR is constitutively phosphorylated on ecto-serine and threonine residues and subsequent ecto-dephosphorylation of these residues might serve to modify TCR-molecular complex formation or even antigen binding affinity (149). CD36 on platelets is ecto-phosphorylated on two residues, Thr-92 and Ser-237 (71, 150). The Thr-92 is constitutively phosphorylated while on the cytoplasmic side of the platelet and expressed on the cell surface in the phosphorylated state. Upon platelet activation acid phosphatases are released and dephosphorylation of this residue modifies the binding properties of CD36. Ser-237 is thought to be phosphorylated after it is expressed by an ecto-PKA system found on platelets (150). The functional consequence of this latter ecto-PKA kinase system has not been established.

1.4 Rationale for study

A receptor-ligand interaction is one in which a receptor binds its specific ligand with high affinity and stereospecific chemical specificity and in so doing, elicits a conformational change of the receptor that ultimately results in an intracellular signal. This dual recognition-signaling property distinguishes receptors from tissue-targeting proteins that may be involved only in cell localization, but not in transmembrane signaling. In falciparum malaria, it is not known whether adhesion molecules on endothelial cells act as true receptors for IRBC, or simply provide points of attachment. A related question is whether intracellular activation of endothelial cells by IRBC leads to modification of the adhesion molecules such as a change in affinity or avidity, best described as inside-out signaling involving integrins.

Several lines of evidence in the literature suggest that IRBC signaling via CD36 might be a possibility. IRBC adhesion to CD36 on monocytes induces a respiratory burst (151) and crosslinking CD36 with an anti-CD36 mAb activates both ERK 1/2 and p38 MAPK pathways in these cells (74). Dendritic cell maturation can be inhibited through a direct cell-cell interaction with IRBC (152) and this effect is specifically mediated by IRBC interaction with dendritic cell surface CD36 (57). It is currently not known if the IRBC-CD36 interaction on endothelial cells initiates a cell signal.

We propose to test a novel model of cytoadherence that includes both outside-in and inside-out signaling mechanisms. This model suggests that the initial IRBC-CD36 interaction initiates endothelial cell signal pathways (outside-in)

leading to the modification of cytoadherence at the cell surface (inside-out). Based on the available information on CD36 signaling in the literature, we will investigate the Src-family kinase and MAPK family of signaling molecules as part of an outside-in mechanism. We will also investigate the possible role of ecto-GPI-AP as part of an inside-out mechanism capable of modulating cytoadherence by altering the phosphorylation state of CD36.

1.5 Statement of hypothesis and specific aims

Hypothesis: CD36 is the major vascular endothelial receptor for *P. falciparum*. Adhesion of infected erythrocytes to CD36 activates intracellular signaling pathways, leading to increased adhesion. Targeting CD36 will reduce cytoadherence and potentially some of the complications seen in severe falciparum malaria.

Specific aim 1: To study the roles of accessory adhesion molecules in modulating cytoadherence of IRBC to CD36 in an intact human microvasculature in vivo.

Objective 1: To investigate the accessory role of ICAM-1 and VCAM-1 on cytoadherence of IRBC to CD36 in vivo.

Objective 2: To investigate the accessory role of P-selectin on cytoadherence of IRBC to CD36 in vivo.

Specific aim 2: To evaluate novel anti-adhesive molecules in inhibiting and reversing cytoadherence in an intact human microvascular system.

Objective 1: To determine if the recombinant PfEMP1 peptide y179 can inhibit IRBC cytoadherence to HDMEC in vitro.

Objective 2: To investigate the anti-adhesive potential of y179 on resting endothelium in vivo.

Objective 3: To investigate the anti-adhesive potential of y179 on TNF-α stimulated endothelium in vivo.

Objective 4: To determine if anti-y179 antibodies inhibit IRBC cytoadherence to HDMEC in vitro.

Specific aim 3: To investigate if adhesion of IRBC to CD36 activates intracellular signaling pathways in the endothelial cell that may play a role in modulating subsequent parasite-host cell interactions.

Objective 1: To characterize CD36-dependent signaling in HDMEC.

Objective 2: To determine if PfEMP1 can directly initiate an intracellular signal in HDMEC.

Objective 3: To determine the consequences of the PfEMP1 induced- CD36 cell signaling to subsequent cytoadherence on HDMEC.

Objective 4: To determine the mechanism by which CD36 signaling increases IRBC firm adhesion to HDMEC.

CHAPTER 2

METHODS AND MATERIALS

2.1 Experimental Models

2.1.1 Materials

2.1.1a. Tissue culture reagents.

Unless otherwise stated, all tissue culture reagents were obtained from Invitrogen Canada Inc. (Burlington, Ontario). Recombinant human TNF-α was purchased from R & D Systems, Inc. (Minneapolis, MN). Histamine was purchased from Sigma-Aldrich (Oakville, Ontario) The cell signal inhibitors were purchased from; src kinase-inhibitor PP1 and the inactive analogue (Biomol, Plymouth Meeting, PA), the p38 inhibitors SKF86002 (Calbiochem, La Jolla, CA) and SB203580 (AG Scientific, San Diego, CA), the ERK 1/2 inhibitors PD098059 (Upstate, Lake Placid, NY) and U0126 (Upstate, Lake Placid, NY) and the phosphatase inhibitor sodium orthovanadate (SOV)(Sigma-Aldrich). Calf intestine alkaline phosphatase (Calbiochem) was used at 200U/ml in HBSS for 30 minutes at 37°C. Levamisole was obtained from Sigma-Aldrich.

2.1.1b Recombinant y179.

The recombinant protein y179 was provided by Dr. Dror Baruch, Laboratories for Parasitic Diseases, National Institute of Allergy and Infectious Diseases, National Institutes of Health, Bethesda, MD. The recombinant protein y179 was expressed in *Pichia pastoris* (Ciaran Brady, manuscript in preparation). In brief, a synthetic gene of the MC-179 (optimized for codon usage in *Pichia* and containing a His_6-tag on the C-terminus) was cloned into pPIC9K vector contains the alpha-factor secretion signal that directs the recombinant protein into the

secretory pathway. The protein was expressed in shaker flasks and harvested at 48 hours post-induction. The protein was purified using nickel-nitriltriacetic acid-agarose (Ni-NTA) followed by size exclusion chromatography on a Superdex 75 column (Amersham Pharmacia Biotech, Piscataway, N. J.) and reverse-phase HPLC using a C4 column (Vydac).

2.1.1c. Antibodies.

The anti-y179 mAb 4B3-A11 and 6A2-B1 were provided by Dr. Dror Baruch. (45). mAb 4B3-A11 recognized amino acids 81-141 of the C1-2 region of CIDR1, while 6A2-B1 reacted with the more conserved 1-87 region. A rat polyclonal antiserum against y179 was also provided by Dr. Baruch. The anti-ICAM-1 mAb 84H10, known to inhibit IRBC interactions with ICAM-1, was purchased from R and D Systems, Inc. Monoclonal antibody OKM5 (a gift from Ortho-Clinical Diagnostics, Raritan, NJ) was used in flow cytometry assays (5μg/ml), adhesion blocking assays in vitro (10μg/ml) and in vivo (20μg/ml). OKM5 was also used as the primary antibody (5μg/ml) followed by a goat anti-mouse $F(ab')_2$ (2.5μg/ml) secondary antibody to hypercrosslink endothelial CD36. The inhibitory anti-VCAM-1 antibody used for in vivo studies (20μg/ml) was a kind gift of Dr. R. Lobb (Biogen, Boston, MA). The anti-P-selectin mAb TS 10-6-6, which specifically inhibits IRBC-P-selectin interaction, was prepared in our laboratory and extensively characterized (9).

Western blot analysis was performed with either a rabbit polyclonal phosphospecific anti-active ERK 1/2 antibody (1:4000) (Promega, Madison, WI)

followed by a goat anti-rabbit horseradish peroxidase secondary antibody (1:20000) (Amersham Pharmacia Biotech, Piscataway, NJ) or a mouse mAb for total ERK 1/2 (1:1000) (BD Biosciences, Transduction Laboratories, Mississauga, Ontario) antibody followed by a goat anti-mouse horseradish peroxidase secondary antibody (1:20000) (Amersham Pharmacia Biotech).

2.1.2 Human dermal microvascular endothelial cells (HDMEC)

Human dermal microvascular endothelial cells (HDMEC) were harvested from discarded neonatal human foreskins as described previously (9). Foreskins were carefully dissected into 2-5mm^2 sections and then treated overnight at 4°C with 0.5 mg/ml Type IA collagenase (Boerhringer Mannheim Biochemicals, Indianapolis, IN) in M199. Endothelial cells were removed from the tissue by gently compressing the digested tissue segments with a spatula. A 100μm nylon mesh filter (Becton Dickinson, San Jose, CA) was used to remove the large debris from the cell suspension. The remaining cells were pelleted by centrifugation (200g for 7minutes), resuspended in EBM medium (Clonetics, San Diego, CA) with supplements provided by the manufacturer and seeded onto gelatin coated (0.2%) tissue culture dishes. Cells were maintained in EBM containing supplements supplied by the manufacturer as well as 100U/ml penicillin, 100μg/ml streptomycin and 1ug/ml amphotericin B in 5% $C0_2$ at 37°C. Using immunohistochemistry cells were found to be 95% positive for two endothelial cell markers, von Willebrand factor and PECAM-1 (CD31).

Experiments were performed with cells from passage one to five on which adhesion molecule expression was shown to be stable.

2.1.3 Parasite isolates.

Clinical isolates of *P. falciparum* were obtained from acutely infected Thai patients and cryopreserved. Patient blood was taken prior to antimalarial therapy. Erythrocytes were washed to remove platelets and leukocytes, cryopreserved in glycerolyte, stored in liquid nitrogen and transported to Calgary on dry ice. The collection of specimens was approved by the Ethics Committee of the Faculty of Tropical Medicine, Mahidol University, Bangkok, Thailand and the Conjoint Medical Research Ethics Board of the University of Calgary. For each experiment, a fresh aliquot was thawed and the parasites were allowed to grow to maturity (approximately 24-30h) in RPMI 1640 medium supplemented with $NaHCO_3$, 2mM L-glutamine (Sigma-Aldrich), gentamycin and 0.5% AlbuMAX II. All in vitro experiments were done at 5-7% parasitemia and 1% hematocrit. For in vivo experiments, the parasites were administered as a bolus (150-200µl) at approximately 50% hematocrit and 5-7% parasitemia.

2.1.4 Parallel plate flow chamber.

The cytoadherence of IRBC was studied using a parallel plate flow chamber as previously described (9). Confluent monolayers of endothelium in 35mm tissue culture dishes (Corning, New York, NY) were assembled in a parallel plate flow chamber in which a uniform wall shear stress was generated.

The flow chamber was mounted on the stage of an inverted phase contrast microscope with an attached video camera (Figure 2.1). The IRBC (1% hematocrit, 5 to 7 % parasitemia in RPMI 1640, pH 7.2) was drawn through the flow chamber at 1 dyne/cm^2 with an infusion pump attached to the outlet. The experiment was videotaped for off-line analysis of rolling and adhesion. A rolling IRBC was defined as one which displays a typical end-on-end rolling motion at a velocity of < 150 μm/sec, compared to a centerline flow rate of red blood cells of > 1000 μm/sec, and a velocity of >150 μm/sec for non-interacting cells in close proximity to the endothelial monolayer. The flux of rolling IRBC was determined as the number that rolled past a fixed line per minute on the monitor screen for the duration of the experiment. An IRBC was considered adherent if it remained stationary for >10 seconds, and the results were expressed as the number of adherent IRBC per mm^2 of surface area. For each experiment, IRBC interactions were visualized in one field for 7 minutes before randomly moving to three different fields for thirty seconds each. Flow rate within the chamber was determined using the following equation; $Q = (RB^2W) / (6\mu)$. Where Q = flow rate (ml/second), R = shear force (dynes/ cm^2), B = gasket thickness (cm), W = chamber width (cm) and μ = viscosity (poise).

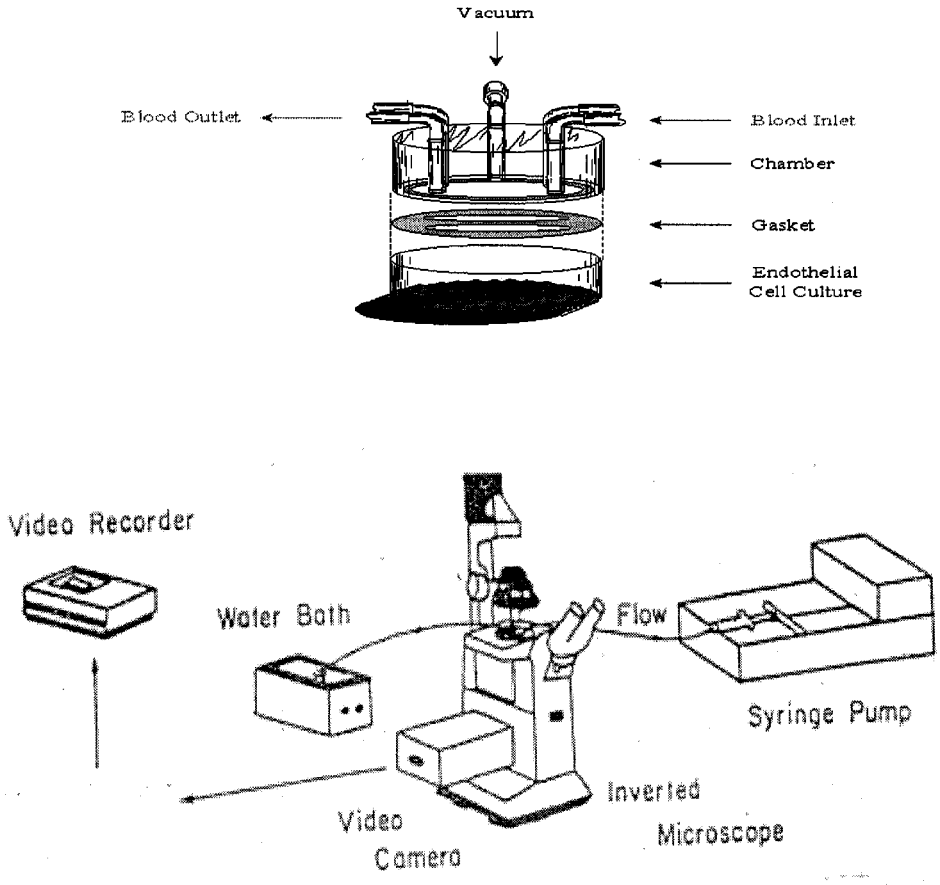

Figure 2.1 Diagram of the flow chamber apparatus used to examine IRBC interactions with endothelial monolayers under shear conditions.

2.1.5 Preparation of the human skin graft in SCID mice.

CB-17 SCID/beige mice (Harlan, Indianapolis, IN) were grafted with split thickness human skin as described previously (113) under a protocol approved by the Animal Care Committee and the Health Research Ethics Board of the University of Calgary. Briefly, split thickness grafts were prepared using a 1 mm dermatome from discarded human skin from donors undergoing plastic surgery. Recipient mice were anesthetized using halothane. A 0.5x0.5 cm defect was excised from the posterior thorax and covered with human skin anchored using skin staples (US Surgical, Norwalk, CT). The grafts were allowed to heal for a minimum of 3 weeks and were used in intravital microscopy experiments within 3-5 weeks following the grafting procedure.

2.1.6 Intravital microscopy.

Animals were prepared for intravital microscopy as previously described (114). The procedure was approved by the Animal Care Committee, University of Calgary. Briefly, the jugular vein of anesthetized animals was cannulated for administration of additional anaesthetic, boluses of IRBC, and recombinant peptide. A midline dorsal incision was made from the neck to the lower back, without disrupting the lateral dermal blood supply. The skin was reflected onto a pedestal and examined using an upright microscope (Nikon Optiphot) with a 20X water immersion objective (Nikon). To identify human vessels, 100 µg of FITC-*Ulex europaeus* (Sigma) was injected i.v. immediately before microscopic visualization. FITC-derived fluorescence was visualized by epi-illumination at

450-490 nm, using a 520 nm emission filter. IRBCs, but not uninfected red cells, were labeled with the nuclear dye rhodamine 6G (Sigma-Aldrich) (25 mg/ml), and visualized by excitation at 510-560 nm, using a 590 nm emission filter. Each 200µl bolus of IRBC contained IRBC at approximately 50% haematocrit and 5-7% parasitaemia. Images of the labeled IRBC and human microvessels were visualized using a silicon-intensified CCD camera (C-2400-08, Hamamatsu Photonics, Hamamatsu City, Japan) and recorded with a VCR for playback analysis. The numbers of rolling and adherent IRBC were determined off-line. IRBC rolling was expressed as rolling flux fraction, determined by counting the IRBC interacting in an individual vessel over the period of observation and expressing this relative to the total number of IRBC passing through the vessel over the same period (determined by frame by frame analysis). IRBC that remained stationary on the vascular wall for at least 30 s were defined as adherent. Adhesive interactions in 4 to 7 postcapillary venules per skin graft were counted.

2.1.7 Western blot analysis.

HDMEC were grown in 60mm tissue culture dishes (Corning) and used for Western blot analysis one day post-confluence. Treated or untreated cells were washed twice with PBS and lysed using 200µl of 2X SDS Laemmli's sample buffer heated to 80°C and then scraped off the plate. The samples were loaded into the wells of a 10% SDS-polyacrylamide gel and electrophoresis was performed at 1100V/hrs overnight. Proteins were transferred onto pure

nitrocellulose membranes (Schleicher & Shuell Inc. Keene, NH) using 0.800amps for 2h. Membranes were blocked with either 5% nonfat dry milk in Tris-buffered saline (TBS) (5mM Tris, 135mM NaCl, 5mM KCl) with 0.5% NP-40 and 0.1% Tween-20 for non-phospho-specific antibodies, or 5% bovine serum albumin in TBS with only 0.1% Tween-20 for the phospho-specific antibodies. Membranes were blocked for 1h at room temperature. Primary antibodies were incubated for 1h at room temperature in their respective blocking buffers. Membranes were given 3 ten-minute washes with either TBS-Tween-20 with or without NP-40 depending on the primary antibody. The appropriate horseradish peroxidase (HRP) conjugated secondary antibody was used at 1:20000 dilution in the appropriate blocking solution for 30 minutes at room temperature. Washes were carried out as described above. The membranes were developed using an enhanced chemiluminescence substrate (ECL)(Amersham Pharmacia Biotech).

2.1.8 Flow cytometry.

The level of CD36 on HDMEC was determined using flow cytometry. Confluent HDMEC monolayers were treated with 0.05% trypsin / 0.53mM EDTA for 5 minutes at room temperature. The dishes were then gently rinsed with phosphate buffered saline (PBS) to detach the cells. The endothelium was centrifuged and resuspended at $5x10^5$ cells/100µl. OKM5, an anti-CD36 mAb was used at 5µg/ml for 30 minutes at 4°C. Cells were washed once with 4 ml of PBS and the mouse mAb was detected using a FITC-conjugated goat anti-

mouse IgG for 30 minutes at 4°C. Control cells were stained with the secondary Ab only. Cells were analyzed in a FACScan flow cytometer (Becton Dickinson).

2.2 Experimental protocols

2.2.1 TNF-α modulates IRBC cytoadherence to CD36 in an intact human microvasculature in vivo.

The human/SCID mouse model previously described was used to investigate the roles of the accessory adhesion molecules ICAM-1 and VCAM-1 in cytoadherence in vivo. 100ng of human TNF-α in 50μl of filter-sterilized PBS containing 2mg/ml bovine serum albumin (BSA) was injected intradermally at the edge of the skin graft. The role for each adhesion molecule was examined at 4 and 24h post-injection. To determine baseline cytoadherence a bolus of IRBC was administered before any inhibitory antibodies were given. Two protocols were used to study the inhibitory effect of mAb on cytoadherence. Mice were either injected with one of the blocking antibodies prior to the administration of a bolus of IRBC, or mAb was administered following an initial bolus of IRBC to determine baseline cytoadherence. The inhibitory antibodies were allowed to circulate for at least ten minutes before the injection of a second bolus of IRBC. The second protocol was adopted to minimize the number of human/SCID mice necessary to obtain sufficient data.

2.2.2 Histamine modulates IRBC cytoadherence to CD36 in an intact human microvasculature in vivo.

The role of P-selectin in the cytoadherence cascade in vivo was investigated by treating the skin-grafted SCID mice with the potent secretagogue histamine. Human endothelial cells rapidly express cell surface P-selectin in response to histamine in vitro (102). As well, previous studies have shown that an intraperitoneal injection of histamine induced cell surface P-selectin within minutes in mouse microvascular beds (153). In our studies, grafted mice received an i.p injection (200µl) of 1mM histamine in saline immediately after jugular cannulation and approximately 30 minutes prior to the administration of IRBC. Baseline rolling and adhesion data for the parasite isolates used in these experiments were obtained under unstimulated conditions in other grafted animals. The role of P-selectin was investigated by using mAb TS 10-6-6.

2.2.3 Recombinant PfEMP1 peptide inhibits and reverses cytoadherence of multiple clinical isolates in vitro and in vivo.

2.2.3a The recombinant PfEMP1 peptide y179 inhibits cytoadherence under resting and TNF-α stimulated conditions in vitro.

The ability to inhibit cytoadherence with y179, the functional PfEMP1 binding domain, was assessed in vitro using confluent HDMEC monolayers in parallel plate flow chamber assays. Confluent endothelial monolayers were pretreated with 2µM of the y179 peptide for 30 minutes at 37°C. The flow

chamber apparatus was inserted into the 35mm endothelial dish and the monolayer was washed for 1 minute with warm HBSS at 1 dyne/cm^2. A 1% hematocrit suspension of IRBC was then perfused over the HDMEC at 1 dyne/cm^2 and IRBC interactions were visualized for 7 minutes. We also studied the ability of y179 to inhibit cytoadherence on HDMEC monolayers treated with 10ng/ml of human TNF-α for 24 h, in order to increase cell surface ICAM-1 and induce VCAM-1 expression.

The parallel plate flow chamber was also used to examine the inhibitory effect of anti-y179 antibodies. IRBC were resuspended in RPMI (10% hematocrit and 5-8% parasitemia) and incubated with one of the anti-y179 mAb (6A2-B1 and 4B3-A11) at 1mg/ml for 30 minutes at 37°C. The cell suspension was diluted to 1% hematocrit in RPMI before being used in the flow chamber assay. A rat anti-y179 polyclonal Ab was used at a 1:100 dilution and incubated with IRBC using the same procedure as for the mAb.

2.2.3b Recombinant PfEMP1 peptide (y179) inhibits and reverses cytoadherence of IRBC within intact human microvasculature under resting and TNF-α stimulated conditions in vivo.

The human-SCID mouse model was used to investigate the ability of y179 to inhibit and reverse adhesion of IRBC within an intact human microvasculature under resting and cytokine-stimulated conditions. Inhibition studies were carried out by administering 2μM of y179 intravenously 10-15 minutes prior to an IRBC bolus injection. Baseline rolling and adhesion values were determined for each

parasite in untreated mice. To study reversal, parasites were administered prior to y179 and allowed to circulate and adhere for 5-10 minutes. Following visual confirmation of IRBC adherence, 2μM of y179 was given i.v. IRBC detachment was visualized and recorded. Inhibition and reversal experiments were also performed on TNF-α stimulated skin grafts. In these experiments, skin grafts were pretreated with an intradermal injection of human TNF-α (100ng/graft, 4h) at the edge of the skin graft.

2.2.4 PfEMP1-CD36 interaction activates a Src-family kinase dependent cell signal within the endothelium resulting in increased firm adherence.

2.2.4a The PfEMP1-CD36 interaction activates an endothelial cell signal cascade.

Initial experiments were performed on HDMEC to determine which cell signal pathways were activated through CD36. We used an antibody cross-linking technique to artificially induce receptor activation. Confluent HDMEC monolayers in 60mm tissue culture dishes were starved in M199 with 0.5% BSA for 4h prior to crosslinking. The mAb OKM5 was used as the primary Ab at 5μg/ml for 30 minutes at 4°C. A goat anti-mouse $F(ab')_2$ fragment was used as the secondary Ab to hyperlink the receptor. The secondary Ab was used at 2μg/ml for 15 minutes at 37°C. After 5 minutes 100 μM of sodium orthovanadate (SOV) was added to the cells to protect against dephosphorylation. At 15 minutes the cells were lysed with 2x sample buffer (200μl at 80°C) and 100μl of

sample was loaded onto a 10% PAGE gel. Western blot analysis was performed in order to determine the amount of phosphorylated ERK 1/2 (activated). A modified procedure was used to determine if PfEMP1 could directly activate cell-signaling pathways. The recombinant y179 peptide was incubated with the HDMEC monolayers at 2μM at 37°C. Sodium orthovanadate (100μM) was added after 5 minutes. Cell lysates were harvested at 5, 15, 30 and 60 min. In experiments with the Src-family kinase inhibitor PP1 (154), HDMEC were pretreated with the inhibitor (10μM) during the last 30minutes of cell starvation.

2.2.4b Inhibition of Src-family kinase activation, but not ERK 1/2 or p38-MAPK, decreases IRBC firm adhesion, but can be restored with exogenous alkaline phosphatase in vitro.

We used the parallel plate flow chamber assay to determine if the CD36 dependent cell signal impacted on IRBC cytoadherence. Confluent HDMEC monolayers were pretreated with a number of cell signal inhibitors. All inhibitors were incubated for 30 minutes at 37°C. The following inhibitors and concentrations were used: PP1 (src-kinase specific, 1-10μM), PP3 (inactive control analogue of PP1, 10-20μM), SB203580 (p38-MAPK, 10-20μM), SKF86002 (p38-MAPK, 10-20μM), U0126 (inhibits MEK1/2 thereby inhibiting ERK1/2, 10μM), PD098059 (inhibits activation of MEK1/2), thereby inhibiting ERK1/2, 25μM). The monolayers were washed for 2 minutes with HBSS before the perfusion of IRBC. To determine if alkaline phosphatase could reverse the inhibitory effect of PP1 monolayers were pretreated with PP1 (10μM) for 30

minutes. The monolayer was washed 3 times with warm HBSS and 1 ml of calf alkaline phosphatase (200U/ml HBSS, 37°C, 30 minutes) was added. The monolayers were washed before IRBC perfusion. In some experiments the HDMEC were pretreated with levamisole, a specific alkaline phosphatase inhibitor (100μM- 1mM, 30 minutes at 37°C), prior to IRBC infusion. To ensure that the level of cell surface CD36 was unaffected by the addition of inhibitors, monolayers were incubated with the inhibitors and CD36 expression determined by flow cytometry.

2.2.4c Systemic inhibition of Src-family kinase activation decreases IRBC cytoadherence in vivo.

We used the human-SCID mouse model and intravital microscopy to determine if Src-family kinase inactivation resulted in decreased cytoadherence in vivo. Mice received an i.p injection of PP1 or PP3 (1.5mg/kg) in 200μl saline just prior to starting the jugular cannulation (1 hour prior to the administration of IRBC). Normal C57BL/6 mice were used in pilot experiments to verify that the PP1 would not affect the mouse microcirculation in terms of blood flow.

2.3 Statistical analysis.

All data are presented as mean ± SEM. For in vitro experiments "n" refers to the number of independent experiments performed. The "n" value for the in vivo experiments refers to the number of individual human vessels analyzed in several grafted animals. This method of counting has previously been

established for analyzing leukocyte recruitment using intravital microscopy (155-157). Raw data between two groups were compared by Student's t-test for paired samples. ANOVA with post hoc analysis, with Bonferroni's correction for multiple comparisons, was used when comparing data from more than two groups. Probabilities of 0.05 or less were considered statistically significant. The following symbols were used to denote significance; * = $p < 0.05$, ** = $p < 0.01$, *** = $p < 0.001$, when compared to the appropriate control group.

CHAPTER 3

UPREGULATION OF ACCESSORY ADHESION MOLECULE MODULATES IRBC CYTOADHERENCE TO CD36 IN AN INTACT HUMAN MICROVASCULATURE IN VIVO

Specific aim 1: To study the roles of accessory adhesion molecules in modulating cytoadherence of IRBC to CD36 within an intact human microvasculature in vivo.

Objective 1: To investigate the accessory role of ICAM-1 and VCAM-1 on cytoadherence of IRBC to CD36 in vivo.

Objective 2: To investigate the accessory role of P-selectin on cytoadherence of IRBC to CD36 in vivo.

3.1 Results.

Using the human/SCID mouse chimera model, we have shown previously that IRBC rolled and adhered on resting human microvessels in the skin grafts (114). Rolling was mediated by both CD36 and ICAM-1, as either antibody could partially inhibit the adhesive interaction. The addition of OKM5 that specifically inhibits IRBC-CD36 interaction resulted in 90% reduction in adhesion. An-anti-ICAM-1 was also able to inhibit IRBC adhesion by 60%, even though clinical parasite isolates adhere poorly to this molecule. The administration of both antibodies inhibited the adhesive interactions completely.

In this study, we further assessed the role of ICAM-1 and VCAM-1 in IRBC cytoadherence in vivo using TNF-α stimulated microvasculature. TNF-α stimulation was used based on our previous observations that the cytokine upregulates ICAM-1 expression and induces VCAM-1 expression on HDMEC in vitro (Figure 3.1)

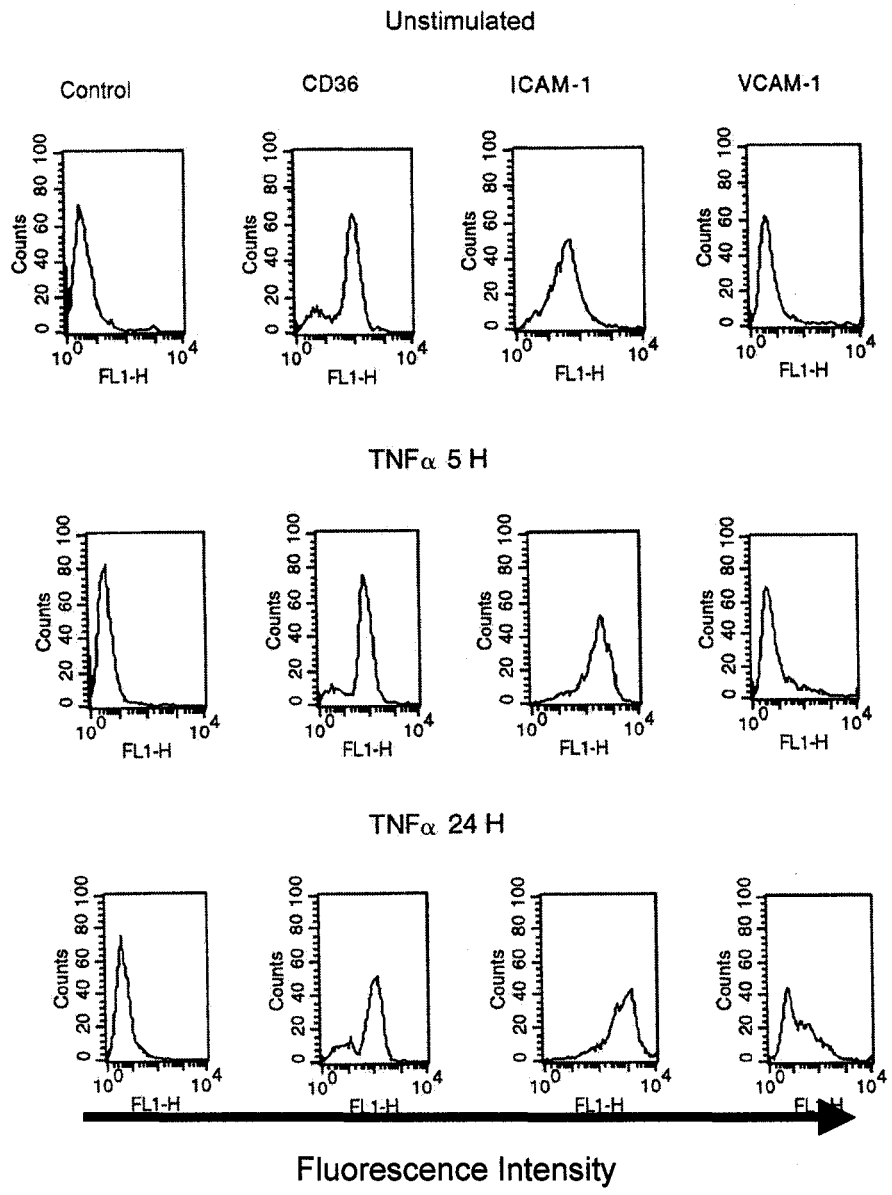

Figure 3.1. Flow cytometric analysis of adhesion molecule expression on resting HDMECs and HDMECs stimulated with 5 ng/mL of TNF-α for 5 and 24 h. The results are representative of 5 different HDMEC preparations.

ICAM-1 mediates increased IRBC adhesion after 4 hours of TNF-α stimulation in vivo. To determine the role of ICAM-1 on IRBC interactions with inflamed endothelium, the human skin graft was stimulated with TNF-α (100ng) for 4h. Cytokine stimulation resulted in a dramatic reduction in rolling flux, from 4.1± 1.3% on resting human microvessels to 1.5 ± 0.7 % in TNF-α stimulated skin grafts ($p < 0.05$)(Figure 3.2A). The decrease in rolling flux was associated with a 1.7-fold increase in the number of firmly adherent IRBC in stimulated microvessels (2.0 ± 0.2 to 3.4 ± 0.4 IRBC / 100μm, $p < 0.05$) (Figure 3.2B). The majority of the IRBC adhered directly without rolling.

In two animals, an anti-ICAM-1 mAb (20μg) was administered prior to IRBC and 13 vessels were analyzed for adhesion. No significant change in the rolling flux fraction was observed (Figure 3.2A). However, the number of adherent IRBC returned to resting levels (Figure 3.2B). Similar effects were seen when OKM5 (20μg) was injected prior to IRBC. There was no change in the rolling flux fraction (Figure 3.3A), but the number of adherent IRBC was reduced from 2.2 ± 0.3 to 0.9 ± 0.2 IRBC / 100μm, $p < 0.01$ (Figure 3.3B). The effect of CD36 blockade on IRBC adhesion was greater than the blockade of ICAM-1 ($p < 0.05$), but the inhibition of adhesion by either antibody was not complete. An isotype-matched mouse IgG mAb had no effect on the rolling flux fraction or adhesion (Figure 3.4A and B).

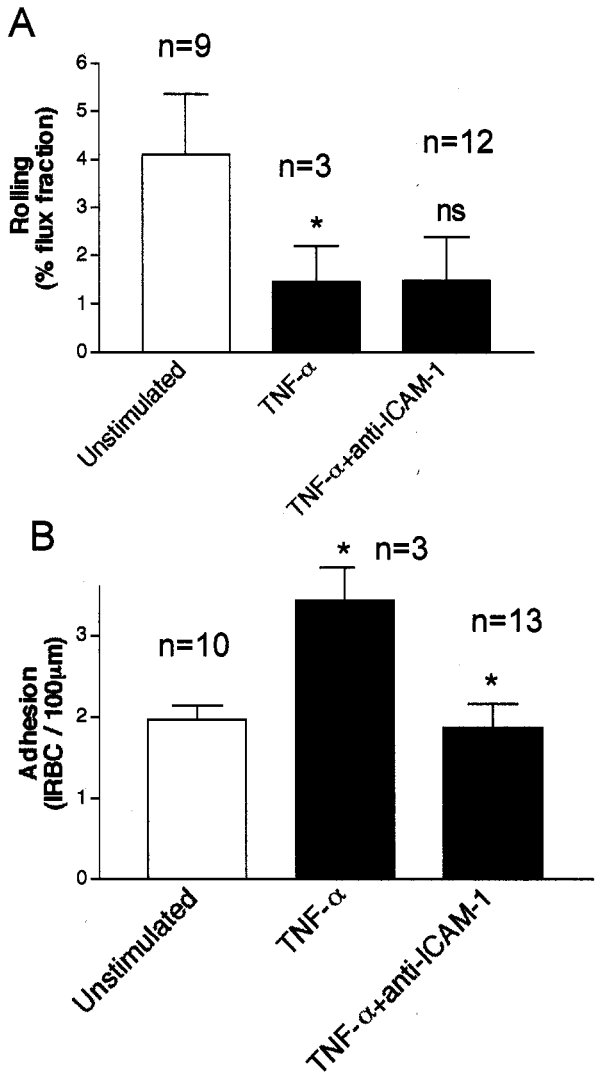

Figure 3.2. The role of ICAM-1 on IRBC rolling and adhesion to TNF-α stimulated human microvessels in vivo. Human skin grafts were either untreated or stimulated with TNF-α (100ng/graft, 4h) and A) Rolling and B) Adhesion were directly visualized. For inhibition studies, 20μg of anti-ICAM-1 mAb 84H10 was administered. Two different clinical parasite isolates were used in 6 mice.

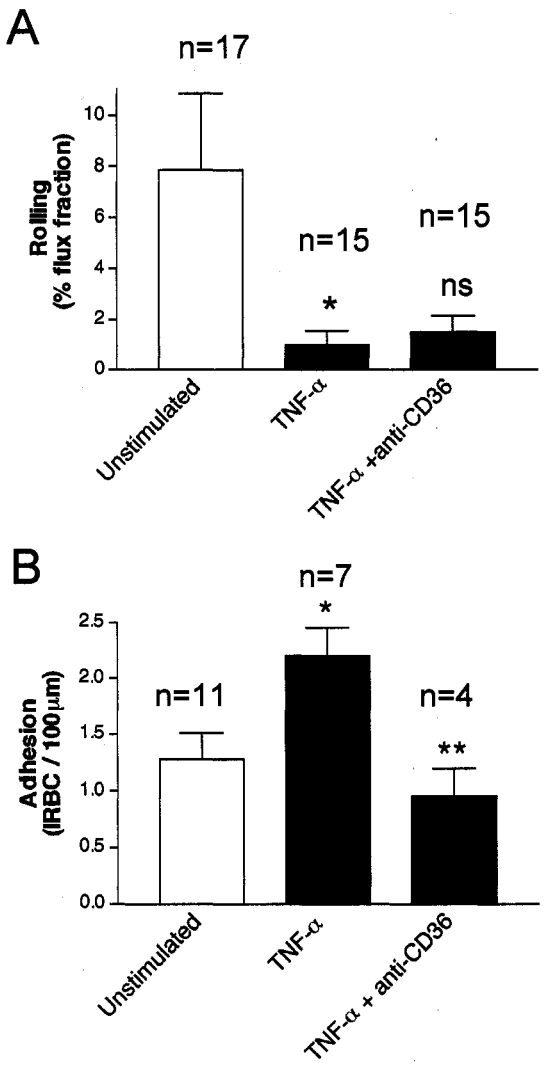

Figure 3.3. The role of CD36 on IRBC rolling and adherence to TNF-α stimulated human microvessels in vivo. Human skin grafts were either untreated or stimulated with TNF-α (100ng/graft, 4h) and A) Rolling and B) Adhesion were directly visualized. For inhibition studies, 20μg of anti-CD36 mAb OKM5 was administered. Three different clinical parasite isolates were used in 8 mice.

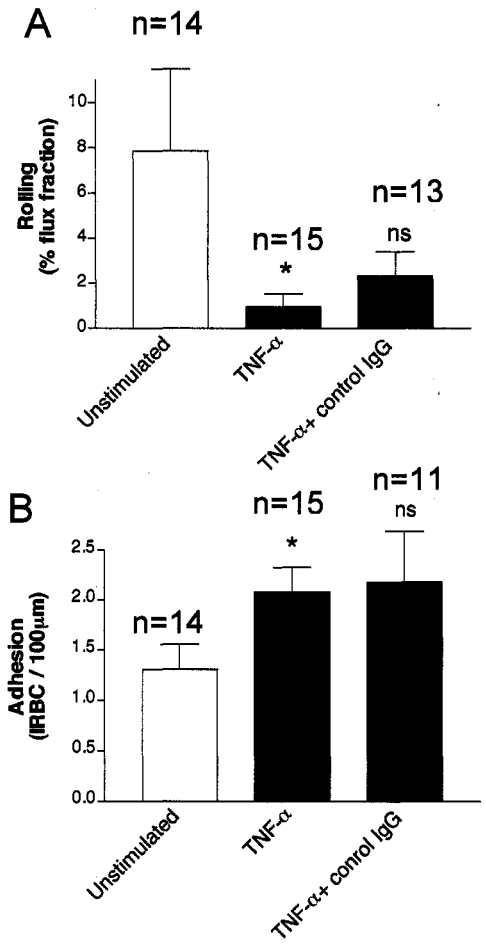

Figure 3.4. The effect of an isotype matched-mouse IgG mAb on IRBC rolling and adhesion in vivo. This data was generated from two different clinical parasite isolates and 6 animals.

ICAM-1, but not VCAM-1, is responsible for the increase in IRBC cytoadherence in human microvessels stimulated with TNF-α for 24h. When human microvessels were stimulated with TNF-α for 24h, there was a further reduction in the rolling flux fraction from 6.2 ± 3.0% to 0.7± 0.5 %, $p < 0.01$ (Figure 3.5A). This represents a drop in the rolling flux fraction of 89.0% compared to a drop of 64.3% on HDMEC stimulated with TNF-α for 4h. The decrease in rolling flux fraction was associated with a 5.4-fold increase in the number of adherent cells from 0.5 ± 0.2 to 2.7 ± 0.4 IRBC / 100 μm (Figure 3.5B).

To determine the relative roles of ICAM-1 and VCAM-1 in IRBC adhesion on HDMEC stimulated with TNF-α for 24h, animals were pretreated with receptor-specific antibodies prior to the administration of IRBC. The addition of anti-ICAM-1 had no effect on the rolling flux fraction (Figure 3.5A), but returned the number of adherent IRBC to baseline levels (Figure 3.5B). In contrast, 4B9, an anti-VCAM-1 mAb that partially inhibits the adhesion of IRBC to VCAM-1 (9, 49), had no effect on IRBC rolling (Figure 3.6A) or adhesion (Figure 3.6B) on cytokine-stimulated microvessels in vivo.

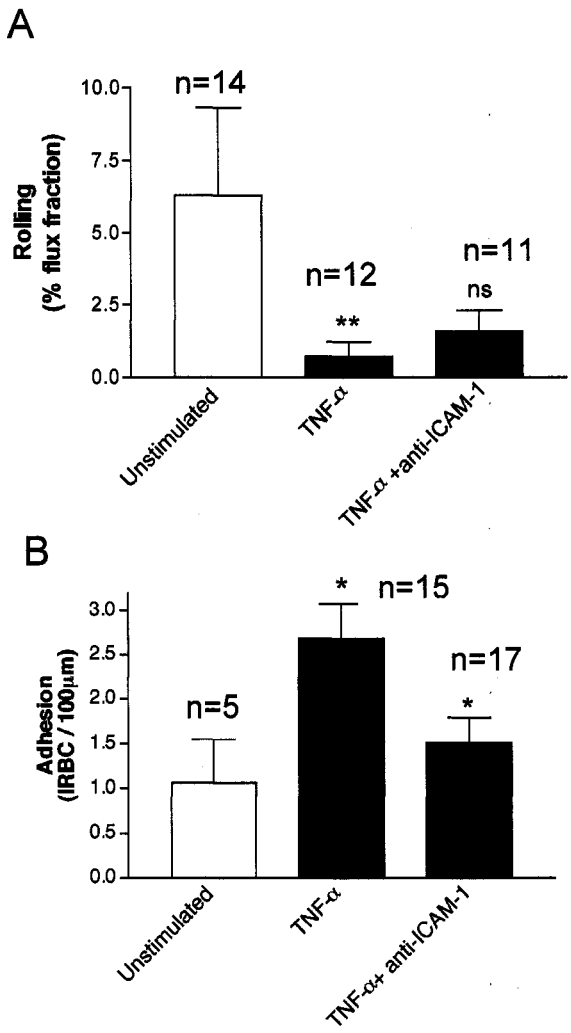

Figure 3.5. The role of ICAM-1 on IRBC rolling and adhesion to TNF-α stimulated (24h) human microvessels in vivo. Human skin grafts were either untreated or stimulated with TNF-α (100ng/graft, 24h) and A) Rolling and B) Adhesion were directly visualized. For inhibition studies, 20μg of anti-ICAM-1 mAb 84H10 was administered. One clinical parasite isolate was studied in 4 mice.

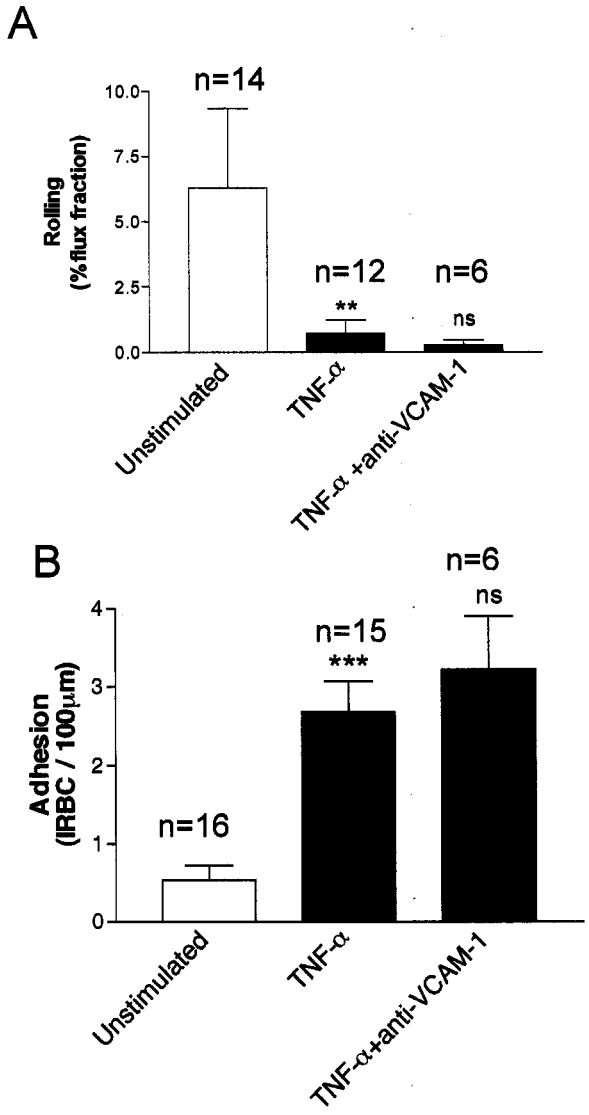

Figure 3.6. The role of VCAM-1 on IRBC rolling and adhesion to TNF-α stimulated (24h) human microvessels in vivo. Human skin grafts were either untreated or stimulated with TNF-α (100ng/graft, 24h) and A) Rolling and B) Adhesion were directly visualized. For inhibition studies, 20μg of anti-VCAM-1 mAb 4B9 was administered. Two clinical parasite isolates were tested in 4 mice.

P-selectin increases IRBC adhesion in vivo through an increase in cell recruitment. Recent work from our lab demonstrated that P-selectin is a receptor for PfEMP1 and that P-selectin (43), but not E-selectin, can significantly increase the number of rolling and adherent IRBC to HDMEC in vitro (9). The role that of this adhesion molecule in IRBC cytoadherence in vivo is unknown. In this study, we induced P-selectin expression on human microvessels by the systemic administration of histamine 30 minutes prior to IRBC injection. This method of histamine administration has been shown to significantly increase cell surface P-selectin expression in multiple vascular beds in a mixed background mouse strain C57BL/6J/129Sv (153).

Induction of P-selectin on microvessels resulted in a dramatic increase in IRBC rolling flux fraction from a baseline of 2.0 ± 0.3 % to 5.7 ± 0.9%($p < 0.05$), representing a 2.9 fold increase (Figure 3.7A). Thus the effect of histamine on the microvasculature was in direct contrast to that of TNF-α in terms of rolling flux fraction. More importantly, the increase in the percentage of rolling cells induced by histamine translated into a significant increase in IRBC adhesion. Figure 3.7B shows that the number of adherent IRBC increased from 1.8 ± 0.1 to 2.9 ± 0.3 IRBC / 100μm ($p < 0.05$) a 1.6 fold increase. The increase in IRBC rolling and adhesion was entirely mediated by P-selectin, as an inhibitory mAb TS10-6-6 completely abolished the histamine response ($p < 0.05$).

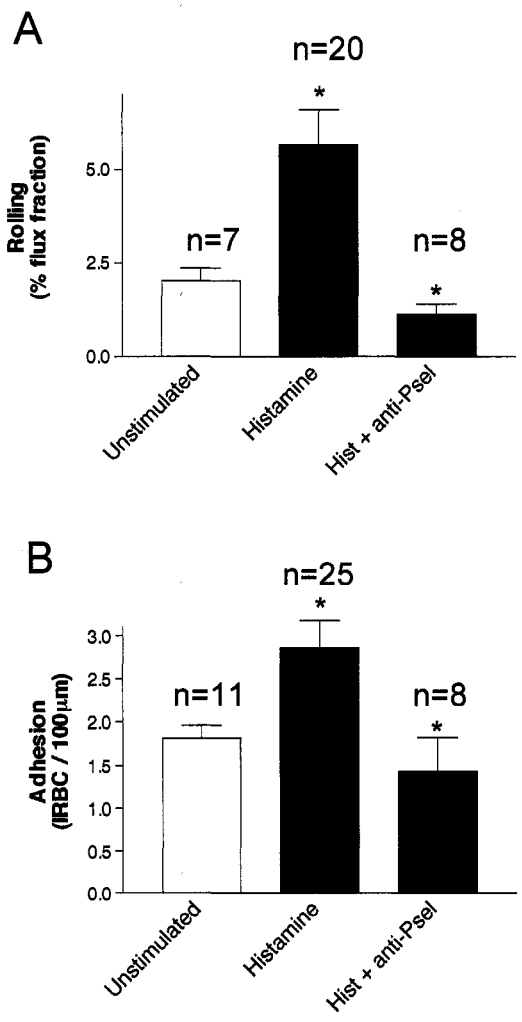

Figure 3.7. The effect of P-selectin on IRBC rolling and adherence in vivo. Stimulated mice were treated with histamine (200µl of 1mM, 30minutes, i.p.) and A) Rolling and B) Adhesion were directly visualized. For inhibition studies, the anti-P-selectin mAb TS 10-6-6 was administered. The experiments were performed with 3 different clinical parasite isolates from 6 grafted animals.

3.2 Discussion

IRBC cytoadherence under shear flow conditions is a series of adhesive events involving multiple receptors, mimicking the leukocyte recruitment cascade. The roles for different adhesion molecule involved in this cascade have been studied extensively in vitro. Under flow conditions in vitro, IRBC can tether and roll on CD36, ICAM-1, VCAM-1 and P-selectin, while adhesion is almost exclusively to CD36. There is strong evidence that the rolling interaction enhances subsequent adhesion, either by increasing the percentage of rolling cells that eventually adhere (ICAM-1 and VCAM-1), or by actually increasing the number of infected erythrocytes recruited from the bloodstream to vascular endothelium (P-selectin). Whether these accessory molecules have a similar role in cytoadherence in vivo has not been determined.

In this study, we have used the human-SCID mouse model and intravital microscopy to investigate the roles of different adhesion molecules in mediating cytoadherence under clinically relevant conditions in vivo. Increased TNF-α levels (158) and activated endothelium (79, 159) have been well documented in severe falciparum malaria. Therefore, we investigated the molecular mechanisms of cytoadherence to TNF-α stimulated human microvasculature. Analogous to the in vitro situation, adhesion in vivo to activated endothelium was significantly increased on stimulated endothelium. However, although the increase in adhesion was mediated without a change in the rolling flux in vitro, IRBC rolling in vivo was substantially decreased in TNF-α stimulated microvessels Inhibition experiments revealed that ICAM-1 was the molecule

responsible for the TNF-α induced increase in adhesion. Since IRBC from clinical parasite isolates with few exceptions adhere poorly to ICAM-1 (6 to 14 fold lower than CD36), these findings suggest that increased ICAM-1 expression in vivo serves to stabilize the adhesion to CD36.

The mechanism underlying the ICAM-1-dependent increase in adhesion is not known. The increased adhesion may be accomplished through ICAM-1 dependent stabilization of the PfEMP1-CD36 interaction leading to immediate adhesion. ICAM-1 dependent stabilization may be due to a number of possibilities. ICAM-1 exists as dimers and large multimers on the cell surface, and dimerization of ICAM-1 is essential for efficient binding of the physiological ligand lymphocyte function-associated antigen-1 (LFA-1) even though LFA-1 is capable of binding monomeric ICAM-1 (160). The ICAM-1 dimer provides two LFA-1 binding sites thereby increasing the avidity of the ligand-receptor interaction (161). Similar changes in avidity may be important for IRBC adhesion. Binding of PfEMP1 to ICAM-1 occurs within the first and second Ig domains of ICAM-1 in a region distinct from the binding site of LFA-1 (162, 163) but lies within the ICAM-1 dimer interface (164). It is possible that dimerized ICAM-1 promotes stabilization by providing two binding domains for two PfEMP-1 molecules similar to the LFA-1 model. Our experiments were performed with TNF-α and it has been shown that TNF-α stimulation of endothelium results in an increase of covalent dimer formation of a fraction of ICAM-1(160).

PfEMP1 interacts with ICAM-1 using a complex of the DBLβ and C2 domains (42), distinct from the CD36 binding domain CIDR1. As PfEMP-1 can

contain the necessary domains to bind CD36 and ICAM-1 simultaneously, increasing ICAM-1 may result in more individual PfEMP-1 molecules binding both CD36 and ICAM-1 resulting in an increased avidity of the interaction. Our results suggest that the level of cell surface ICAM-1, and possibly the number of dimerized molecules, may be critical in determining if the IRBC roll or if they immediately adhere. In other words, there may be a gradation in functional ICAM-1 expression, where basal levels of ICAM-1 expression promote IRBC rolling. Higher levels of ICAM-1 expression may cause more rolling cells to adhere and at the highest level of ICAM-1 expression, the progression from rolling to firm adhesion may become instantaneous.

Contrary to the findings in vitro, we could not identify a role for VCAM-1 in promoting IRBC adhesion on TNF-α stimulated microvessels in vivo. Three possible explanations exist: 1) VCAM-1 was not induced in our skin grafts or 2) VCAM-1 plays no detectable role in the cytoadherence cascade in vivo or 3) The mAb 4B9 does not effectively block the VCAM-1 binding domain. Many reports have demonstrated that VCAM-1 is consistently expressed in human microvascular endothelial cells stimulated with TNF-α for 24hr (9, 165, 166), so it is unlikely the human microvessels in the skin graft would not be expressing this molecule. A more likely explanation is that in vivo, IRBC-VCAM-1 interaction is unstable because the shear forces and centerline red blood cell velocity are much greater in vivo than in vitro. We have previously shown that the rolling velocity of IRBC on VCAM-1 stable transfectants was 5-10 fold higher than that on CD36 and ICAM-1, indicating an interaction with a high off rate and hence low

affinity (10). The mAb 4B9 can inhibit IRBC adherence in vitro by approximately 60% (49), as well we have demonstrated that 4B9 can decrease adhesion of IRBC to TNF-α stimulated (24hr) HDMEC (9). To confirm that VCAM-1 is not playing a role in vivo, further experiments could be performed using a panel of anti-VCAM-1 antibodies or with soluble VCAM-1. This would test if sites on VCAM-1, other than the epitope recognized by 4B9, might play a more significant role in promoting IRBC firm adhesion.

The role of P-selectin in IRBC rolling and adhesion in vivo was also assessed in this study. In direct contrast to TNF-α stimulation, IRBC rolling flux fraction was substantially increased in histamine-stimulated human microvessels, and resulted in a significant increase in the number of adherent IRBC. Therefore, an obvious difference in mechanism exists between P-selectin mediated and ICAM-1 mediated enhancement of firm adhesion to CD36, as we demonstrated in vitro (9). P-selectin extends past the glycocalyx (99), giving it optimal positioning to form a quick strong bond with a ligand traveling at high velocity (167). As a result, more IRBC are recruited to the vessel wall allowing for a greater number of interactions with CD36. The identification of the P-selectin interacting domains on PfEMP1 in relation to the CD36 and ICAM-1 domains will be of particular interest and importance in determining how all of these adhesion molecules can interact with the same ligand.

Unlike ICAM-1 and VCAM-1, the transcription of the human P-selectin gene is not induced by TNF-α. This raises the question of how P-selectin could be relevant during *P. falciparum* malaria. Increased levels of circulating

histamine have been demonstrated in falciparum malaria (168), and in a recent report, *P. falciparum* was shown to produce a histamine releasing factor (HRF) homologue termed translationally controlled tumor protein (TCTP)(169). This protein is found in the sera of patients with falciparum malaria, and stimulates the release of histamine from human leukocytes. As well, P-selectin gene transcription can be induced by oncostatin M (OSM), a cytokine in the IL-6 family. Although OSM has not been measured in falciparum malaria, IL-6 is markedly elevated during the infection and its level is significantly associated with disease severity (158).

Over the past two decades, many endothelial molecules have been identified as ligands for IRBC. These include CD36, ICAM-1, PECAM-1, VCAM-1, thrombospondin-1 (TSP-1), hyaluronic acid (HA), CSA, E-selectin and P-selectin. The contribution of most of these adhesion molecules has been determined under static conditions using lab-adapted parasite lines and clones on immobilized proteins or transfectants expressing unphysiological levels of adhesion molecules. In addition the molecules have been studied individually, making it difficult to infer co-operative functions in vivo. To directly address these problems, we first adapted a flow chamber assay and more recently a model of human microvasculature in vivo in order to investigate the contributions of multiple adhesion molecules acting interdependently in cytoadhesion. In doing so, we have developed a paradigm for IRBC-endothelial interaction that unequivocally shows that cytoadherence is a dynamic process in keeping with other cell-cell interactions in the circulation (114). Two distinct pathways of

enhanced IRBC firm adhesion to CD36 have been identified, that involve either an increase or a decrease in the rolling flux fraction. We have clearly shown that ICAM-1 dramatically increases IRBC adhesion while decreasing the total rolling flux fraction, suggesting that this molecule may be involved in stabilizing the PfEMP-1-CD36 adhesive interaction. In sharp contrast P-selectin mediates a rolling dependent increase in IRBC adhesion due to its ability to recruit more IRBC to the endothelium allowing for more IRBC-CD36 interaction.

There are limitations even of the human/SCID mouse model. The IRBC adhesion cascade in the human skin may differ from the adhesive events in other tissues and organs. For instance, adhesion of IRBC to CSA and HA is specific to the placenta, and there is preliminary evidence to indicate that vascular adhesion protein-1 (VAP-1) may be involved in the cytoadherence within the tortuous architecture and lower shear forces found in the liver sinusoids (Rinfret & Ho, unpublished observation). The low expression of CD36 in the cerebral vasculature raises the possibility that other adhesion molecules may be involved in cerebral complications. These and related tissues warrant further investigation.

CHAPTER 4

RECOMBINANT PfEMP1 PEPTIDE INHIBITS AND REVERSES CYTOADHERENCE OF MULTIPLE CLINICAL ISOLATES IN VIVO

Specific aim 2: To evaluate novel anti-adhesive molecules in inhibiting and reversing cytoadherence in an intact human microvascular system.

Objective 1: To determine if the recombinant PfEMP1 peptide y179 can inhibit IRBC cytoadherence to HDMEC in vitro.

Objective 2: To investigate the anti-adhesive potential of y179 on resting endothelium in vivo.

Objective 3: To investigate the anti-adhesive potential of y179 on TNF-α stimulated endothelium in vivo.

Objective 4: To determine if anti-y179 antibodies inhibit IRBC cytoadherence to HDMEC in vitro.

4.1 Results.

Inhibition of IRBC cytoadherence on resting HDMEC by recombinant y179 in vitro.

We first tested if y179 was capable of inhibiting IRBC rolling and adhesion in vitro. Resting endothelial monolayers that expressed CD36 and ICAM-1 constitutively were pre-incubated with 2mM y179 for 30 minutes prior to flow chamber experiments. The results show that the total number of adherent IRBC decreased from 96.8 ± 20.5 to 15.1 ± 9.0 / mm^2 ($p < 0.01$) after 7 minutes of IRBC perfusion, representing an inhibition of 84.4% (Figure 4.1A). Rolling flux, however, was not significantly affected by y179, suggesting that the same number of IRBC interacted with the endothelium with the potential to adhere

(Figure 4.1B). The results demonstrate that the inhibitory effect of y179 was not limited to the MC strain from which it was derived and that blocking CD36 alone significantly inhibits adhesion even in the presence of basal ICAM-1 expression.

Inhibition of IRBC cytoadherence on TNF-α-stimulated HDMEC by recombinant y179 in vitro. We have shown previously that IRBC adhesion on HDMEC stimulated with TNF-α for 24 h is significantly increased due to a higher percentage of rolling cells becoming arrested (an increase from 45 to 100%) (5). The effect is mediated largely by the cytokine-induced upregulation of ICAM-1 expression, although VCAM-1 expression also appears to play a minor role. A similar increase in the number of adherent IRBC was seen on TNF-α-stimulated-endothelium in this study (Figure 4.1C). Treatment of stimulated HDMEC with only y179 inhibited IRBC adhesion by 62.8% (133.2 ± 20.4 to 49.5 ± 21.8 IRBC/mm^2, $p < 0.05$) without affecting the number of rolling cells (Figure 4.1D). The combination of an inhibitory anti-ICAM-1 mAb and y179 inhibited adhesion by 90.4 ± 3.69%, $p < 0.01$ (Figure 4.1C) and rolling flux by 78.3 ± 11.5%, $p < 0.05$ (Figure 4.1D). The inhibitory effect was observed using four different clinical isolates in five separate experiments. An IgG isotype-matched mAb CL3 directed against E-selectin had no inhibitory effect on IRBC rolling or adhesion on HDMEC (data not shown).

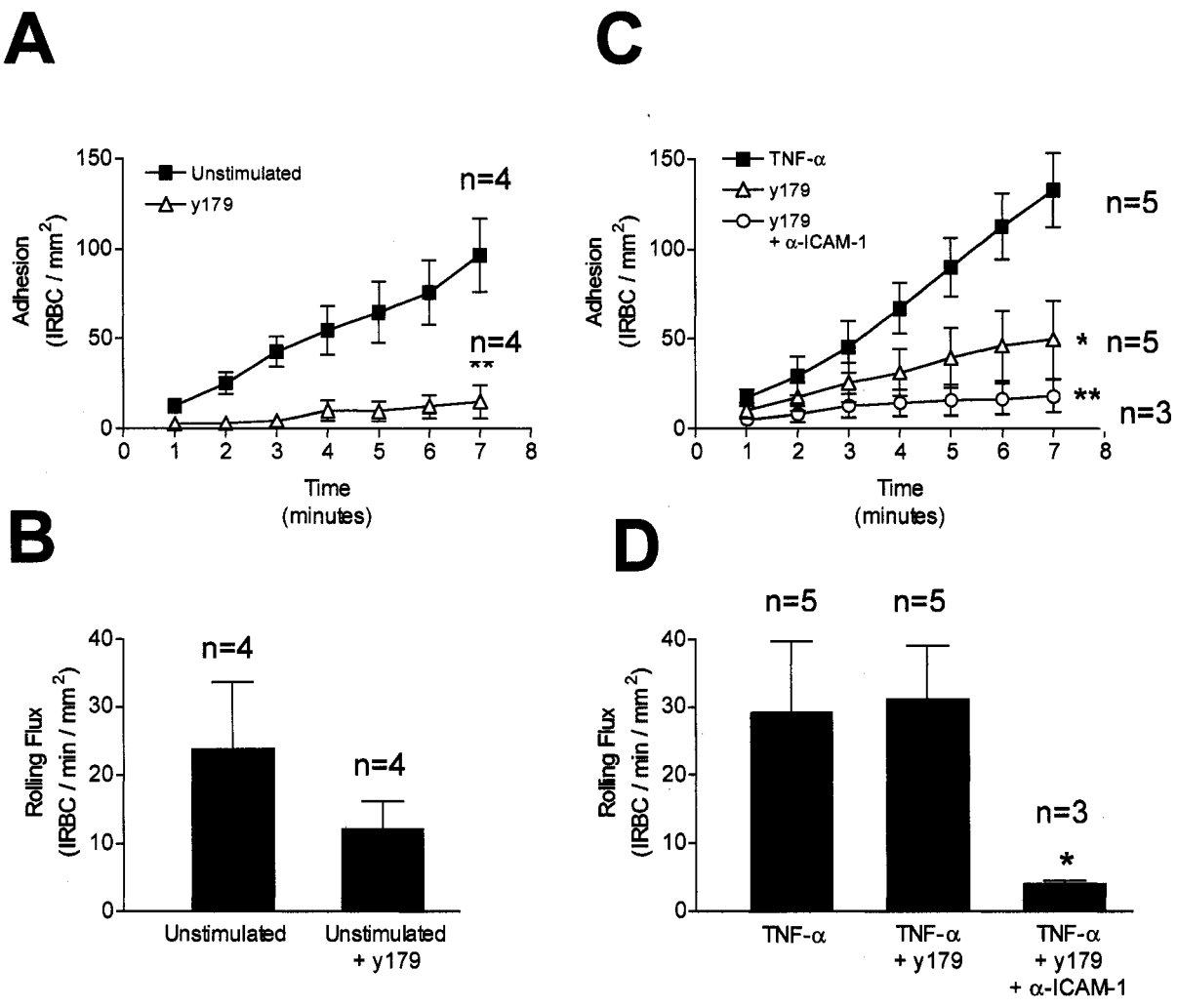

Figure 4.1. Inhibition of cytoadherence on resting and stimulated HDMEC by y179 in vitro. Resting and TNF-α stimulated (10ng/ml, 24h) endothelial monolayers were pre-incubated with 2μM y179 (30 min.). IRBC were then perfused at 1 dyne / cm^2. y179 was used alone or in combination with the inhibitory anti-ICAM-1 mAb 84H10 at 5μg/ml. A) Adhesion and B) Rolling on unstimulated cells. C) Adhesion and D) Rolling on stimulated cells. A and B represent 3 different parasite isolates, while C and D represent 4 different parasite isolates.

Inhibition of IRBC cytoadherence in human microvasculature by recombinant y179 in vivo. To determine if y179 could inhibit the adhesive interactions between IRBC and human microvessels under the much higher shear stress in vivo, experiments were performed by observing by intravital microscopy the adhesive interactions of IRBC in the microvasculature of human skin grafted on to a SCID mouse. In inhibition experiments, the grafted mice received a bolus of 2μM y179 via the jugular vein. The peptide was allowed to circulate for 10 to 15 minutes before the administration of the bolus of IRBC. Rolling and adhesion of IRBC observed in animals treated with y179 were compared to that observed in untreated animals. The results show that firm adhesion was inhibited from a baseline of 1.4 ± 0.24 to 0.18 ± 0.13 IRBC/100 μm for parasite isolate P00-24 ($p < 0.01$) and 1.94 ± 0.13 to 0.28 ± 0.13 IRBC/100 μm for P99-14 ($p < 0.001$) (Figure 4.2A). The drop in adhesion represented an inhibition of 86.4 %. However, the effect of y179 on the rolling flux fraction was different between the two parasites isolates. Inhibiting firm adhesion of P00-24 significantly increased the rolling flux fraction from 1.46 ± 0.77 to 6.02 ± 2.0 ($p < 0.05$) while the rolling of P99-14 did not appear to be affected (Figure 4.2B).

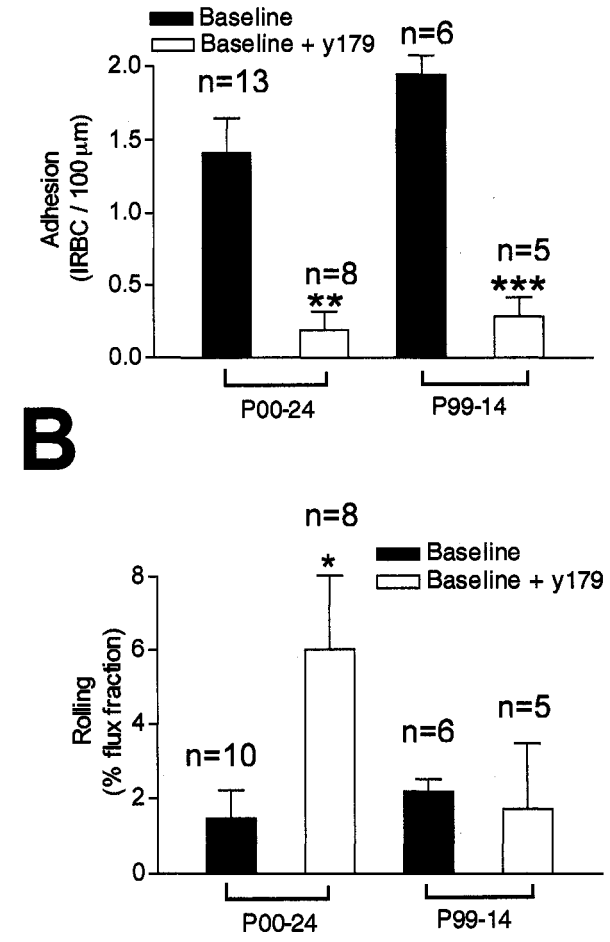

Figure 4.2. Inhibition of IRBC cytoadherence in human microvasculature by recombinant y179 in vivo. 2µM of y179 in a volume of 100µl was administered intravenously into the unstimulated SCID mice. The peptide was allowed to circulate for 10 minutes before IRBC were injected. A) Adhesion and B) Rolling. Data were obtained in seven animals using two different clinical parasite isolates.

Inhibition of IRBC cytoadherence in TNF-α-stimulated human microvasculature by recombinant y179 in vivo. The peptide y179 was next tested for its ability to inhibit cytoadherence within TNF-α stimulated microvasculature, simulating the clinical situation in severe falciparum malaria where there is a marked elevation of pro-inflammatory cytokines. Human TNF-α (100 ng in 50µl sterile PBS) was injected intradermally at the edge of the human skin graft and experiments were conducted 4 hours later. Compared to baseline values, y179 reduced adhesion dramatically from 2.0 ± 0.25 to 0.15 ± 0.05 IRBC/100 mm ($p < 0.001$) and 3.44 ± 0.4 to 0.63 ± 0.27 IRBC/100 mm ($p < 0.001$) for P00-24 and P99-14, respectively (Figure 4.3A). Thus pre-incubation with y179 inhibited the adhesion of parasite isolate P00-24 by 87.5 % and parasite isolate P99-14 by 81.7%. The reduction in adhesion was associated with a significant increase in the rolling flux fraction for both parasite isolates (Figure 4.3B).

Reversal of IRBC cytoadherence in human microvasculature by recombinant y179 in vivo. To determine if y179 was able to detach IRBC that were already adherent, a bolus of IRBC was allowed to circulate and adhere within the human microvasculature for 5 to10 minutes prior to the administration of 2µM y179. In untreated animals, the number of circulating IRBC gradually decreased over 15 to 20 min due to IRBC adhesion within the human microvasculature, as well as trapping in the mouse liver and spleen (Ho et al., unpublished observation). In animals treated with y179, an increase in the

number of circulating IRBC was repeatedly observed immediately following y179 administration. The number of adherent IRBC dropped from 1.4 ± 0.2 to 0.4 ± 0.2 IRBC/100 μm for P00-24 ($p < 0.01$) and from 2.0 ± 0.3 to 0.2 ± 0.2 IRBC/100 μm for P98-10 ($p < 0.01$), representing a 71.4% and a 90.0% reversal of cytoadherence respectively and an average reversal of 80.7% (Figure 4.4A). As IRBC became detached, the rolling flux fraction for P98-10 increased significantly ($p < 0.05$), indicating that the IRBC were still able to interact with the human microvessels but a stable firm adhesion could no longer be established.

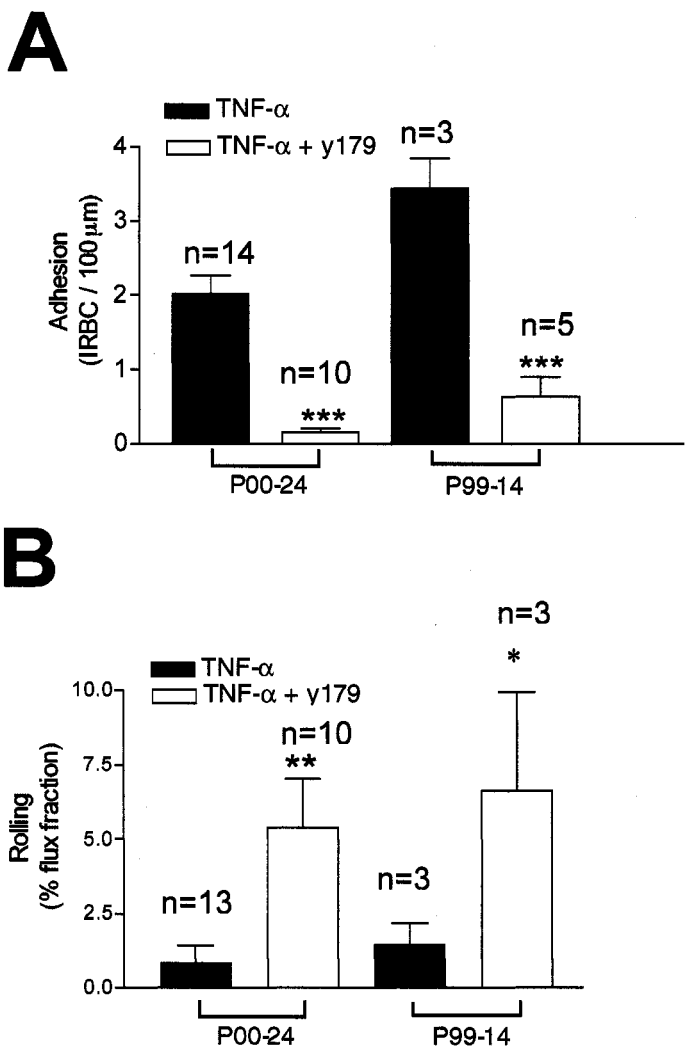

Figure 4.3. Inhibition of IRBC cytoadherence in TNF-α-stimulated human microvasculature by recombinant y179 in vivo. 2µM of y179 in a volume of 100µl was administered intravenously into TNF-α-stimulated (100ng / graft, 4h) SCID mice. The peptide was allowed to circulate for 10 minutes before IRBC were injected. A) Adhesion and B) Rolling. Data were collected in six animals using two different clinical parasite isolates.

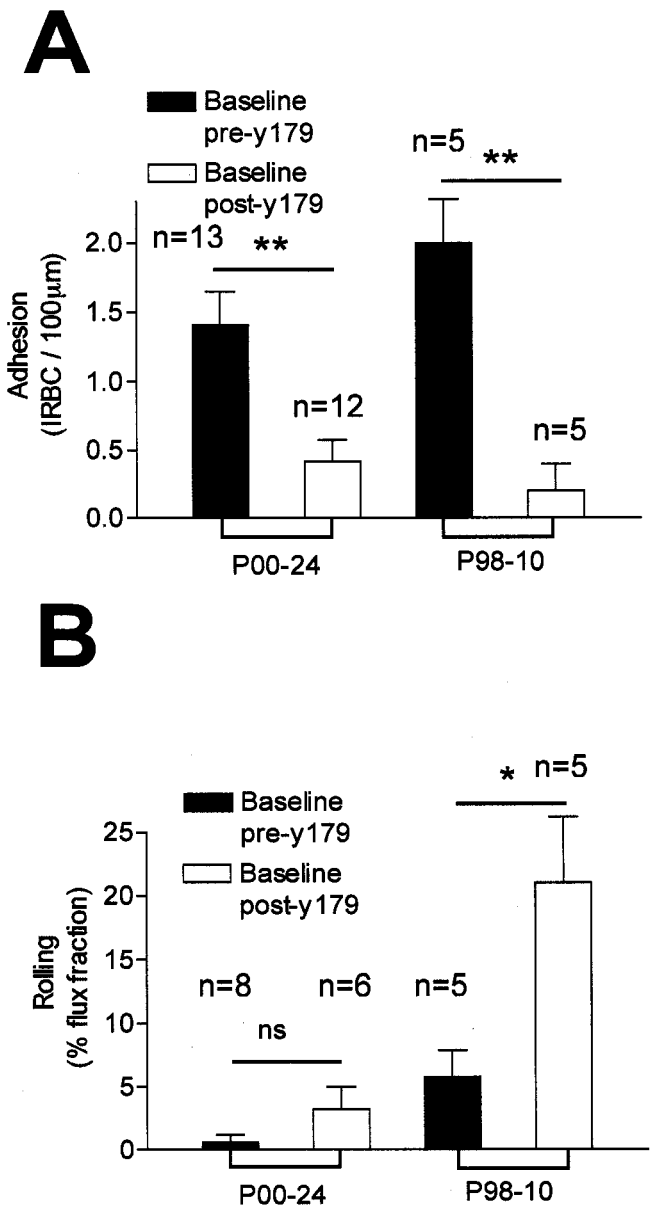

Figure 4.4. Reversal of IRBC cytoadherence in resting human microvasculature by recombinant y179 in vivo. IRBC were allowed to firmly adhere to human microvessels in unstimulated skin grafts for 5-10 minutes. 2µM of y179 was then administered i.v. A) Adhesion and B) Rolling. Data were collected from six mice using two different clinical parasite isolates.

Reversal of IRBC cytoadherence in TNF-α-stimulated human microvasculature by recombinant y179 in vivo. Reversal experiments were also conducted in TNF-α treated skin grafts. Adhesion of P94-59 was reversed from 2.4±0.7 to 0.6±0.2 IRBC/100 μm, P00-24 from 2.0±0.3 to 0.4±0.2 and P99-26 from 2.0±0.2 to 0.2±0.2, $p < 0.001$ (Figure 4.5A). These results represent a mean reversal of 81.6 %. The detachment of IRBC from the blood vessel wall was associated with an increase in the number of rolling cells, but this difference did not reach statistical significance (Figure 4.5B).

Videotaped images depicting the reversal of cytoadherence are shown in Figure 4.6. Panel A1 shows a human microvessel labeled with FITC-*Ulex europaeus* prior to the administration of either y179 or parasites. A2 and A3 were sequential images taken 20 seconds apart after IRBC injection. Numerous IRBC could be seen within the lumen of the human vessel. Adherent and slow rolling cells appeared round, while non-interacting and fast rolling cells appeared as streaks. The same microvessel was visualized 5 minutes after the administration of y179. Panels B1-3 show that all of the previously adherent IRBC had detached. A second bolus of IRBC was injected 25 minutes after y179 addition and the same vessel was observed. Panel C1-3 show the ability of y179 to inhibit the adhesion of newly administered IRBC, demonstrating that the reversal and inhibitory effect of y179 was not transient.

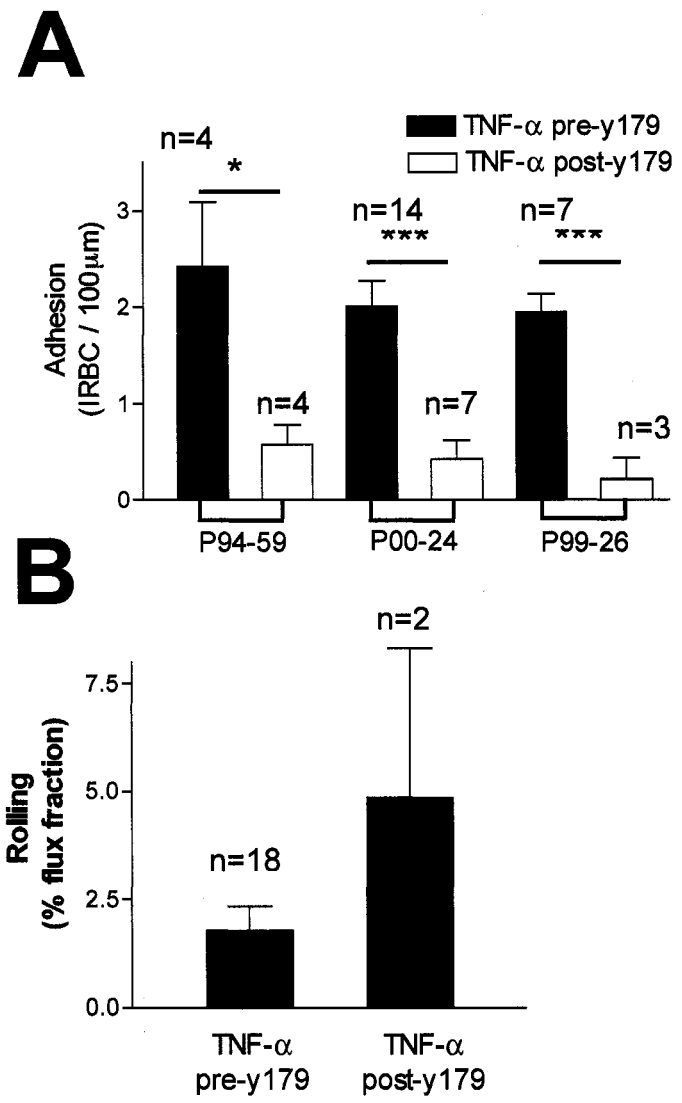

Figure 4.5. Reversal of IRBC cytoadherence in TNF-α-stimulated human microvasculature by recombinant y179 in vivo. IRBC were allowed to firmly adhere to TNF-α-stimulated skin grafts for 5-10minutes prior to the administration of 2μM y179 i.v. A) Adhesion and B) Rolling. Data were collected using three different clinical isolates in 7 animals.

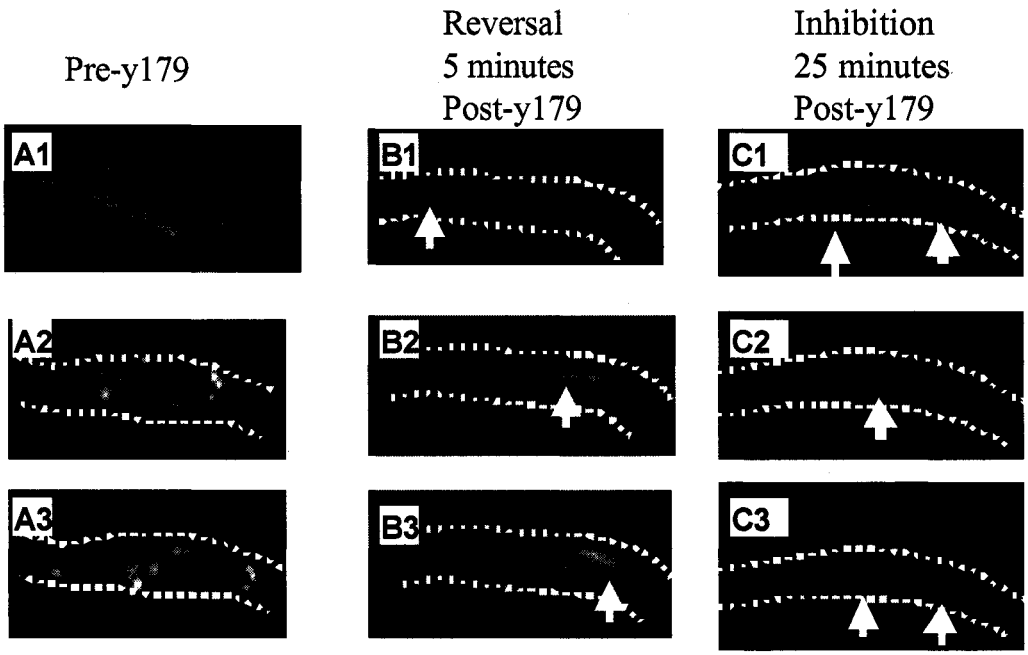

Figure 4.6. Visualization of reversal and inhibition of cytoadherence on TNF-α stimulated human microvasculature in vivo. Each frame in columns A to C was an image of the same microvessel taken at 20 sec intervals. A1) Microvessel labeled with *Ulex europaeus*-FITC prior to IRBC injection. A2-A3) Following IRBC injection, interacting and adherent parasites appeared as distinct bright circles while non-interacting IRBC appeared as streaks. B1-B3) 2μM of y179 was administered i.v. and the same microvessel was observed 5 minutes later. C1-C3) A second bolus of IRBC was administered 25 minutes after y179. No further adhesion of IRBC could be detected.

Lack of effect of anti-y179 antibodies on IRBC cytoadherence in vitro. Antibodies recognizing cross-reactive epitopes of the CIDR1 of MC PfEMP1 were also tested for their ability to inhibit cytoadherence of clinical parasite isolates to HDMEC in a flow chamber assay. 6A2-B1 and 4B3-A11, two mAb that are known to bind different regions within C1-2, a sub-region of CIDR1, were pre-incubated for 30 minutes with IRBC. Treated and untreated IRBC were then perfused over resting HDMEC monolayers. Importantly, neither mAb inhibited adhesion (Figure 4.7A) or rolling (Figure 4.7B) of any of the four clinical isolates tested. An anti- rC1-2 rat polyclonal antibody also had no effect on IRBC adhesion (Figure 4.7A) or rolling flux (Figure 4.7B). These experiments were performed on three clinical isolates that were inhibited by the y179 peptide.

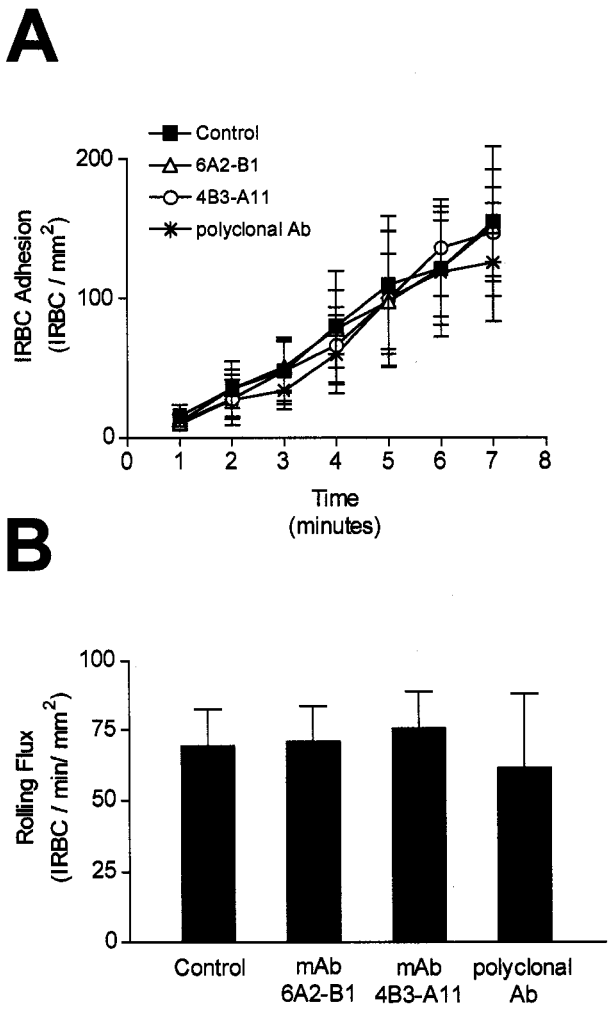

Figure 4.7. The effect of anti-y179 antibodies on IRBC cytoadherence in vitro. Two mAbs, either 6A2-B1 or 4B3-A11 or a rat anti-y179 polyclonal Ab were used to pre-treat IRBC cell suspensions. IRBC were perfused over the monolayers at 1dyne / cm ^{2}. A) Adhesion and B) Rolling. These experiments were performed with four different clinical parasite isolates.

4.2 Discussion.

Antimalarials are the mainstay of treatment for *P. falciparum* infections. However, for some patients this intervention may come too late to save their lives. This is particularly true for comatose patients and for those developing life-threatening syndromes before antimalarials become effective. The spread of drug resistant parasites increases the likelihood of such events and requires the development of novel adjunct therapies to rapidly halt the disease process. In the past few years, anti-cytokine therapy in the form of anti-TNF-α antibodies (170, 171) and pentoxifylline (172) that inhibits TNF-α production has been tried with limited clinical improvement. Exchange transfusion is used to correct hyperparasitemia (173), but this therapy is difficult to administer in developing countries and carries obvious risks in transmission of diseases.

With increasing understanding of the molecular mechanisms of cytoadherence, an alternative therapeutic modality for severe falciparum malaria might be anti-adhesive therapy. This type of therapy has been shown to be efficacious in inflammatory diseases such as rheumatoid arthritis in which the recruitment of lymphocytes to the synovium is successfully inhibited by anti-LFA-1 (174). Soluble ICAM-1 has also been used successfully to inhibit the binding of rhinovirus, the causative agent of the common cold, to nasal epithelium (175).

There is also precedent in the use of anti-adhesive therapy in the treatment of malaria in animal models. In Aotus and Saimiri monkeys infected with *P. falciparum,* passive transfer of hyperimmune sera resulted in parasite detachment and subsequent clearance by the spleen (176, 177). In addition, it

has been reported that soluble CSA was able to inhibit and reverse adhesion of CSA-adherent parasites in splenectomized Saimiri monkeys (178). However, the degree of detachment in these experiments was not established.

Among the various host receptors, adhesion to CD36 appears to be a vital component for parasite sequestration in microvasculature beds. With few exceptions, all non-placental parasites including those from cerebral malaria patients exhibit binding to CD36. This interaction is mediated by the M2 region of the CIDR1 domain of PfEMP1 (41). In this study, we show that a 179 amino acid peptide from the CIDR domain of *MCvar1* PfEMP1 inhibited and reversed the adhesion of IRBC from multiple clinical parasite isolates to HDMEC under flow conditions in vitro, and to human microvessels in skin grafts on SCID mice in vivo. This is the first demonstration that cytoadherence of diverse wild type parasite strains on a physiological substratum can be inhibited by a single parasite protein under shear stress. On HDMEC monolayers in vitro, the peptide was effective in inhibiting IRBC adhesion on resting endothelium, and acted synergistically with an anti-ICAM-1 antibody on endothelium that had been stimulated with TNF-α, which results in an augmentation of ICAM-1 expression. These results are similar to our previous observations using OKM5, the mAb against CD36 (9). In human microvessels, y179 alone was able to inhibit approximately 80 to 85 % of the adhesion under both resting and stimulated conditions. This finding suggests that the interaction between IRBC and ICAM-1 might play a more minor role in cytoadherence under the higher shear stress in vivo. The inhibition of adhesion was associated to a variable degree with an

increase in rolling flux fraction, which suggests that y179 specifically affects stationary binding to CD36 but not the interaction with other host receptors involved with IRBC rolling. Indeed, large numbers of IRBC were observed to remain circulating while they generally disappeared from the circulation within 15 to 20 minutes in control animals.

The inhibitory effect of y179 lasted for the duration of the experiments that was at least 30 to 40 minutes. Thus, y179 is stable in vivo (at least when bound to CD36) for a significant length of time, an important factor for a potential therapeutic agent. More striking was the observation that y179 could rapidly detach already adherent IRBC in vivo, suggesting that the peptide can have both a preventive and curative role in relation to cytoadherence. No further IRBC adhesion occurred once they were displaced, even when a second bolus of IRBC was administered after the peptide. The rapid reversal within 5 minutes was different from previous results from an in vitro flow chamber assay in which perfusion of recombinant peptide for over two hours was needed for reversal (44). We believe that the human microvasculature in the human/SCID mouse chimera used in this study represents a much more physiological model for cytoadherence under flow than immobilized CD36 protein in a flow chamber.

In contrast to the anti-adhesive effect of the peptide, mAbs and a polyclonal antibody against y179 did not have any effect on rolling or adhesion of clinical isolates to microvascular endothelial cells under flow conditions, although they inhibited the adhesion of the homologous strain (MC) to purified CD36 in a static binding assay (45). These antibodies have also been shown to agglutinate

IRBC from various parasite clones and lines expressing different PfEMP1 variants (45). Collectively, the observations suggest that the antibodies recognize cross-reactive epitopes on y179 that are not directly involved in CD36 binding, but appears to be immunodominant in eliciting an antibody response.

We recognize that even the human/SCID mouse model has its limitations. Reversal of adhesion was substantial but never complete, and may not be sufficient for altering the course of disease progression. In addition, questions remain of the importance of CD36 binding in adhesion to cerebral microvascular endothelium that expresses very little CD36 by immunohistochemical staining. However, a distinction must be made between the inability to detect surface expression using relative insensitive methods such as immunohistochemistry, and the absence of function. It is well established that surface expression of P-selectin on endothelial cells is notoriously difficult to demonstrate (105), and yet its critical role in leukocyte recruitment is indisputable (103).

In conclusion, we demonstrated that it is possible to inhibit and reverse parasite sequestration with a small functional peptide from PfEMP1. The peptide has a universal effect on all parasite isolates tested. The finding strongly suggests that anti-adhesive therapy based on y179 is feasible and will offer a therapeutic intervention with immediate effect.

CHAPTER 5

IRBC FIRM ADHESION IS DEPENDENT ON A PfEMP1-CD36 INDUCED SRC-FAMILY KINASE ACTIVATION AND REQUIRES AN ECTO-ALKALINE PHOSPHATASE

Specific aim 3: To investigate if adhesion of IRBC to CD36 activates intracellular signaling pathways within endothelium that may play a role in modulating subsequent parasite-host cell interactions.

Objective 1: To characterize the CD36-dependent signaling in HDMEC.

Objective 2: To determine if PfEMP1 can directly initiate an intracellular signal in HDMEC.

Objective 3: To determine the consequences of the PfEMP1 induced-CD36 cell signaling to subsequent cytoadherence.

Objective 4: To determine the mechanisms by which CD36 signaling increases IRBC firm adhesion to HDMEC.

5.1 Results.

CD36 Can Activate the ERK 1/2 Pathway Through Direct Interaction with PfEMP1.

We first used an antibody crosslinking approach to determine the signaling pathways that might be elicited by IRBC in human microvascular endothelial cells. OKM5, an anti-CD36 mAb that inhibits IRBC adhesion was used as the primary antibody and was crosslinked with a goat anti-mouse $F(ab')_2$. Western blot analysis clearly shows that crosslinking CD36 with both antibodies resulted in a significant increase in total tyrosine phosphorylated proteins, demonstrating that cell signaling pathways are activated (Figure 5.1A). Further analysis with

phospho-specific anti-MAPK antibodies reveal that ERK 1/2 is one of the pathways that becomes activated downstream of crosslinked CD36 (Figure 5.1B). However, antibody crosslinking is an artificial means of inducing a signal and may not reflect what happens when PfEMP1 binds CD36. In order to directly determine if PfEMP1-CD36 interaction results in a cell signal in endothelium, we used y179, the minimal CD36 binding region of PfEMP1. Endothelial monolayers were treated with the recombinant peptide at 2μM for 15 minutes at 37°C. The y179-CD36 interaction resulted in phosphorylation of ERK 1/2 to the same degree as crosslinking CD36 (Figure 5.2). Kinetic studies of the y179-induced signal further revealed that ERK 1/2 phosphorylation was a transient event that reached a maximum within 15 minutes of interaction (Figure 5.3) and could be detected as early as after the first 5 minutes.

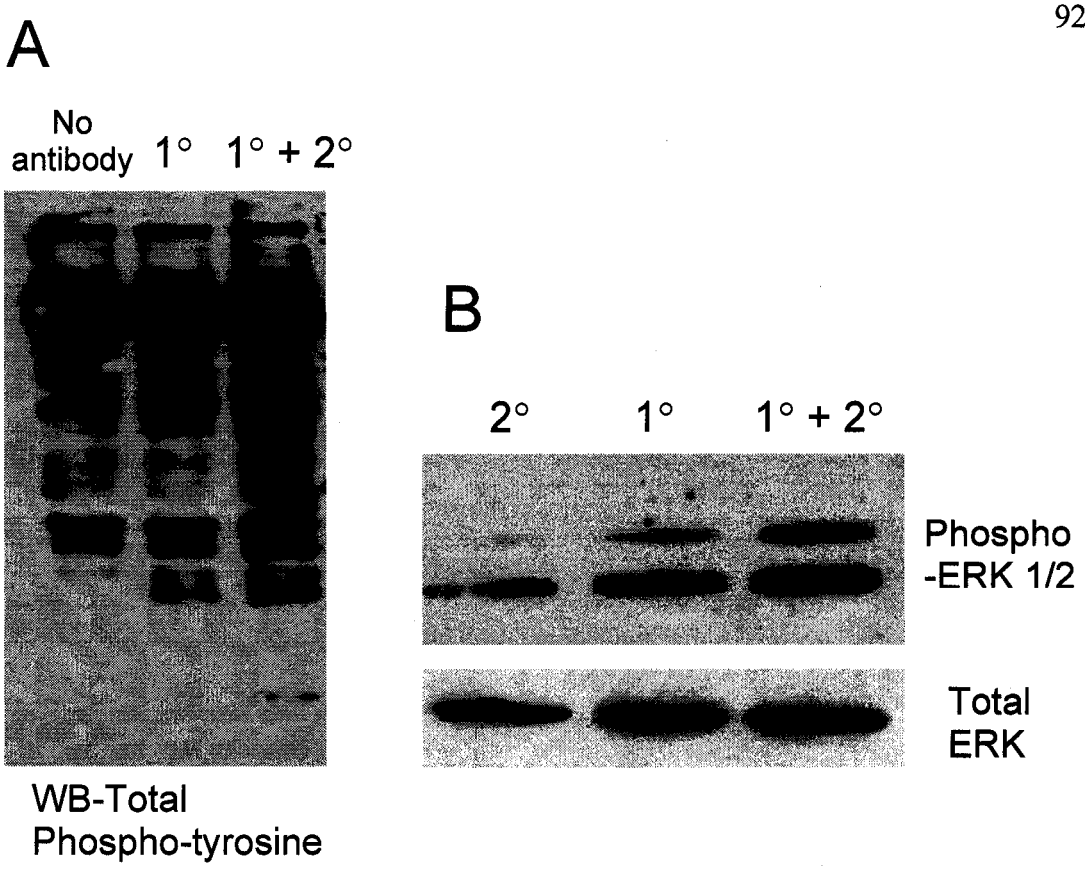

Figure 5.1. Antibody crosslinking CD36 results in the activation of cell signaling pathways. Confluent HDMEC monolayers were incubated with either the anti-CD36 1° mAb (OKM5) or a 2° Ab (goat anti-mouse $F(ab')_2$) or both. Western blots were performed on whole cell lysates and probed for A) total tyrosine phosphorylation or B) activated ERK 1/2 (phospho-ERK 1/2) or re-probed for total ERK as the loading control.

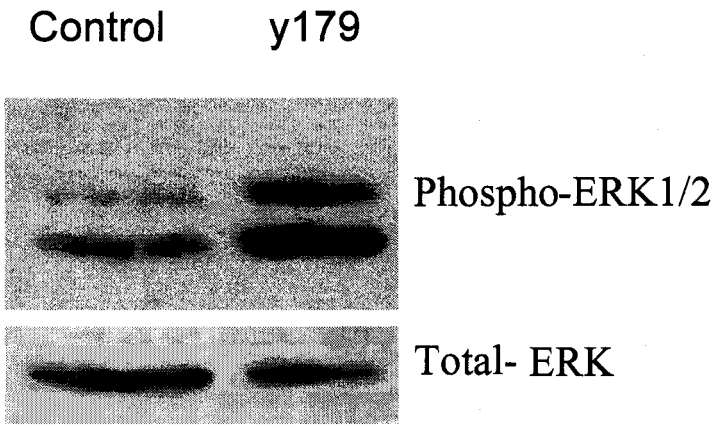

Figure 5.2. The recombinant peptide y179 activates the ERK 1/2 pathway in HDMEC. Confluent HDMEC monolayers were treated with 2μM y179 for 15 minutes. Western blots were performed on whole cell lysates and probed for activated ERK 1/2 (phospho-ERK 1/2) or re-probed for total ERK as the loading control.

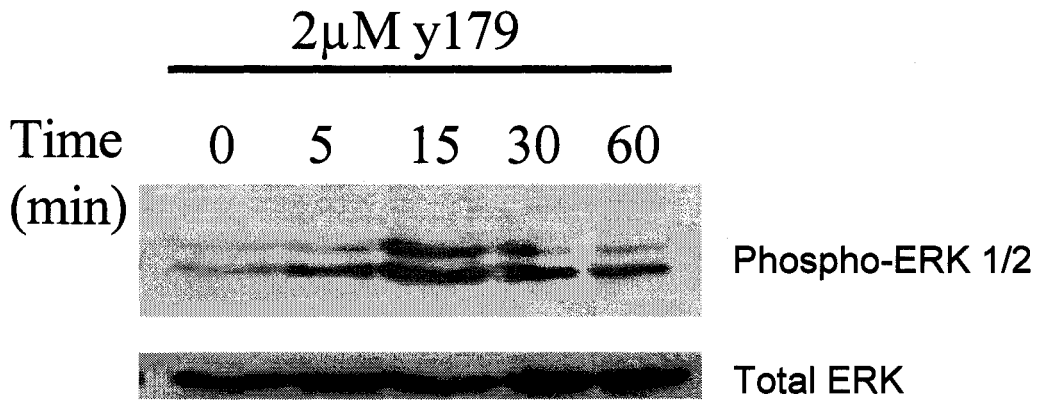

Figure 5.3. Time course of the effect of y179 on ERK 1/2 activation. Confluent HDMEC monolayers were treated with 2μM y179 for between 0-60 minutes. Western blots were performed on whole cell lysates and probed for activated ERK 1/2 (phospho-ERK 1/2) or re-probed for total ERK as the loading control

Inhibition of Erk1/2 Activation Does Not Affect IRBC Cytoadherence.

To determine what consequence, if any, PfEMP1 induced MAP-kinase activation has on cytoadherence, we pretreated confluent HDMEC monolayers with either PD098059 (25μM, 30minutes) or U0126 (10μM, 30 minutes), both specific inhibitors of the ERK 1/2 MAPK pathway. IRBC suspensions were perfused over the monolayers and adhesion was visualized using a parallel plate flow chamber assay. The inhibitors did not affect the rolling (Figure 5.4A) or the adhesion (Figure 5.4B) of four different parasite isolates on HDMEC. As the p38 MAPK is activated through CD36 in monocytes (74) and by thrombospondin-1 (TSP-1) interaction with CD36 on HDMEC (60), the functional effect of two p38 MAPK pathway inhibitors, SB 203580 and SKF 86002, on IRBC rolling and adhesion was also studied. Inhibiting the p38 pathway had no affect on IRBC rolling (Figure 5.5A) and adhesion (Figure 5.5B)(n = 3 for each inhibitor). As redundancy or crosstalk may exist for the MAPK pathways we combined the ERK 1/2 (U0126) and p38 (SB203580) inhibitors using identical concentrations and conditions as in the previous experiments. There was no effect on IRBC rolling (Figure 5.6A) and adherence (Figure 5.6B) in ERK 1/2, p38 inactive endothelium (n = 3).

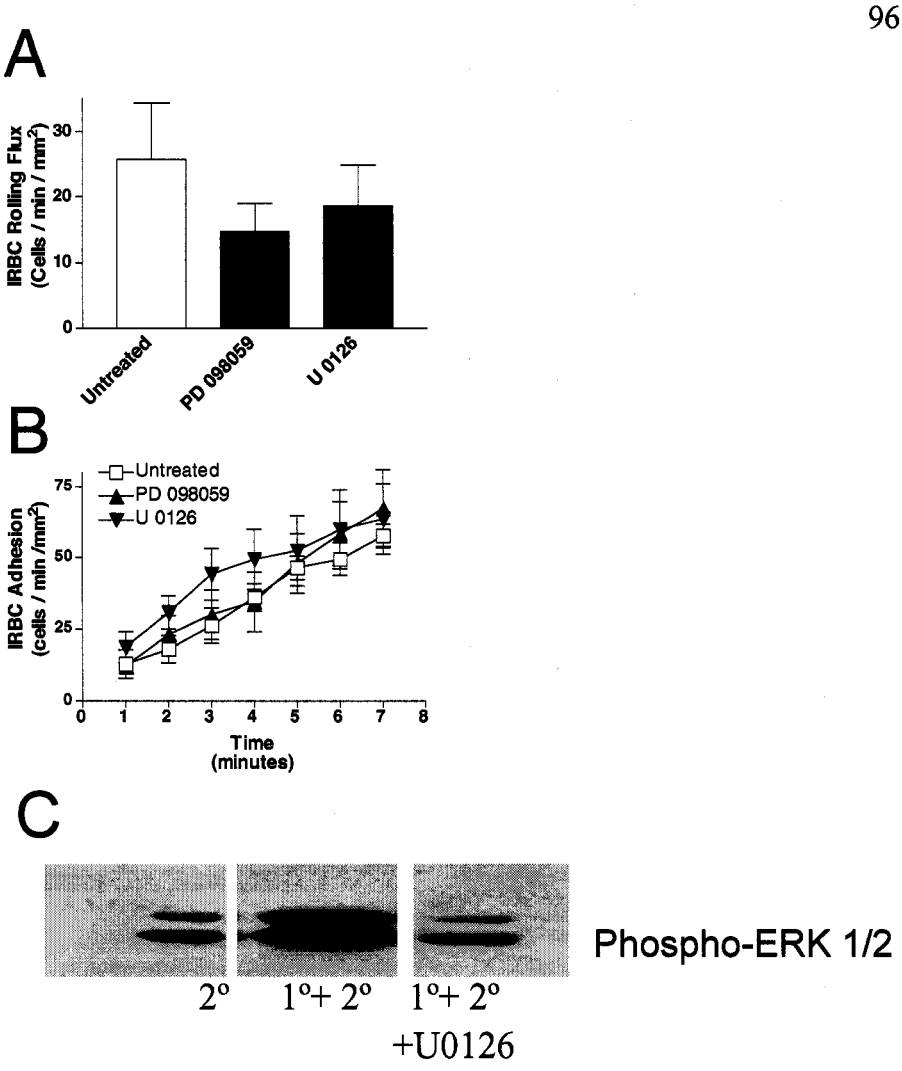

Figure 5.4. The effect of ERK 1/2 inhibitors on cytoadherence. Confluent HDMEC monolayers were pre-treated with either PD098059 (25μM, 30 min) or U0126 (10μM, 30min). IRBC suspensions were perfused through the flow chamber at 1 dyne / cm^2 and A) rolling and B) adhesion was determined. These experiments were performed four times with four different clinical parasite isolates. C) Western blot analysis of crosslinked CD36 demonstrates that the U0126 effectively inhibited ERK1/2 activation.

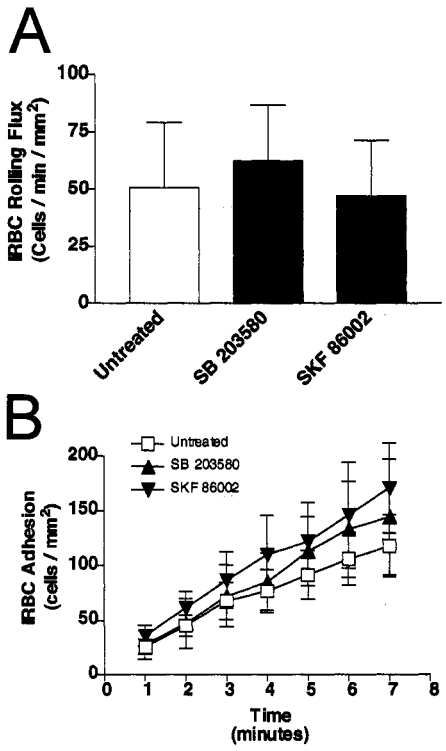

Figure 5.5. The effect of p38 inhibitors on cytoadherence. Confluent HDMEC monolayers were pre-treated with either SB 203580 (10μM, 30 min) or SKF 86002 (10μM, 30min) and IRBC suspensions were perfused through the flow chamber at 1 dyne / cm^2. These experiments were repeated three times.

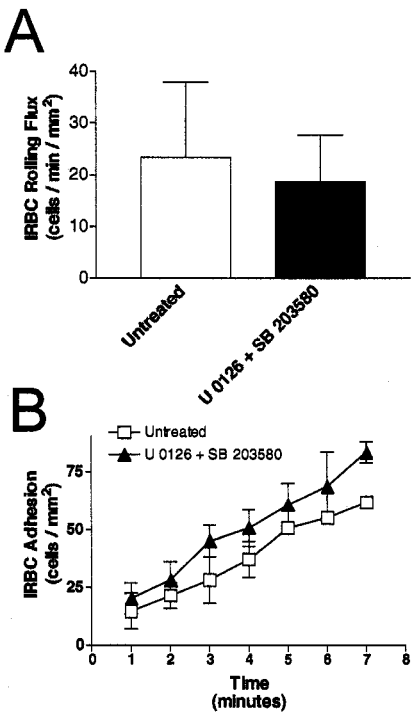

Figure 5.6. The combined effect of the ERK 1/2 and p38 inhibitors on IRBC cytoadherence. Confluent HDMEC monolayers were pre-treated with both SB 203580 (10μM, 30 min) and U0126 (10μM, 30min) and IRBC suspensions were perfused through the flow chamber at 1 dyne / cm^2. These experiments were repeated three times.

Erk1/2 Activation is Dependent on Src-family Kinase Activity.

CD36 co-localizes with a number of Src-family kinases in endothelial caveolae. The physical proximity suggests that ERK 1/2 activation may be a downstream result of src-kinase activity. Confluent endothelial monolayers were pretreated for 30 minutes with 10μM PP1, a specific Src-family kinase inhibitor. ERK 1/2 activation due to y179 stimulation was significantly reduced in Src-family kinase inactive cells (Figure 5.7).

Firm Adhesion of IRBC to Microvascular Endothelium is Src-family Kinase Dependent.

To determine the functional consequences for Src-family kinase activation in HDMEC, we pretreated HDMEC monolayers with various concentrations of the Src-family kinase inhibitor PP1. Using the flow chamber assay, IRBC rolling flux was seen to be decreased significantly at 10μM PP1 from 15.4±2.5 to 9.0±0.8 IRBC / min / mm^2 a change of 41.6% ($p < 0.05$) (Figure 5.8). Lower concentrations of the inhibitor had no effect on IRBC rolling flux. Firm adhesion was decreased in a dose dependent manner, with 5μM inhibiting adhesion from 155.9±54 in untreated cells to 98.7±37.7 IRBC / mm^2 in treated cells, a 36.7% reduction ($p < 0.05$)(Figure 5.9B). 10μM of PP1 inhibited adhesion by 72.4%, a decrease from 107.0±18.7 to 29.5±6.3 IRBC / mm^2 ($p < 0.001$) (Figure 5.9C). The inactive analogue PP3 had no effect on either rolling or adhesion (Figure 5.9D) indicating the effect is specific to Src-family kinase inactivation. These results include six parasite isolates and multiple HDMEC preparations. Flow

cytometry was used to exclude the possibility that the reduction in adhesion was due to a change in the level of CD36 expression. PP1 did not affect the percentage of CD36 positive endothelium or the mean fluorescence intensity (Figure 5.10).

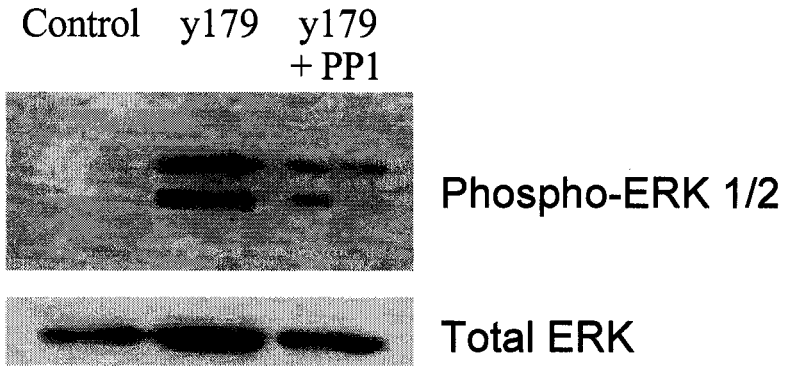

Figure 5.7. The effect of the Src-family kinase inhibitor PP1 on ERK 1/2 activation. Confluent HDMEC monolayers were treated with 2μM y179 for 15 minutes. Western blots were performed on whole cell lysates and probed for activated ERK 1/2 (phospho-ERK 1/2) or total ERK 1/2 as the loading control.

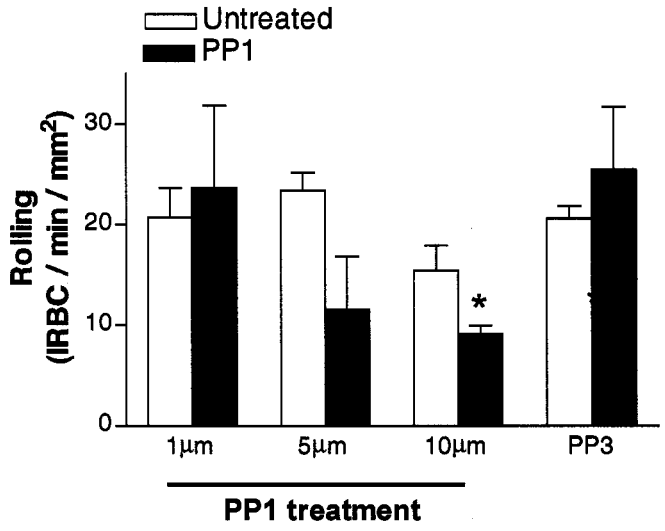

Figure 5.8 The effect of the Src-family kinase inhibitor PP1 on IRBC rolling under flow conditions. Confluent HDMEC monolayers were pre-treated with 1, 5 or 10µM of PP1 or 10µM PP3 (the inactive analogue) for 30 minutes. IRBC suspensions were perfused at 1 dyne / cm^2. These experiments were repeated 3 times for 1, 5µM PP1 and 10µM PP3, and 6 times for PP1 10µM.

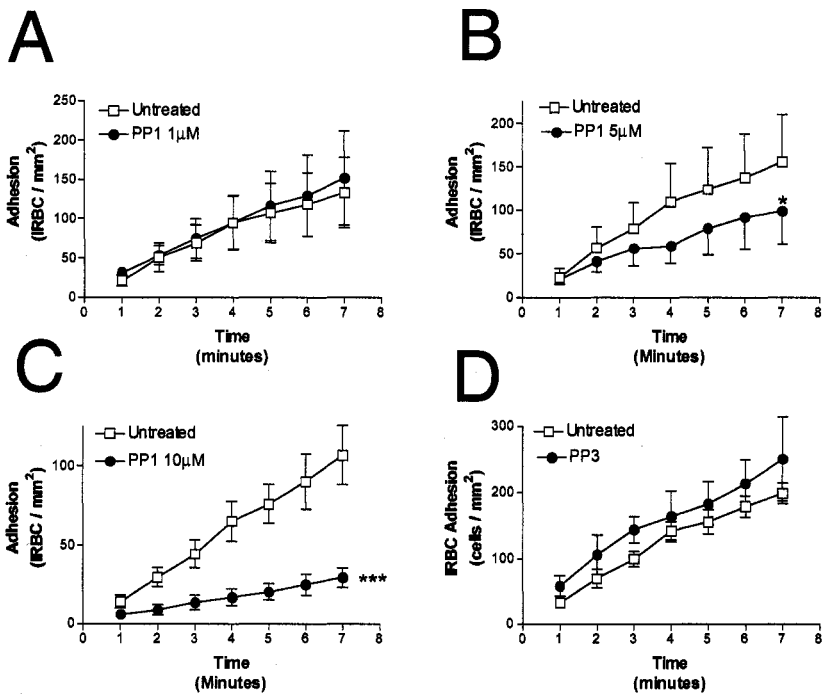

Figure 5.9. The effect of the Src-family kinase inhibitor PP1 on IRBC adhesion under flow conditions. Confluent HDMEC monolayers were pre-treated with 1, 5 or 10μM of PP1 or 10μM PP3 (the inactive analogue) for 30 minutes. IRBC suspensions were perfused at 1 dyne / cm^2. These experiments were repeated 3 times for 1, 5μM PP1 and 10μM PP3, and 6 times for PP1 10μM.

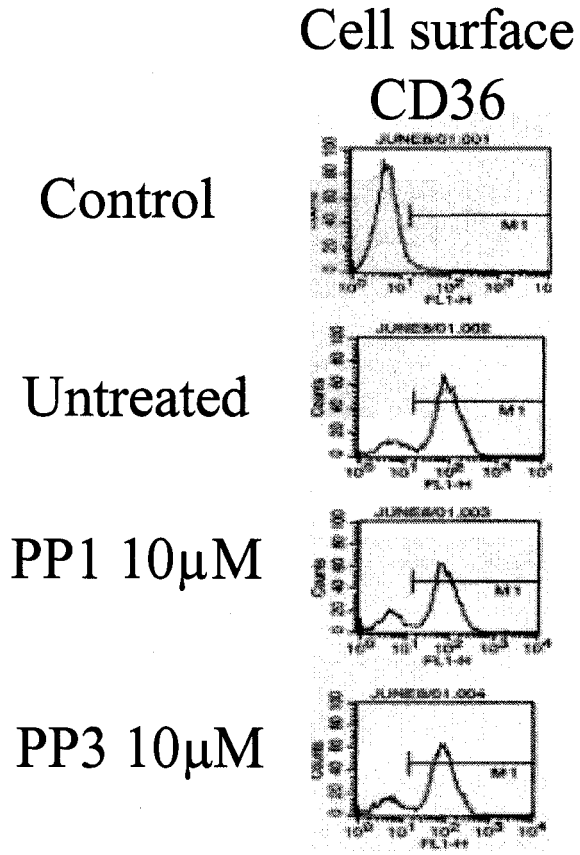

Figure 5.10. The effect of the Src-family kinase inhibitor PP1 on CD36 cell surface expression. Confluent HDMEC monolayers were pre-treated with either PP1 (10μM, 30min) or with the inactive analogue PP3 (10μM, 30 min) and then analyzed using flow cytometry.

We extended the previous *in vitro* findings by examining the role of src-kinase activity on adhesion *in vivo* using our human-SCID mouse model of intact human microvasculature. Grafted animals were either untreated or pretreated with either PP1 (1.5mg/kg, 1 hour) or PP3 (1.5mg/kg, 1 hour). This dose of inhibitor was used in a study to examine the protective effect of PP1 against cerebral infarct following an experimentally induced stroke (179). We found that PP1 had no effect on the percentage of rolling cells compared to untreated animals (Figure 5.11A). However, Src-family kinase inactivation did decrease IRBC adhesion from 1.9±0.1 to 0.6±0.1 IRBC / 100μm, a significant change of 68.4% ($p < 0.001$). The inactive analogue PP3 had no effect on adhesion (Figure 5.11B). In pilot experiments, no changes in shear rate, red blood cell velocity, vessel diameter, leukocyte rolling flux, leukocyte adhesion and emigration were observed in C57BL/6 mice treated with PP1.

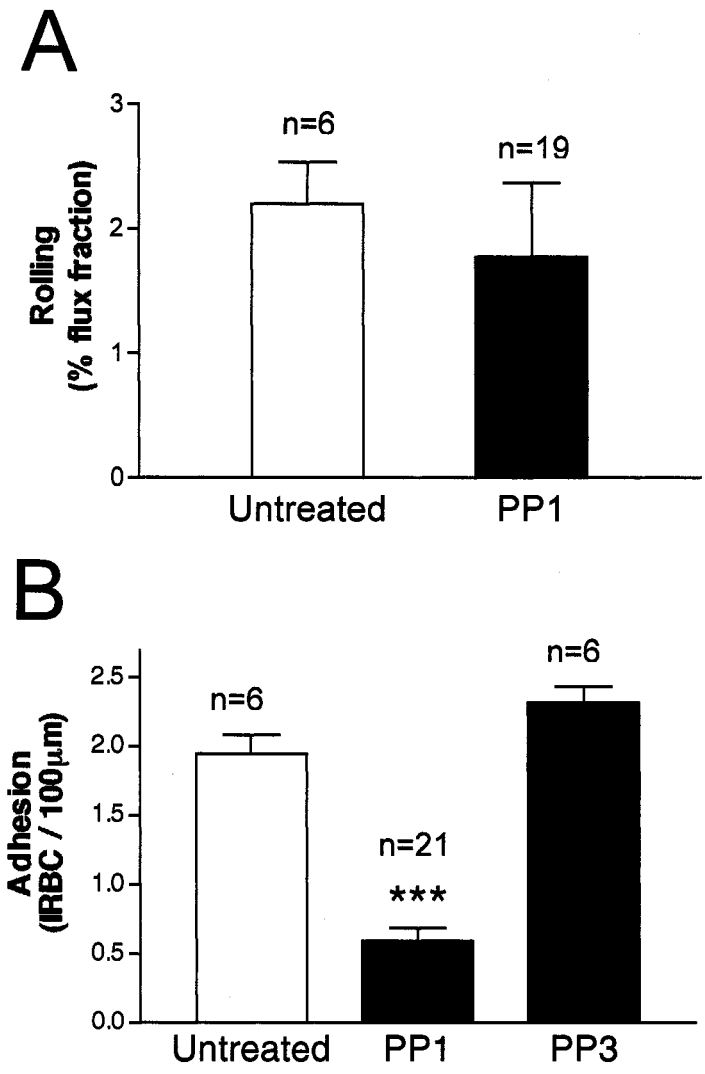

Figure 5.11. The effect of the Src-family kinase inhibitor PP1 on IRBC cytoadherence in vivo. Grafted SCID mice were treated with PP1 or PP3 (1.5mg/kg, 1h, i.p.) and the skin graft was exposed for direct visualization of the human microvasculature using intravital microscopy. Baseline data was obtained from untreated animals. The data are from one clinical parasite isolate used in 5 animals.

IRBC cytoadherence is modulated by either an intra- or extracellular protein phosphatase.

To explain how the inhibition of intracellular cell signaling could affect extracellular firm adhesion without changing the level of CD36 expression, a mechanism involving modulation of the CD36 ectodomain via an ecto-alkaline phosphatase was investigated. To assess the possibility that a phosphatase was involved in the modulation of IRBC binding to CD36, as reported for adhesion of TSP-1 to platelet CD36 (71), a broad specificity inhibitor of protein phosphatases was used to pre-treat endothelial monolayers. Sodium orthovanadate (SOV) is a potent inhibitor of multiple families of phosphatases. Endothelial monolayers were pretreated for 30 minutes with 5 and 25μM of SOV and a 1:1 ratio of sodium phosphate (NaH_2PO_4) to balance the changes in pH due to the SOV alone. IRBC rolling was significantly decreased from 52.5±16.2 to 12.4±6.1 IRBC / min / mm^2 at 25μM ($p < 0.05$) but was not significantly affected with 5μM SOV (Figure 5.12). Adhesion, however was significantly inhibited at both doses, but was more profound at 25μM. Phosphatase inhibition reduced adhesion from 74.3±9.0 to 41.6±12.4 IRBC / mm^2 for 5μM SOV ($p < 0.05$) and was further reduced to 12.4±2.7 IRBC / mm^2 with 25μM SOV ($p < 0.01$), an overall 83.3% decrease (Figure 5.13A and B). Clearly a phosphatase is involved in the firm adhesion process however, SOV is a small soluble molecule that is capable of crossing the outer cell membrane thereby inhibiting both extracellular and intracellular protein phosphatases. In fact, the SOV may be acting to block the CD36 signaling pathway by inhibiting the src-kinase family, similar to the effects

of PP1. Src-family kinases require dephosphorylation in order to become activated, so it is possible that the effect of SOV is at the level of src-kinase activation. SOV did not affect the level of CD36 on the endothelial cell surface when assayed by flow cytometry (data not shown). These experiments provided good evidence of the involvement of a phosphatase, but did not provide any insight regarding its location, site of activity or mechanism.

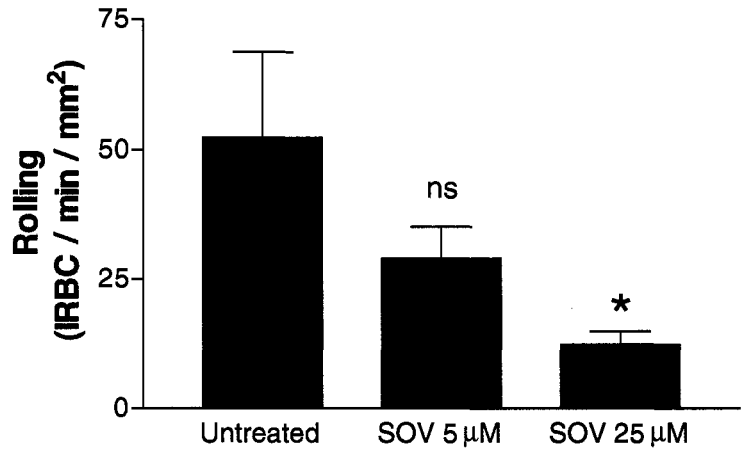

Figure 5.12. The effect of inhibiting phosphatase activity with SOV on IRBC rolling under flow. Confluent HDMEC monolayers were pre-treated with 5 or 25 µM of SOV for 30 minutes. IRBC cell suspensions were perfused at 1 dyne / cm^2. These experiments were repeated three times with three different clinical parasite isolates.

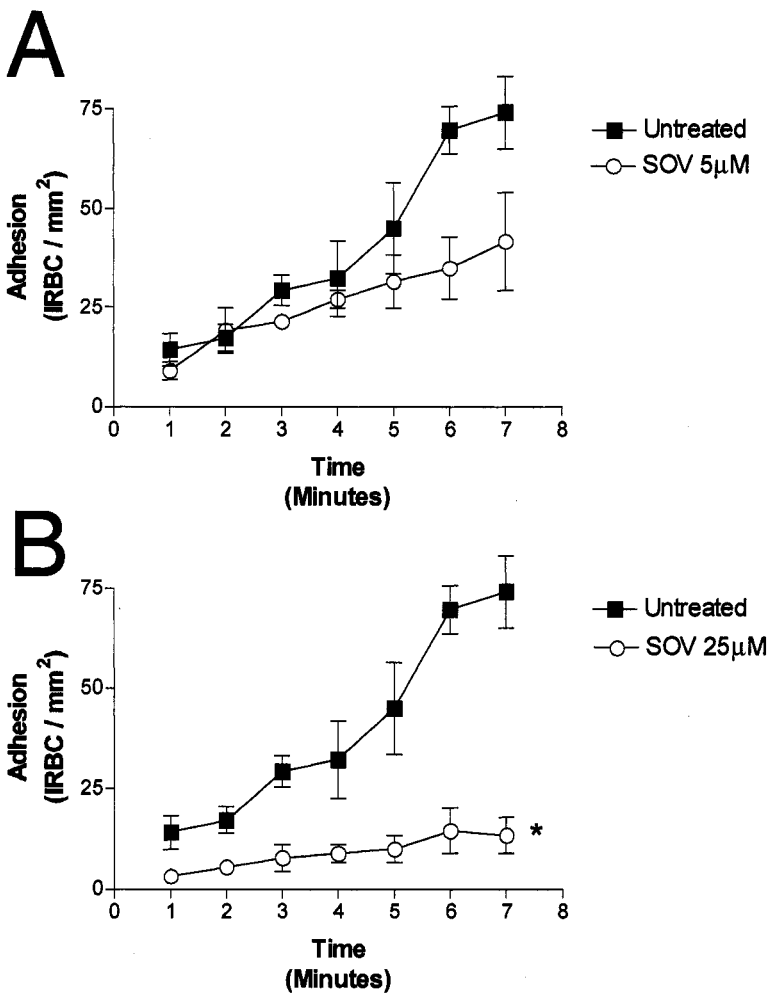

Figure 5.13 The effect of inhibiting phosphatase activity with SOV on IRBC adhesion under flow. Confluent HDMEC monolayers were pre-treated with 5 or 25 μM of SOV for 30 minutes. IRBC cell suspensions were perfused at 1 dyne / cm^2. These experiments were repeated three times with three different clinical parasite isolates.

Exogenous AP Completely Restores Adhesion in Src-kinase inactive HDMEC.

To more directly test the requirement for an ecto-phosphatase in IRBC firm adhesion we treated the HDMEC with exogenous AP (200U/ml) for 30 minutes at 37°C. AP is a large protein enzyme that would not be able to cross the endothelial plasma membrane and should therefore only affect cell surface proteins. Based on the model of low affinity (CD36-phosphorylated) and high affinity (CD36-dephosphorylated) CD36 demonstrated for TSP-1-CD36 interaction, we expected that treatment of HDMEC with additional exogenous AP would result in increased adhesion. However, the addition of AP did not result in any change in rolling (Figure 5.14) or adhesion (Figure 5.15A).

We repeated the Src-family kinase inhibition studies with PP1 to determine if exogenous AP could reverse the inhibitory effects of src-kinase inactivation. PP1 (10μM) treatment slightly decreased the rolling flux (Figure 5.14) and significantly decreased IRBC adhesion (Figure 5.15B) similar to the effects observed in figures 5.7 and 5.8 respectively. Src-family kinase inactive cells were then treated with exogenous AP (200U/ml, 30 minutes at 37°C) and rolling and adhesion was quantitated. Rolling flux was unchanged in PP1 + AP treated cells compared to untreated cells (Figure 5.14). PP1 treatment lowered adhesion 58.7% from 128.3±20.6 to 53.0±20.2 IRBC / mm^2 ($p < 0.01$), but the level of adhesion was restored to normal levels (180.4±56.5/ mm^2) in PP1 + AP treated cells ($p < 0.001$ compared to PP1 alone) (Figure 5.15C). This result demonstrates a link between the intracellular signal transduced from CD36 after

PfEMP1 engagement and an ectodomain alkaline phosphatase in modulating IRBC firm adhesion to endothelium.

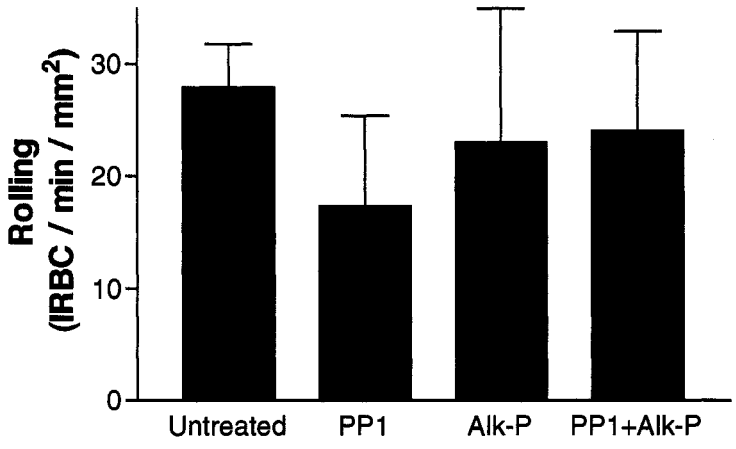

Figure 5.14. The effect of exogenous AP on IRBC rolling under flow. Confluent HDMEC monolayers were treated with exogenous AP (200U /ml, 30 min) and IRBC suspensions were perfused at 1 dyne / cm^2. In some experiments HDMEC were treated with the src-kinase inhibitor PP1 (10μM, 30min) before AP addition. These experiments were repeated five times using three different clinical parasite isolates.

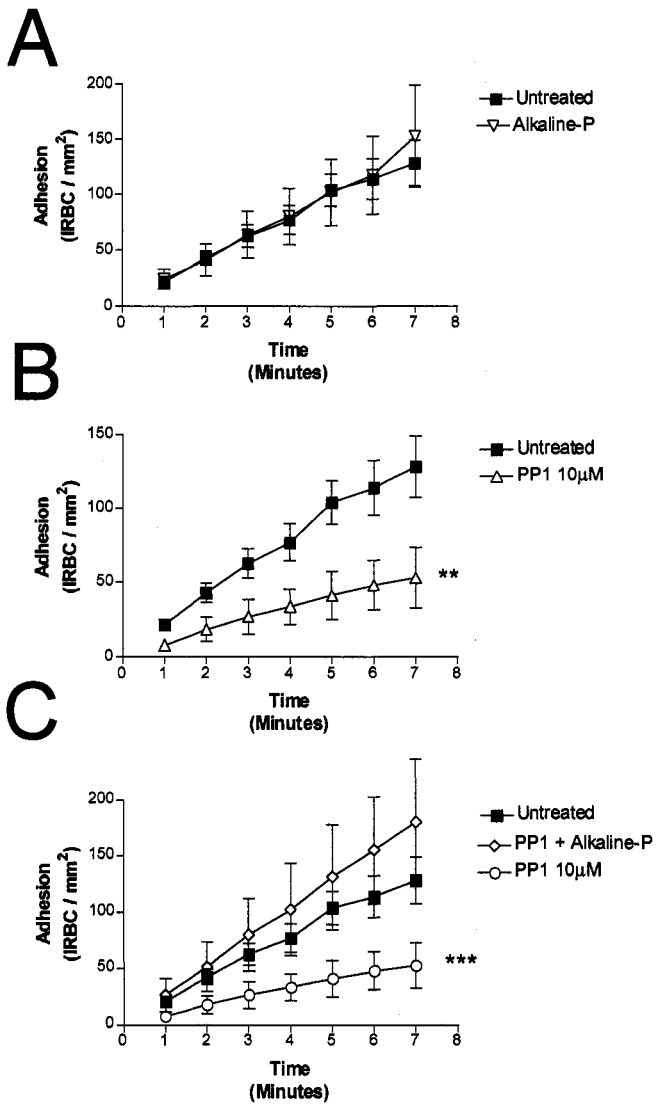

Figure 5.15. The effect of exogenous AP on IRBC adhesion under flow. Confluent HDMEC monolayers were treated with exogenous AP (200U /ml, 30 min) and IRBC suspensions were perfused at 1 dyne / cm^2. In some experiments HDMEC were treated with the Src-family kinase inhibitor PP1 (10μM, 30min) before AP addition. These experiments were repeated five times using three different clinical parasite isolates.

Levamisole, an alkaline phosphatase specific inhibitor decreases firm adhesion of IRBC to HDMEC.

A role for alkaline phosphatase in cytoadherence was directly investigated by using levamisole, a specific AP inhibitor. Levamisole is a licensed pharmaceutical drug that inhibits purified and cell bound AP at physiological pH, without inhibiting the phosphatase activity of any other known membrane enzymes. Confluent HDMEC monolayers were pretreated with levamisole (100μM-1mM) for 30 minutes at 37°C. Rolling flux showed a trend towards increased rolling in the presence of increased concentrations of the AP inhibitor with 1mM levamisole increasing rolling from 18.2±5.2 to 30.0±6.2 IRBC / min /mm^2 (Figure 5.16). Adhesion was significantly decreased from 119.9±24.8 to 58.1±17.2 IRBC / mm^2, a 51.0% reduction ($p < 0.05$) with 500μM (Figure 5.17B) and from 137.3±13.9 to 67.7±9.0 IRBC / mm^2, a 51.0% ($p < 0.05$) reduction with 1mM (Figure 5.17C) concentrations of levamisole, but was unaffected with the 100μM dose (Figure 5.17A).

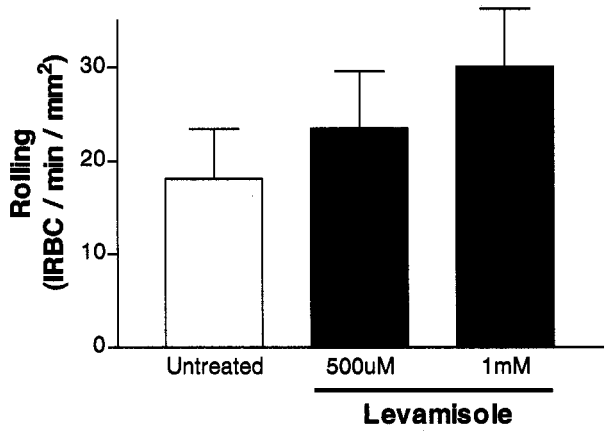

Figure 5.16. The effect of the specific AP inhibitor, levamisole on IRBC rolling under flow. Confluent HDMEC monolayers were treated with either 500μM or 1mM levamisole (30 min) and IRBC suspensions were perfused at 1 dyne / cm^2. These experiments were repeated five times using five different clinical parasite isolates.

.

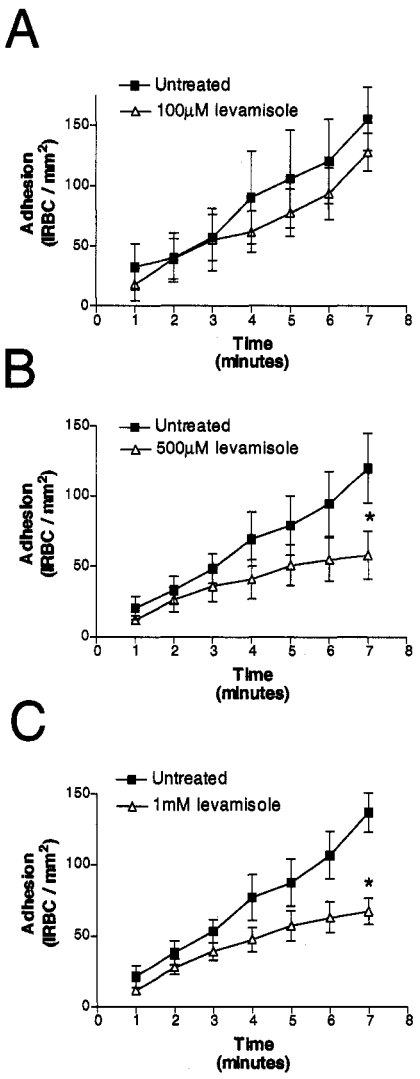

Figure 5.17. The effect of the specific AP inhibitor, levamisole on IRBC adhesion under flow. Confluent HDMEC monolayers were treated with 100μM, 500μM or 1mM levamisole (30 min) and IRBC suspensions were perfused at 1 dyne / cm^2. These experiments were repeated five times using five different clinical parasite isolates.

5.2 Discussion

In current models of cytoadherence, whether in vitro or in vivo, endothelial adhesion molecules are viewed as mere points of attachment for IRBC, with the endothelium acting as an inactive substratum. The possibility that endothelial cells may play a more dynamic role in the cytoadherence cascade has not been explored. In this study, we tested the hypothesis that IRBC adhesion to the endothelial molecule CD36 represents a true ligand-receptor interaction, resulting in cellular consequences capable of modulating the adhesion process. Our current data support a novel model of cytoadherence involving outside-in and inside-out signaling mechanisms. This model proposes that the initial attachment of IRBC to CD36 under flow conditions triggers a Src-family kinase dependent intracellular signal (outside-in) that is responsible for increasing subsequent firm adhesion to CD36 by means of an ecto-AP (inside-out) (Figure 5.18)

Several lines of evidence in the literature suggest that IRBC signaling via CD36 might be a possibility. IRBC adhesion to CD36 on monocytes induces a respiratory burst (151) and activates both ERK 1/2 and p38 MAPK pathways (74). Dendritic cell maturation can be inhibited through a direct cell-cell interaction with IRBC (152) and this effect is specifically mediated by IRBC interaction with dendritic cell surface CD36 (57). No corresponding data exists for the interaction of IRBC with endothelial cells. Here we showed that crosslinking CD36 with OKM5, and more specifically with the recombinant peptide y179, led to the activation of the ERK 1/2 MAPK pathway in HDMEC. The y179 peptide represents the functional binding domain of the parasite

cytoadherent ligand PfEMP1, and our finding is therefore the first demonstration that this protein can directly generate a cell signal in any type of cell.

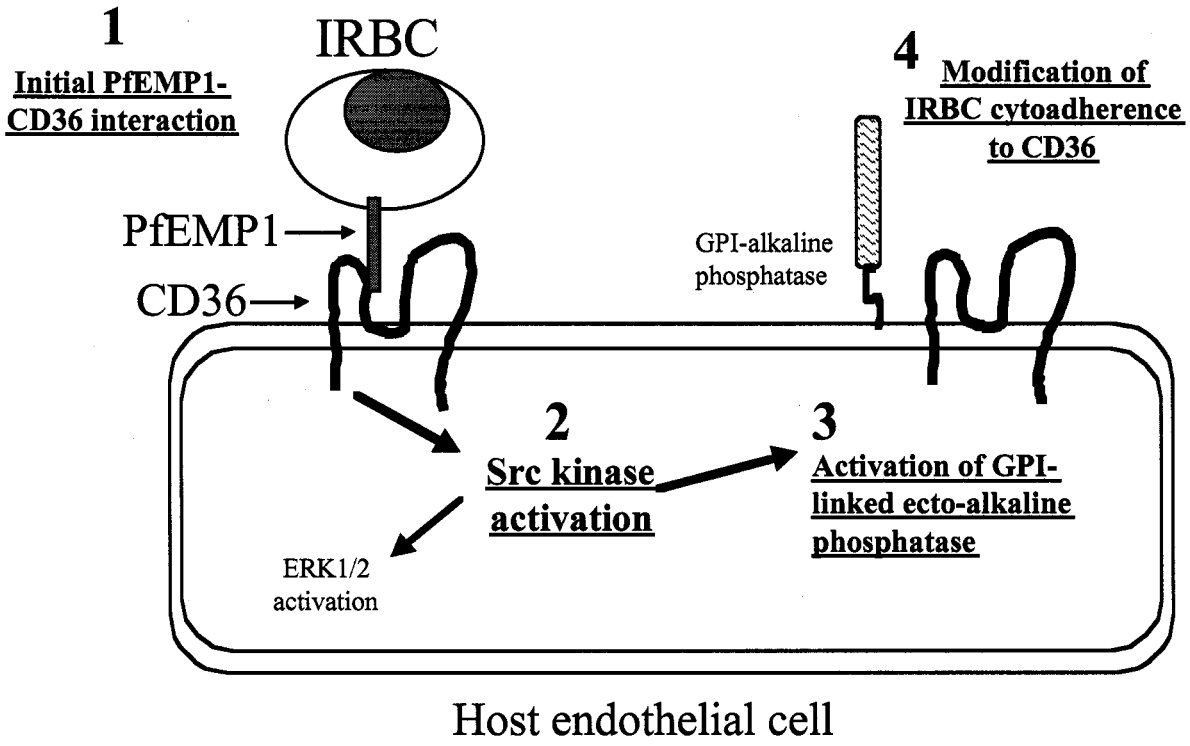

Figure 5.18. A proposed model of cytoadherence. 1) The initial PfEMP1-CD36 interaction causes an outside-in signaling event mediated by 2) Src-family kinase molecules. The Src-family kinases activate the ERK 1/2 pathway and are linked to the activation of 3) ecto-AP (possibly GPI-anchored). 4) Ecto-AP enhances cytoadherence in an inside-out event.

The functional consequence of an activated ERK 1/2 MAPK pathway in the endothelium remains to be determined. What we do know is that its inhibition had no detectable effect on IRBC adhesion to HDMEC for the duration of the experiment. Downstream cellular responses may include induction of gene transcription and protein synthesis of molecules that would affect the outcome of the infection, such as cytokines, adhesion molecules or nitric oxide. It has been shown that activation of the p38 MAPK pathway by the binding of TSP-1 to CD36 on HDMEC leads to apoptosis of the endothelial cells and inhibition of angiogenesis.

To determine if a CD36-mediated signal had any immediate effects on adhesion we investigated the upstream signaling molecules preceding ERK 1/2. Members of the Src-family kinase are physically associated with the intracellular tails of CD36 in microvascular endothelium (72) and Fyn, a member of the Src-family kinases, is activated when TSP-1 binds CD36 (60). We found that Src-family kinase activation was critical for maintaining firm adhesion of IRBC to HDMEC in vitro and in vivo. The exact mechanism whereby Src-family kinases modulate cytoadherence is not known. Src-family kinases are targeted for localization to the plasma membrane due to protein myristoylation within the N-terminus (126, 127). Much of the Src-family kinase activity therefore lies at the inner leaflet of the plasma membrane in close proximity with the intracellular tails of transmembrane protein receptors. The cytoplasmic tails of CD36 can associate with Src-family kinases so it is possible that after CD36 interaction with the PfEMP1 peptide, tyrosine residues become phosphorylated within CD36 and

this allows recruitment and activation of members of the Src-family kinase family. The ERK 1/2 activation could result from a previously defined pathway where Src-family kinases activate focal adhesion kinases (FAK) that subsequently activate Ras, MEK, and ERK (180).

A second molecule found to be highly important in maintaining normal levels of cytoadherence was an ecto-AP. Activated AP probably functions as an ecto-phosphatase, acting either on extracellular substrates or on cell surface membrane proteins. A role for an ecto-AP fits into our model of firm adhesion by being a modulator of the ecto-domain of CD36 thereby influencing CD36 binding affinity. As previously described (71) CD36 on platelets exists in two different binding states depending on ectodomain phosphorylation. Low affinity TSP-1 binding is due to a phosphorylated threonine-92 while the transition to the high affinity receptor requires dephosphorylation of this residue (71). Although the two forms of CD36 have not been identified in endothelium, the amino acid sequence between platelet and endothelial CD36 are almost identical, and the PKC-dependent targeting sequence RGPYTYRVRFLA for threonine-92 phosphorylation is conserved in the endothelial protein. The results suggest that ecto-AP might be an important therapeutic target for the treatment of severe falciparum malaria. Indeed, we demonstrated that the reduction in cytoadherence resulting from AP inhibition could be achieved with a preexisting licensed drug, levamisole. The use of levamisole as an anti-adhesive agent would provide an immediate halt to the chain of pathophysiological events in

severe falciparum malaria before the more specific antimalarial treatment can take effect.

The data demonstrate a connection between the CD36-induced Src-family kinase signal and the ecto-AP modulated adhesion, but the mechanistic link has not been determined. Ecto-alkaline phosphatase is found on the endothelial cell surface as a GPI-anchored protein. As the GPI anchor does not cross the plasma membrane, it is not entirely clear how information is transduced in either an outside-in or inside-out fashion upon ligand-recognition. One commonality shared between CD36, src and GPI-AP is they can all be found within caveolae, which are specialized lipid rafts and all bind to the defining membrane protein caveolin-1 (181). This scaffolding protein may serve as a linkage between the extracellular and intracellular molecules in our model. An emerging idea is that caveolae and Src-family kinases might be involved in transmembrane crosstalk with GPI-anchored outer membrane proteins (182, 183). Src-family kinases are localized to caveolae due to the addition of palmitoyl groups to myristoylated Src-family kinases. This lipid modification within the SH4 domain helps stabilize the membrane interaction within the caveolae (128, 184). Src-family kinases interact with caveolin-1 when it is phosphorylated on tyrosine 14 providing an SH2 binding domain (185) while CD36 and GPI-proteins interact with caveolin-1 through modified lipid moieties. CD36, Src-family kinases and GPI-AP can all interact with caveolin-1 but not all simultaneously as it has been shown that molecules can displace one another (183). Although it is not known if activated CD36 translocates to membrane microdomains, signaling by the epidermal

growth factor receptor (EGFR) requires relocation and mobilization that is dependent on caveolin and Src-family kinases (186). GPI-AP is known to concentrate to caveolae upon stimulation (147). Caveolin-1 could serve as an information conduit interacting with different molecules or different combinations of molecules as they migrate into or out of the membrane microdomain.

In summary, our data suggests a novel model of cytoadherence that involves the endothelium in a more dynamic role than previously appreciated. The PfEMP1-CD36 interaction results in a Src-family kinase dependent cell signal and Src-family kinase activity is critical for mediating IRBC cytoadherence. Although we showed that the PfEMP1-CD36 interaction initiated a Src-family kinase-dependent signal biochemically, we did not demonstrate conclusively that the enhancement of IRBC adhesion in functional experiments was due solely to signaling through CD36. Microvascular endothelium does express ICAM-1 and perhaps even other adhesion molecules that might interact with IRBC. To confirm that the Src-family kinase effect is mediated by CD36, the functional experiments need to be repeated with a parasite clone that interacts only with CD36. Adhesion is also dependent on the activity of an ecto-AP, which is linked to Src-family kinase activity through an as yet undetermined mechanism. It is reasonable to speculate that the IRBC have exploited a preexisting physiological cellular pathway, giving rise to the possibility that we have identified a novel cellular pathway linking CD36, the Src-family kinases and ecto-AP.

CHAPTER 6

CONCLUSIONS AND FUTURE DIRECTION

6.1 Summary and Conclusions

The pathophysiology of severe falciparum malaria is still incompletely understood. The ability of IRBC containing mature stages of *P. falciparum* to adhere to host endothelium is considered to be a key pathogenic process that may ultimately lead to the demise of the host. It is now known that the process of cytoadherence involves the parasite protein PfEMP1 and multiple host receptor molecules acting synergistically and mimics the leukocyte recruitment cascade under physiological flow conditions. Understanding the molecular mechanisms underlying cytoadherence is critical for the rational development of anti-adhesive therapies. The focus of this thesis was to determine the molecular basis of IRBC firm adhesion to CD36. Three major aspects of firm adhesion were investigated, including the roles of accessory molecules in the enhancement of IRBC adhesion to CD36 in vivo, the effectiveness of an anti-adhesive therapy based on a recombinant parasite protein in vivo and the characterization of a novel regulatory pathway of cytoadherence that involves host outside-in and inside-out signaling mechanisms.

Using the human/SCID mouse model, we have identified two distinct pathways of enhanced IRBC adhesion in vivo, associated with either increased rolling or decreased rolling. In TNF-α treated skin grafts, we observed a dramatic increase in the number of IRBC that adhered immediately after tethering. The increase in adhesion was entirely due to the presence of ICAM-1 with no detectable role for VCAM-1. Associated with the increase in adhesion, we observed a significant decrease in the rolling flux fraction. In histamine treated

animals, we observed a significant increase in both the number of rolling IRBC and the number of firmly adherent IRBC. The increase in rolling flux fraction was mediated by P-selectin, as it could be completely inhibited by an anti-P-selectin mAb. These results firmly establish the paradigm that multiple host molecules contribute to cytoadherence and that inducible accessory molecules can significantly affect the level of IRBC adhesion. As CD36 expression does not appear to change during falciparum malaria, the contribution of inducible molecules that enhance cytoadherence may be critical for the progression to severe disease.

The second major aim of this thesis was to evaluate a novel therapeutic strategy for severe falciparum malaria based on an anti-adhesive molecule. Inhibiting the adhesion of IRBC and detaching already adherent IRBC might stop the chain of pathological events and constitute a more rapid therapy than antimalarial drugs. We used the human/SCID mouse model to test the anti-adhesive effect of a recombinant molecule, based on the parasite derived cytoadherence ligand PfEMP1. The critical binding region of PfEMP1 to CD36 was used to generate the recombinant peptide y179. This peptide has been shown to inhibit and reverse the adhesion of a few CD36-binding laboratory adapted parasite strains to immobilized CD36 protein under static and flow conditions in vitro (35, 44). We significantly extended these findings in vitro and more importantly in vivo. The y179 peptide was effective in universally inhibiting adhesion of diverse clinical isolates both in vitro and in vivo, even in the presence of TNF-α-induced ICAM-1 expression. More importantly, we demonstrated that

y179 could rapidly detach already adherent IRBC in vivo, within minutes of administration and the effect was stable for at least 40 minutes, the duration of the experiment. Once the adherent IRBC detached no further adhesion was observed even when a second bolus of IRBC was administered into the dermal microvessels. These findings suggest that an anti-adhesive therapy based on y179 has significant therapeutic potential, and warrants similar trials in non-human primates and eventually patients.

The third part of this investigation focused on whether IRBC cytoadherence induces endothelial cell signaling and what consequences, if any, this may have on the adhesion process. A novel model of cytoadherence can be proposed based on our findings. This model proposes that initial IRBC-CD36 interaction triggers a Src-family kinase signal that is responsible for an increase in firm adhesion due to an ecto-AP-dependent modulation at the extracellular cell surface. The data show that PfEMP1, by interacting with CD36, can directly induce a Src-family kinase dependent ERK 1/2 activation. Using the specific Src-family kinase inhibitor PP1, we demonstrated that Src-family kinase activation was absolutely critical for mediating IRBC adhesion to human microvasculature in vitro, and more importantly in vivo. We further investigated how an intracellular signal could modify the IRBC-endothelial interaction. Based on the ability of CD36 to exist in a high and low affinity form due to ecto-phosphorylation on platelets we investigated if ecto-AP on endothelium could modulate adhesion and if this effect was linked to PfEMP1-CD36 induced Src-family kinase activation. A role for ecto-AP was demonstrated by the ability of exogenous AP

to restore adhesion levels in Src-family kinase inactive HDMEC. Moreover, levamisole, an AP specific inhibitor, significantly decreased adhesion to HDMEC, firmly establishing a role for ecto-AP in the cytoadherence cascade. These results demonstrate that optimal cytoadherence requires outside-in (CD36-Src-family kinase) and inside-out (Src-family kinase-ecto-AP) signaling mechanisms.

6.2 Future directions

We have demonstrated the human/SCID mouse chimera to be a valuable model for the evaluation of an anti-adhesive peptide based on the parasite protein PfEMP1. This model appears to be ideal for testing other anti-adhesive agents. An obvious candidate is the licensed drug levamisole, which reduced cytoadherence on HDMEC in vitro presumably through its specific inhibitory effect on ecto-AP. The drug could be administered to grafted SCID mice either prior to or following the administration of IRBC to determine the importance of maintaining CD36 dephosphorylation on cytoadherence in vivo. Another agent that could be tested in the human/SCID mouse model is nitric oxide (NO) that is known to be an anti-adhesive molecule for leukocytes, and has recently been shown to have an anti-adhesive effect on IRBC cytoadherence to HDMEC in vitro (Serirom and Ho, manuscript in preparation). The in vivo model would allow us to examine the direct effect of NO on vascular endothelium under physiological shear stress, as well as its effect on perivascular cellular elements such as mast cells.

A number of questions remain regarding the src-family kinase dependent mechanism for IRBC firm adhesion. We need to demonstrate directly that endothelial CD36 is phosphorylated in its physiological state. To do this, HDMEC will be metabolically labeled with radioactive [γ-ATP], so that only proteins on the cell surface will be able to incorporate the radioactive compound. Whole cell lysates will be subjected to immunoprecipitation with an anti-CD36 antibody, and resolved on an SDS-PAGE gel followed by autoradiography. It is anticipated that in control cells, a "hot" band at 88 kDa will be visualized, whereas in HDMEC pre-treated with y179, the band would be missing or diminished. The combination of y179 and levamisole should restore the pattern to that of untreated cells.

An alternative approach involves the use of mutant constructs that contain a substitution at the threonine 92 position. Asch *et al.* has previously generated a CD36-mutant construct in which Thr-92 was replaced with alanine (CD36ala92), an amino acid that cannot be phosphorylated (71). They found that the mutated CD36 was expressed in COS cells in an unphosphorylated state and that TSP-1 bound the mutant CD36 to a higher degree than the wild-type (phosphorylated) CD36. We will use the construct to make stable transfected mouse L cells that will be used in parallel-plate flow chamber studies. With this construct we could directly determine if phosphorylation of Thr-92 affects IRBC adhesion to CD36 under flow conditions.

Finally, a direct link between IRBC adhesion and ecto-AP activity could be established by treating HDMEC with y179 and assaying for AP activity in the

supernatant with a malachite green detection kit. The recombinant protein should increase the activity of the ecto-AP. This experiment could also be repeated with PP1-treated HDMEC to link the src-kinase with ecto-AP activity.

Future studies should also focus on the function of activated ERK 1/2. In our study, we were unable to demonstrate a functional effect of the activation of this pathway on IRBC cytoadherence. However, the downstream events associated with activated ERK 1/2 might require hours as opposed to minutes to occur. It would be interesting to investigate if activation of this pathway results in new gene transcription and protein synthesis of molecules associated with the adhesion process or its regulation. In particular, upregulation of pertinent adhesion molecules or pro-inflammatory cytokines would have a tremendous impact on the outcome of the infection.

BIBLIOGRAPHY

1. White, N. J., and M. Ho. 1992. The pathophysiology of malaria. *Adv Parasitol 31:83.*

2. 1986. Severe and complicated malaria. World Health Organization Malaria Action Programme. *Trans R Soc Trop Med Hyg 80 Suppl:3.*

3. 1990. Severe and complicated malaria. World Health Organization, Division of Control of Tropical Diseases. *Trans R Soc Trop Med Hyg 84 Suppl 2:1.*

4. MacPherson, G. G., M. J. Warrell, N. J. White, S. Looareesuwan, and D. A. Warrell. 1985. Human cerebral malaria. A quantitative ultrastructural analysis of parasitized erythrocyte sequestration. *Am J Pathol 119:385.*

5. Su, X. Z., V. M. Heatwole, S. P. Wertheimer, F. Guinet, J. A. Herrfeldt, D. S. Peterson, J. A. Ravetch, and T. E. Wellems. 1995. The large diverse gene family var encodes proteins involved in cytoadherence and antigenic variation of Plasmodium falciparum-infected erythrocytes. *Cell 82:89.*

6. Baruch, D. I., B. L. Pasloske, H. B. Singh, X. Bi, X. C. Ma, M. Feldman, T. F. Taraschi, and R. J. Howard. 1995. Cloning the P. falciparum gene encoding PfEMP1, a malarial variant antigen and adherence receptor on the surface of parasitized human erythrocytes. *Cell 82:77.*

7. Smith, J. D., C. E. Chitnis, A. G. Craig, D. J. Roberts, D. E. Hudson-Taylor, D. S. Peterson, R. Pinches, C. I. Newbold, and L. H. Miller. 1995. Switches in expression of Plasmodium falciparum var genes correlate with

changes in antigenic and cytoadherent phenotypes of infected erythrocytes. *Cell 82:101.*

8. Smith, J. D., B. Gamain, D. I. Baruch, and S. Kyes. 2001. Decoding the language of var genes and Plasmodium falciparum sequestration. *Trends Parasitol 17:538.*

9. Yipp, B. G., S. Anand, T. Schollaardt, K. D. Patel, S. Looareesuwan, and M. Ho. 2000. Synergism of multiple adhesion molecules in mediating cytoadherence of Plasmodium falciparum-infected erythrocytes to microvascular endothelial cells under flow. *Blood 96:2292.*

10. Udomsangpetch, R., P. H. Reinhardt, T. Schollaardt, J. F. Elliott, P. Kubes, and M. Ho. 1997. Promiscuity of clinical Plasmodium falciparum isolates for multiple adhesion molecules under flow conditions. *J Immunol 158:4358.*

11. Ho, M., T. Schollaardt, X. Niu, S. Looareesuwan, K. D. Patel, and P. Kubes. 1998. Characterization of Plasmodium falciparum-infected erythrocyte and P-selectin interaction under flow conditions. *Blood 91:4803.*

12. Luse, S. A., and L. H. Miller. 1971. Plasmodium falciparum malaria. Ultrastructure of parasitized erythrocytes in cardiac vessels. *Am J Trop Med Hyg 20:655.*

13. Silamut, K., N. H. Phu, C. Whitty, G. D. Turner, K. Louwrier, N. T. Mai, J. A. Simpson, T. T. Hien, and N. J. White. 1999. A quantitative analysis of

the microvascular sequestration of malaria parasites in the human brain. *Am J Pathol 155:395.*

14. Duarte, M. I., C. E. Corbett, M. Boulos, and V. Amato Neto. 1985. Ultrastructure of the lung in falciparum malaria. *Am J Trop Med Hyg 34:31.*

15. Corbett, C. E., M. I. Duarte, C. L. Lancellotti, M. A. Silva, and H. F. Andrade Junior. 1989. Cytoadherence in human falciparum malaria as a cause of respiratory distress. *J Trop Med Hyg 92:112.*

16. Pongponratn, E., P. Viriyavejakul, P. Wilairatana, D. Ferguson, U. Chaisri, G. Turner, and S. Looareesuwan. 2000. Absence of knobs on parasitized red blood cells in a splenectomized patient in fatal falciparum malaria. *Southeast Asian J Trop Med Public Health 31:829.*

17. Pongponratn, E., M. Riganti, B. Punpoowong, and M. Aikawa. 1991. Microvascular sequestration of parasitized erythrocytes in human falciparum malaria: a pathological study. *Am J Trop Med Hyg 44:168.*

18. Warrell, D. A., N. J. White, N. Veall, S. Looareesuwan, P. Chanthavanich, R. E. Phillips, J. Karbwang, P. Pongpaew, and S. Krishna. 1988. Cerebral anaerobic glycolysis and reduced cerebral oxygen transport in human cerebral malaria. *Lancet 2:534.*

19. White, N. J., D. A. Warrell, S. Looareesuwan, P. Chanthavanich, R. E. Phillips, and P. Pongpaew. 1985. Pathophysiological and prognostic significance of cerebrospinal-fluid lactate in cerebral malaria. *Lancet 1:776.*

20. Grau, G. E., T. E. Taylor, M. E. Molyneux, J. J. Wirima, P. Vassalli, M. Hommel, and P. H. Lambert. 1989. Tumor necrosis factor and disease severity in children with falciparum malaria. *N Engl J Med 320:1586.*

21. Karunaweera, N. D., G. E. Grau, P. Gamage, R. Carter, and K. N. Mendis. 1992. Dynamics of fever and serum levels of tumor necrosis factor are closely associated during clinical paroxysms in Plasmodium vivax malaria. *Proc Natl Acad Sci U S A 89:3200.*

22. Leech, J. H., J. W. Barnwell, L. H. Miller, and R. J. Howard. 1984. Identification of a strain-specific malarial antigen exposed on the surface of Plasmodium falciparum-infected erythrocytes. *J Exp Med 159:1567.*

23. Magowan, C., W. Wollish, L. Anderson, and J. Leech. 1988. Cytoadherence by Plasmodium falciparum-infected erythrocytes is correlated with the expression of a family of variable proteins on infected erythrocytes. *J Exp Med 168:1307.*

24. Leech, J. H., J. W. Barnwell, M. Aikawa, L. H. Miller, and R. J. Howard. 1984. Plasmodium falciparum malaria: association of knobs on the surface of infected erythrocytes with a histidine-rich protein and the erythrocyte skeleton. *J Cell Biol 98:1256.*

25. Crabb, B. S., B. M. Cooke, J. C. Reeder, R. F. Waller, S. R. Caruana, K. M. Davern, M. E. Wickham, G. V. Brown, R. L. Coppel, and A. F. Cowman. 1997. Targeted gene disruption shows that knobs enable malaria-infected red cells to cytoadhere under physiological shear stress. *Cell 89:287.*

26. Coppel, R. L., B. M. Cooke, C. Magowan, and M. Narla. 1998. Malaria and the erythrocyte. *Curr Opin Hematol 5:132.*

27. Trenholme, K. R., D. L. Gardiner, D. C. Holt, E. A. Thomas, A. F. Cowman, and D. J. Kemp. 2000. clag9: A cytoadherence gene in Plasmodium falciparum essential for binding of parasitized erythrocytes to CD36. *Proc Natl Acad Sci U S A 97:4029.*

28. Waller, K. L., B. M. Cooke, W. Nunomura, N. Mohandas, and R. L. Coppel. 1999. Mapping the binding domains involved in the interaction between the Plasmodium falciparum knob-associated histidine-rich protein (KAHRP) and the cytoadherence ligand P. falciparum erythrocyte membrane protein 1 (PfEMP1). *J Biol Chem 274:23808.*

29. Kilejian, A., M. A. Rashid, M. Aikawa, T. Aji, and Y. F. Yang. 1991. Selective association of a fragment of the knob protein with spectrin, actin and the red cell membrane. *Mol Biochem Parasitol 44:175.*

30. Waterkeyn, J. G., M. E. Wickham, K. M. Davern, B. M. Cooke, R. L. Coppel, J. C. Reeder, J. G. Culvenor, R. F. Waller, and A. F. Cowman. 2000. Targeted mutagenesis of Plasmodium falciparum erythrocyte membrane protein 3 (PfEMP3) disrupts cytoadherence of malaria-infected red blood cells. *Embo J 19:2813.*

31. Enderle, T., T. Ha, D. F. Ogletree, D. S. Chemla, C. Magowan, and S. Weiss. 1997. Membrane specific mapping and colocalization of malarial and host skeletal proteins in the Plasmodium falciparum infected

erythrocyte by dual-color near-field scanning optical microscopy. *Proc Natl Acad Sci U S A 94:520.*

32. Wickham, M. E., M. Rug, S. A. Ralph, N. Klonis, G. I. McFadden, L. Tilley, and A. F. Cowman. 2001. Trafficking and assembly of the cytoadherence complex in Plasmodium falciparum-infected human erythrocytes. *Embo J 20:5636.*

33. Scherf, A., R. Hernandez-Rivas, P. Buffet, E. Bottius, C. Benatar, B. Pouvelle, J. Gysin, and M. Lanzer. 1998. Antigenic variation in malaria: in situ switching, relaxed and mutually exclusive transcription of var genes during intra-erythrocytic development in Plasmodium falciparum. *Embo J 17:5418.*

34. Smith, J. D., G. Subramanian, B. Gamain, D. I. Baruch, and L. H. Miller. 2000. Classification of adhesive domains in the Plasmodium falciparum erythrocyte membrane protein 1 family. *Mol Biochem Parasitol 110:293.*

35. Baruch, D. I., X. C. Ma, H. B. Singh, X. Bi, B. L. Pasloske, and R. J. Howard. 1997. Identification of a region of PfEMP1 that mediates adherence of Plasmodium falciparum infected erythrocytes to CD36: conserved function with variant sequence. *Blood 90:3766.*

36. Smith, J. D., S. Kyes, A. G. Craig, T. Fagan, D. Hudson-Taylor, L. H. Miller, D. I. Baruch, and C. I. Newbold. 1998. Analysis of adhesive domains from the A4VAR Plasmodium falciparum erythrocyte membrane protein-1 identifies a CD36 binding domain. *Mol Biochem Parasitol 97:133.*

37. Chen, Q., A. Heddini, A. Barragan, V. Fernandez, S. F. Pearce, and M. Wahlgren. 2000. The semiconserved head structure of Plasmodium falciparum erythrocyte membrane protein 1 mediates binding to multiple independent host receptors. *J Exp Med 192:1*.

38. Fried, M., and P. E. Duffy. 1996. Adherence of Plasmodium falciparum to chondroitin sulfate A in the human placenta. *Science 272:1502*.

39. Reeder, J. C., A. F. Cowman, K. M. Davern, J. G. Beeson, J. K. Thompson, S. J. Rogerson, and G. V. Brown. 1999. The adhesion of Plasmodium falciparum-infected erythrocytes to chondroitin sulfate A is mediated by P. falciparum erythrocyte membrane protein 1. *Proc Natl Acad Sci U S A 96:5198*.

40. Buffet, P. A., B. Gamain, C. Scheidig, D. Baruch, J. D. Smith, R. Hernandez-Rivas, B. Pouvelle, S. Oishi, N. Fujii, T. Fusai, D. Parzy, L. H. Miller, J. Gysin, and A. Scherf. 1999. Plasmodium falciparum domain mediating adhesion to chondroitin sulfate A: a receptor for human placental infection. *Proc Natl Acad Sci U S A 96:12743*.

41. Gamain, B., J. D. Smith, L. H. Miller, and D. I. Baruch. 2001. Modifications in the CD36 binding domain of the Plasmodium falciparum variant antigen are responsible for the inability of chondroitin sulfate A adherent parasites to bind CD36. *Blood 97:3268*.

42. Smith, J. D., A. G. Craig, N. Kriek, D. Hudson-Taylor, S. Kyes, T. Fagen, R. Pinches, D. I. Baruch, C. I. Newbold, and L. H. Miller. 2000. Identification of a Plasmodium falciparum intercellular adhesion molecule-

1 binding domain: a parasite adhesion trait implicated in cerebral malaria. *Proc Natl Acad Sci U S A 97:1766.*

43. Senczuk, A. M., J. C. Reeder, M. M. Kosmala, and M. Ho. 2001. Plasmodium falciparum erythrocyte membrane protein 1 functions as a ligand for P-selectin. *Blood 98:3132.*

44. Cooke, B. M., C. L. Nicoll, D. I. Baruch, and R. L. Coppel. 1998. A recombinant peptide based on PfEMP-1 blocks and reverses adhesion of malaria-infected red blood cells to CD36 under flow. *Mol Microbiol 30:83.*

45. Gamain, B., L. H. Miller, and D. I. Baruch. 2001. The surface variant antigens of Plasmodium falciparum contain cross-reactive epitopes. *Proc Natl Acad Sci U S A 98:2664.*

46. Ockenhouse, C. F., N. N. Tandon, C. Magowan, G. A. Jamieson, and J. D. Chulay. 1989. Identification of a platelet membrane glycoprotein as a falciparum malaria sequestration receptor. *Science 243:1469.*

47. Treutiger, C. J., A. Heddini, V. Fernandez, W. A. Muller, and M. Wahlgren. 1997. PECAM-1/CD31, an endothelial receptor for binding Plasmodium falciparum-infected erythrocytes. *Nat Med 3:1405.*

48. Berendt, A. R., D. L. Simmons, J. Tansey, C. I. Newbold, and K. Marsh. 1989. Intercellular adhesion molecule-1 is an endothelial cell adhesion receptor for Plasmodium falciparum. *Nature 341:57.*

49. Ockenhouse, C. F., T. Tegoshi, Y. Maeno, C. Benjamin, M. Ho, K. E. Kan, Y. Thway, K. Win, M. Aikawa, and R. R. Lobb. 1992. Human vascular endothelial cell adhesion receptors for Plasmodium falciparum-infected

erythrocytes: roles for endothelial leukocyte adhesion molecule 1 and vascular cell adhesion molecule 1. *J Exp Med 176:1183.*

50. Roberts, D. D., J. A. Sherwood, S. L. Spitalnik, L. J. Panton, R. J. Howard, V. M. Dixit, W. A. Frazier, L. H. Miller, and V. Ginsburg. 1985. Thrombospondin binds falciparum malaria parasitized erythrocytes and may mediate cytoadherence. *Nature 318:64.*

51. Swerlick, R. A., K. H. Lee, T. M. Wick, and T. J. Lawley. 1992. Human dermal microvascular endothelial but not human umbilical vein endothelial cells express CD36 in vivo and in vitro. *J Immunol 148:78.*

52. Knowles, D. M., 2nd, B. Tolidjian, C. Marboe, V. D'Agati, M. Grimes, and L. Chess. 1984. Monoclonal anti-human monocyte antibodies OKM1 and OKM5 possess distinctive tissue distributions including differential reactivity with vascular endothelium. *J Immunol 132:2170.*

53. Edelman, P., G. Vinci, J. L. Villeval, W. Vainchenker, A. Henri, R. Miglierina, P. Rouger, J. Reviron, J. Breton-Gorius, C. Sureau, and et al. 1986. A monoclonal antibody against an erythrocyte ontogenic antigen identifies fetal and adult erythroid progenitors. *Blood 67:56.*

54. Abumrad, N. A., M. R. el-Maghrabi, E. Z. Amri, E. Lopez, and P. A. Grimaldi. 1993. Cloning of a rat adipocyte membrane protein implicated in binding or transport of long-chain fatty acids that is induced during preadipocyte differentiation. Homology with human CD36. *J Biol Chem 268:17665.*

55. Tandon, N. N., R. H. Lipsky, W. H. Burgess, and G. A. Jamieson. 1989. Isolation and characterization of platelet glycoprotein IV (CD36). *J Biol Chem 264:7570.*

56. Albert, M. L., S. F. Pearce, L. M. Francisco, B. Sauter, P. Roy, R. L. Silverstein, and N. Bhardwaj. 1998. Immature dendritic cells phagocytose apoptotic cells via alphavbeta5 and CD36, and cross-present antigens to cytotoxic T lymphocytes. *J Exp Med 188:1359.*

57. Urban, B. C., N. Willcox, and D. J. Roberts. 2001. A role for CD36 in the regulation of dendritic cell function. *Proc Natl Acad Sci U S A 98:8750.*

58. Talle, M. A., P. E. Rao, E. Westberg, N. Allegar, M. Makowski, R. S. Mittler, and G. Goldstein. 1983. Patterns of antigenic expression on human monocytes as defined by monoclonal antibodies. *Cell Immunol 78:83.*

59. Savill, J., N. Hogg, and C. Haslett. 1991. Macrophage vitronectin receptor, CD36, and thrombospondin cooperate in recognition of neutrophils undergoing programmed cell death. *Chest 99:6S.*

60. Jimenez, B., O. V. Volpert, S. E. Crawford, M. Febbraio, R. L. Silverstein, and N. Bouck. 2000. Signals leading to apoptosis-dependent inhibition of neovascularization by thrombospondin-1. *Nat Med 6:41.*

61. Hajri, T., A. Ibrahimi, C. T. Coburn, F. F. Knapp, Jr., T. Kurtz, M. Pravenec, and N. A. Abumrad. 2001. Defective fatty acid uptake in the spontaneously hypertensive rat is a primary determinant of altered

glucose metabolism, hyperinsulinemia, and myocardial hypertrophy. *J Biol Chem 276:23661.*

62. Aitman, T. J., A. M. Glazier, C. A. Wallace, L. D. Cooper, P. J. Norsworthy, F. N. Wahid, K. M. Al-Majali, P. M. Trembling, C. J. Mann, C. C. Shoulders, D. Graf, E. St Lezin, T. W. Kurtz, V. Kren, M. Pravenec, A. Ibrahimi, N. A. Abumrad, L. W. Stanton, and J. Scott. 1999. Identification of Cd36 (Fat) as an insulin-resistance gene causing defective fatty acid and glucose metabolism in hypertensive rats. *Nat Genet 21:76.*

63. Pravenec, M., V. Landa, V. Zidek, A. Musilova, V. Kren, L. Kazdova, T. J. Aitman, A. M. Glazier, A. Ibrahimi, N. A. Abumrad, N. Qi, J. M. Wang, E. M. St Lezin, and T. W. Kurtz. 2001. Transgenic rescue of defective Cd36 ameliorates insulin resistance in spontaneously hypertensive rats. *Nat Genet 27:156.*

64. Greenwalt, D. E., S. H. Scheck, and T. Rhinehart-Jones. 1995. Heart CD36 expression is increased in murine models of diabetes and in mice fed a high fat diet. *J Clin Invest 96:1382.*

65. Hirooka, K., Y. Yasumura, Y. Ishida, K. Komamura, A. Hanatani, S. Nakatani, M. Yamagishi, and K. Miyatake. 2000. Improvement in cardiac function and free fatty acid metabolism in a case of dilated cardiomyopathy with CD36 deficiency. *Jpn Circ J 64:731.*

66. Glazier, A. M., J. Scott, and T. J. Aitman. 2002. Molecular basis of the Cd36 chromosomal deletion underlying SHR defects in insulin action and fatty acid metabolism. *Mamm Genome 13:108.*

67. Asch, A. S., J. Barnwell, R. L. Silverstein, and R. L. Nachman. 1987. Isolation of the thrombospondin membrane receptor. *J Clin Invest 79:1054.*

68. Silverstein, R. L., A. S. Asch, and R. L. Nachman. 1989. Glycoprotein IV mediates thrombospondin-dependent platelet-monocyte and platelet-U937 cell adhesion. *J Clin Invest 84:546.*

69. Leung, L. L., W. X. Li, J. L. McGregor, G. Albrecht, and R. J. Howard. 1992. CD36 peptides enhance or inhibit CD36-thrombospondin binding. A two-step process of ligand-receptor interaction. *J Biol Chem 267:18244.*

70. Li, W. X., R. J. Howard, and L. L. Leung. 1993. Identification of SVTCG in thrombospondin as the conformation-dependent, high affinity binding site for its receptor, CD36. *J Biol Chem 268:16179.*

71. Asch, A. S., I. Liu, F. M. Briccetti, J. W. Barnwell, F. Kwakye-Berko, A. Dokun, J. Goldberger, and M. Pernambuco. 1993. Analysis of CD36 binding domains: ligand specificity controlled by dephosphorylation of an ectodomain. *Science 262:1436.*

72. Bull, H. A., P. M. Brickell, and P. M. Dowd. 1994. Src-related protein tyrosine kinases are physically associated with the surface antigen CD36 in human dermal microvascular endothelial cells. *FEBS Lett 351:41.*

73. Huang, M. M., J. B. Bolen, J. W. Barnwell, S. J. Shattil, and J. S. Brugge. 1991. Membrane glycoprotein IV (CD36) is physically associated with the Fyn, Lyn, and Yes protein-tyrosine kinases in human platelets. *Proc Natl Acad Sci U S A 88:7844.*

74. McGilvray, I. D., L. Serghides, A. Kapus, O. D. Rotstein, and K. C. Kain. 2000. Nonopsonic monocyte/macrophage phagocytosis of Plasmodium falciparum-parasitized erythrocytes: a role for CD36 in malarial clearance. *Blood 96:3231.*

75. Newbold, C., P. Warn, G. Black, A. Berendt, A. Craig, B. Snow, M. Msobo, N. Peshu, and K. Marsh. 1997. Receptor-specific adhesion and clinical disease in Plasmodium falciparum. *Am J Trop Med Hyg 57:389.*

76. Rogerson, S. J., R. Tembenu, C. Dobano, S. Plitt, T. E. Taylor, and M. E. Molyneux. 1999. Cytoadherence characteristics of Plasmodium falciparum-infected erythrocytes from Malawian children with severe and uncomplicated malaria. *Am J Trop Med Hyg 61:467.*

77. Navazo, M. D., L. Daviet, J. Savill, Y. Ren, L. L. Leung, and J. L. McGregor. 1996. Identification of a domain (155-183) on CD36 implicated in the phagocytosis of apoptotic neutrophils. *J Biol Chem 271:15381.*

78. Baruch, D. I., X. C. Ma, B. Pasloske, R. J. Howard, and L. H. Miller. 1999. CD36 peptides that block cytoadherence define the CD36 binding region for Plasmodium falciparum-infected erythrocytes. *Blood 94:2121.*

79. Turner, G. D., H. Morrison, M. Jones, T. M. Davis, S. Looareesuwan, I. D. Buley, K. C. Gatter, C. I. Newbold, S. Pukritayakamee, B. Nagachinta, and et al. 1994. An immunohistochemical study of the pathology of fatal malaria. Evidence for widespread endothelial activation and a potential role for intercellular adhesion molecule-1 in cerebral sequestration. *Am J Pathol 145:1057.*

80. Turner, G. 1997. Cerebral malaria. *Brain Pathol 7:569.*

81. Pain, A., B. C. Urban, O. Kai, C. Casals-Pascual, J. Shafi, K. Marsh, and D. J. Roberts. 2001. A non-sense mutation in Cd36 gene is associated with protection from severe malaria. *Lancet 357:1502.*

82. Aitman, T. J., L. D. Cooper, P. J. Norsworthy, F. N. Wahid, J. K. Gray, B. R. Curtis, P. M. McKeigue, D. Kwiatkowski, B. M. Greenwood, R. W. Snow, A. V. Hill, and J. Scott. 2000. Malaria susceptibility and CD36 mutation. *Nature 405:1015.*

83. Pober, J. S., M. A. Gimbrone, Jr., L. A. Lapierre, D. L. Mendrick, W. Fiers, R. Rothlein, and T. A. Springer. 1986. Overlapping patterns of activation of human endothelial cells by interleukin 1, tumor necrosis factor, and immune interferon. *J Immunol 137:1893.*

84. Pober, J. S., L. A. Lapierre, A. H. Stolpen, T. A. Brock, T. A. Springer, W. Fiers, M. P. Bevilacqua, D. L. Mendrick, and M. A. Gimbrone, Jr. 1987. Activation of cultured human endothelial cells by recombinant lymphotoxin: comparison with tumor necrosis factor and interleukin 1 species. *J Immunol 138:3319.*

85. Udomsangpetch, R., B. J. Taylor, S. Looareesuwan, N. J. White, J. F. Elliott, and M. Ho. 1996. Receptor specificity of clinical Plasmodium falciparum isolates: nonadherence to cell-bound E-selectin and vascular cell adhesion molecule-1. *Blood 88:2754.*

86. Fernandez-Reyes, D., A. G. Craig, S. A. Kyes, N. Peshu, R. W. Snow, A. R. Berendt, K. Marsh, and C. I. Newbold. 1997. A high frequency African

coding polymorphism in the N-terminal domain of ICAM-1 predisposing to cerebral malaria in Kenya. *Hum Mol Genet 6:1357.*

87. Bellamy, R., D. Kwiatkowski, and A. V. Hill. 1998. Absence of an association between intercellular adhesion molecule 1, complement receptor 1 and interleukin 1 receptor antagonist gene polymorphisms and severe malaria in a West African population. *Trans R Soc Trop Med Hyg 92:312.*

88. Ohashi, J., I. Naka, J. Patarapotikul, H. Hananantachai, S. Looareesuwan, and K. Tokunaga. 2001. Absence of association between the allele coding methionine at position 29 in the N-terminal domain of ICAM-1 (ICAM-1(Kilifi)) and severe malaria in the northwest of Thailand. *Jpn J Infect Dis 54:114.*

89. Adams, S., G. D. Turner, G. B. Nash, K. Micklem, C. I. Newbold, and A. G. Craig. 2000. Differential binding of clonal variants of Plasmodium falciparum to allelic forms of intracellular adhesion molecule 1 determined by flow adhesion assay. *Infect Immun 68:264.*

90. Alon, R., P. D. Kassner, M. W. Carr, E. B. Finger, M. E. Hemler, and T. A. Springer. 1995. The integrin VLA-4 supports tethering and rolling in flow on VCAM-1. *J Cell Biol 128:1243.*

91. Vonderheide, R. H., T. F. Tedder, T. A. Springer, and D. E. Staunton. 1994. Residues within a conserved amino acid motif of domains 1 and 4 of VCAM-1 are required for binding to VLA-4. *J Cell Biol 125:215.*

92. Kitayama, J., R. C. Fuhlbrigge, K. D. Puri, and T. A. Springer. 1997. P-selectin, L-selectin, and alpha 4 integrin have distinct roles in eosinophil tethering and arrest on vascular endothelial cells under physiological flow conditions. *J Immunol 159:3929.*

93. Patel, K. D. 1998. Eosinophil tethering to interleukin-4-activated endothelial cells requires both P-selectin and vascular cell adhesion molecule-1. *Blood 92:3904.*

94. Luscinskas, F. W., H. Ding, P. Tan, D. Cumming, T. F. Tedder, and M. E. Gerritsen. 1996. L- and P-selectins, but not CD49d (VLA-4) integrins, mediate monocyte initial attachment to TNF-alpha-activated vascular endothelium under flow in vitro. *J Immunol 157:326.*

95. Reinhardt, P. H., and P. Kubes. 1998. Differential leukocyte recruitment from whole blood via endothelial adhesion molecules under shear conditions. *Blood 92:4691.*

96. Reinhardt, P. H., J. F. Elliott, and P. Kubes. 1997. Neutrophils can adhere via alpha4beta1-integrin under flow conditions. *Blood 89:3837.*

97. Ibbotson, G. C., C. Doig, J. Kaur, V. Gill, L. Ostrovsky, T. Fairhead, and P. Kubes. 2001. Functional alpha4-integrin: a newly identified pathway of neutrophil recruitment in critically ill septic patients. *Nat Med 7:465.*

98. Johnston, G. I., R. G. Cook, and R. P. McEver. 1989. Cloning of GMP-140, a granule membrane protein of platelets and endothelium: sequence similarity to proteins involved in cell adhesion and inflammation. *Cell 56:1033.*

99. Patel, K. D., M. U. Nollert, and R. P. McEver. 1995. P-selectin must extend a sufficient length from the plasma membrane to mediate rolling of neutrophils. *J Cell Biol 131:1893.*

100. McEver, R. P., J. H. Beckstead, K. L. Moore, L. Marshall-Carlson, and D. F. Bainton. 1989. GMP-140, a platelet alpha-granule membrane protein, is also synthesized by vascular endothelial cells and is localized in Weibel-Palade bodies. *J Clin Invest 84:92.*

101. Hattori, R., K. K. Hamilton, R. D. Fugate, R. P. McEver, and P. J. Sims. 1989. Stimulated secretion of endothelial von Willebrand factor is accompanied by rapid redistribution to the cell surface of the intracellular granule membrane protein GMP-140. *J Biol Chem 264:7768.*

102. Geng, J. G., M. P. Bevilacqua, K. L. Moore, T. M. McIntyre, S. M. Prescott, J. M. Kim, G. A. Bliss, G. A. Zimmerman, and R. P. McEver. 1990. Rapid neutrophil adhesion to activated endothelium mediated by GMP-140. *Nature 343:757.*

103. Lawrence, M. B., and T. A. Springer. 1991. Leukocytes roll on a selectin at physiologic flow rates: distinction from and prerequisite for adhesion through integrins. *Cell 65:859.*

104. Kubes, P., and S. Kanwar. 1994. Histamine induces leukocyte rolling in post-capillary venules. A P-selectin-mediated event. *J Immunol 152:3570.*

105. Yao, L., J. Pan, H. Setiadi, K. D. Patel, and R. P. McEver. 1996. Interleukin 4 or oncostatin M induces a prolonged increase in P-selectin mRNA and protein in human endothelial cells. *J Exp Med 184:81.*

106. Kerfoot, S. M., E. Raharjo, M. Ho, J. Kaur, S. Serirom, D. M. McCafferty, A. R. Burns, K. D. Patel, and P. Kubes. 2001. Exclusive neutrophil recruitment with oncostatin M in a human system. *Am J Pathol 159:1531*.

107. Tardy, Y., N. Resnick, T. Nagel, M. A. Gimbrone, Jr., and C. F. Dewey, Jr. 1997. Shear stress gradients remodel endothelial monolayers in vitro via a cell proliferation-migration-loss cycle. *Arterioscler Thromb Vasc Biol 17:3102*.

108. Resnick, N., H. Yahav, L. M. Khachigian, T. Collins, K. R. Anderson, F. C. Dewey, and M. A. Gimbrone, Jr. 1997. Endothelial gene regulation by laminar shear stress. *Adv Exp Med Biol 430:155*.

109. Topper, J. N., and M. A. Gimbrone, Jr. 1999. Blood flow and vascular gene expression: fluid shear stress as a modulator of endothelial phenotype. *Mol Med Today 5:40*.

110. Bhullar, I. S., Y. S. Li, H. Miao, E. Zandi, M. Kim, J. Y. Shyy, and S. Chien. 1998. Fluid shear stress activation of IkappaB kinase is integrin-dependent. *J Biol Chem 273:30544*.

111. Galbraith, C. G., R. Skalak, and S. Chien. 1998. Shear stress induces spatial reorganization of the endothelial cell cytoskeleton. *Cell Motil Cytoskeleton 40:317*.

112. Chien, S., and J. Y. Shyy. 1998. Effects of hemodynamic forces on gene expression and signal transduction in endothelial cells. *Biol Bull 194:390*.

113. Murray, A. G., P. Petzelbauer, C. C. Hughes, J. Costa, P. Askenase, and J. S. Pober. 1994. Human T-cell-mediated destruction of allogeneic dermal microvessels in a severe combined immunodeficient mouse. *Proc Natl Acad Sci U S A 91:9146.*

114. Ho, M., M. J. Hickey, A. G. Murray, G. Andonegui, and P. Kubes. 2000. Visualization of Plasmodium falciparum-endothelium interactions in human microvasculature: mimicry of leukocyte recruitment. *J Exp Med 192:1205.*

115. Brenner, B., E. Gulbins, K. Schlottmann, U. Koppenhoefer, G. L. Busch, B. Walzog, M. Steinhausen, K. M. Coggeshall, O. Linderkamp, and F. Lang. 1996. L-selectin activates the Ras pathway via the tyrosine kinase p56lck. *Proc Natl Acad Sci U S A 93:15376.*

116. Waddell, T. K., L. Fialkow, C. K. Chan, T. K. Kishimoto, and G. P. Downey. 1995. Signaling functions of L-selectin. Enhancement of tyrosine phosphorylation and activation of MAP kinase. *J Biol Chem 270:15403.*

117. Steeber, D. A., P. Engel, A. S. Miller, M. P. Sheetz, and T. F. Tedder. 1997. Ligation of L-selectin through conserved regions within the lectin domain activates signal transduction pathways and integrin function in human, mouse, and rat leukocytes. *J Immunol 159:952.*

118. Smolen, J. E., T. K. Petersen, C. Koch, S. J. O'Keefe, W. A. Hanlon, S. Seo, D. Pearson, M. C. Fossett, and S. I. Simon. 2000. L-selectin signaling of neutrophil adhesion and degranulation involves p38 mitogen-activated protein kinase. *J Biol Chem 275:15876.*

119. Lorenzon, P., E. Vecile, E. Nardon, E. Ferrero, J. M. Harlan, F. Tedesco, and A. Dobrina. 1998. Endothelial cell E- and P-selectin and vascular cell adhesion molecule-1 function as signaling receptors. *J Cell Biol 142:1381.*

120. Yoshida, M., W. F. Westlin, N. Wang, D. E. Ingber, A. Rosenzweig, N. Resnick, and M. A. Gimbrone, Jr. 1996. Leukocyte adhesion to vascular endothelium induces E-selectin linkage to the actin cytoskeleton. *J Cell Biol 133:445.*

121. Yoshida, M., B. E. Szente, J. M. Kiely, A. Rosenzweig, and M. A. Gimbrone, Jr. 1998. Phosphorylation of the cytoplasmic domain of E-selectin is regulated during leukocyte-endothelial adhesion. *J Immunol 161:933.*

122. Hu, Y., B. Szente, J. M. Kiely, and M. A. Gimbrone, Jr. 2001. Molecular events in transmembrane signaling via E-selectin. SHP2 association, adaptor protein complex formation and ERK1/2 activation. *J Biol Chem 276:48549.*

123. Simon, S. I., Y. Hu, D. Vestweber, and C. W. Smith. 2000. Neutrophil tethering on E-selectin activates beta 2 integrin binding to ICAM-1 through a mitogen-activated protein kinase signal transduction pathway. *J Immunol 164:4348.*

124. Etienne-Manneville, S., J. B. Manneville, P. Adamson, B. Wilbourn, J. Greenwood, and P. O. Couraud. 2000. ICAM-1-coupled cytoskeletal rearrangements and transendothelial lymphocyte migration involve

intracellular calcium signaling in brain endothelial cell lines. *J Immunol 165:3375.*

125. Modderman, P. W., A. E. von dem Borne, and A. Sonnenberg. 1994. Tyrosine phosphorylation of P-selectin in intact platelets and in a disulphide-linked complex with immunoprecipitated pp60c-src. *Biochem J 299 (Pt 3):613.*

126. Pellman, D., E. A. Garber, F. R. Cross, and H. Hanafusa. 1985. An N-terminal peptide from p60src can direct myristylation and plasma membrane localization when fused to heterologous proteins. *Nature 314:374.*

127. Kaplan, J. M., G. Mardon, J. M. Bishop, and H. E. Varmus. 1988. The first seven amino acids encoded by the v-src oncogene act as a myristylation signal: lysine 7 is a critical determinant. *Mol Cell Biol 8:2435.*

128. Robbins, S. M., N. A. Quintrell, and J. M. Bishop. 1995. Myristoylation and differential palmitoylation of the HCK protein-tyrosine kinases govern their attachment to membranes and association with caveolae. *Mol Cell Biol 15:3507.*

129. Roussel, R. R., S. R. Brodeur, D. Shalloway, and A. P. Laudano. 1991. Selective binding of activated pp60c-src by an immobilized synthetic phosphopeptide modeled on the carboxyl terminus of pp60c-src. *Proc Natl Acad Sci U S A 88:10696.*

130. Bibbins, K. B., H. Boeuf, and H. E. Varmus. 1993. Binding of the Src SH2 domain to phosphopeptides is determined by residues in both the SH2 domain and the phosphopeptides. *Mol Cell Biol 13:7278.*

131. Xu, W., S. C. Harrison, and M. J. Eck. 1997. Three-dimensional structure of the tyrosine kinase c-Src. *Nature 385:595.*

132. Xu, W., A. Doshi, M. Lei, M. J. Eck, and S. C. Harrison. 1999. Crystal structures of c-Src reveal features of its autoinhibitory mechanism. *Mol Cell 3:629.*

133. Robbins, D. J., and M. H. Cobb. 1992. Extracellular signal-regulated kinases 2 autophosphorylates on a subset of peptides phosphorylated in intact cells in response to insulin and nerve growth factor: analysis by peptide mapping. *Mol Biol Cell 3:299.*

134. Kyriakis, J. M., H. App, X. F. Zhang, P. Banerjee, D. L. Brautigan, U. R. Rapp, and J. Avruch. 1992. Raf-1 activates MAP kinase-kinase. *Nature 358:417.*

135. Wu, J., J. K. Harrison, L. A. Vincent, C. Haystead, T. A. Haystead, H. Michel, D. F. Hunt, K. R. Lynch, and T. W. Sturgill. 1993. Molecular structure of a protein-tyrosine/threonine kinase activating p42 mitogen-activated protein (MAP) kinase: MAP kinase kinase. *Proc Natl Acad Sci U S A 90:173.*

136. Crews, C. M., A. Alessandrini, and R. L. Erikson. 1992. The primary structure of MEK, a protein kinase that phosphorylates the ERK gene product. *Science 258:478.*

137. Zheng, C. F., and K. L. Guan. 1993. Cloning and characterization of two distinct human extracellular signal-regulated kinase activator kinases, MEK1 and MEK2. *J Biol Chem 268:11435.*

138. Hill, C. S., and R. Treisman. 1995. Transcriptional regulation by extracellular signals: mechanisms and specificity. *Cell 80:199.*

139. Cruzalegui, F. H., E. Cano, and R. Treisman. 1999. ERK activation induces phosphorylation of Elk-1 at multiple S/T-P motifs to high stoichiometry. *Oncogene 18:7948.*

140. Marais, R., J. Wynne, and R. Treisman. 1993. The SRF accessory protein Elk-1 contains a growth factor-regulated transcriptional activation domain. *Cell 73:381.*

141. Hazan-Halevy, I., R. Seger, and R. Levy. 2000. The requirement of both extracellular regulated kinase and p38 mitogen-activated protein kinase for stimulation of cytosolic phospholipase A(2) activity by either FcgammaRIIA or FcgammaRIIIB in human neutrophils. A possible role for Pyk2 but not for the Grb2-Sos-Shc complex. *J Biol Chem 275:12416.*

142. Liu, Z. X., C. F. Yu, C. Nickel, S. Thomas, and L. G. Cantley. 2002. Hepatocyte growth factor induces ERK-dependent paxillin phosphorylation and regulates paxillin-focal adhesion kinase association. *J Biol Chem 277:10452.*

143. Cope, F. O., and J. J. Wille. 1989. Retinoid receptor antisense DNAs inhibit alkaline phosphatase induction and clonogenicity in malignant keratinocytes. *Proc Natl Acad Sci U S A 86:5590.*

144. Calhau, C., F. Martel, S. Pinheiro-Silva, H. Pinheiro, P. Soares-da-Silva, C. Hipolito-Reis, and I. Azevedo. 2002. Modulation of insulin transport in rat brain microvessel endothelial cells by an ecto-phosphatase activity. *J Cell Biochem 84:389.*

145. Scheibe, R. J., H. Kuehl, S. Krautwald, J. D. Meissner, and W. H. Mueller. 2000. Ecto-alkaline phosphatase activity identified at physiological pH range on intact P19 and HL-60 cells is induced by retinoic acid. *J Cell Biochem 76:420.*

146. Gallo, R. L., R. A. Dorschner, S. Takashima, M. Klagsbrun, E. Eriksson, and M. Bernfield. 1997. Endothelial cell surface alkaline phosphatase activity is induced by IL-6 released during wound repair. *J Invest Dermatol 109:597.*

147. Parton, R. G., B. Joggerst, and K. Simons. 1994. Regulated internalization of caveolae. *J Cell Biol 127:1199.*

148. Naik, U. P., E. Kornecki, and Y. H. Ehrlich. 1991. Phosphorylation and dephosphorylation of human platelet surface proteins by an ecto-protein kinase/phosphatase system. *Biochim Biophys Acta 1092:256.*

149. Apasov, S. G., P. T. Smith, M. T. Jelonek, D. H. Margulies, and M. V. Sitkovsky. 1996. Phosphorylation of extracellular domains of T-lymphocyte surface proteins. Constitutive serine and threonine phosphorylation of the T cell antigen receptor ectodomains. *J Biol Chem 271:25677.*

150. Hatmi, M., J. M. Gavaret, I. Elalamy, B. B. Vargaftig, and C. Jacquemin. 1996. Evidence for cAMP-dependent platelet ectoprotein kinase activity

that phosphorylates platelet glycoprotein IV (CD36). *J Biol Chem 271:24776.*

151. Ockenhouse, C. F., C. Magowan, and J. D. Chulay. 1989. Activation of monocytes and platelets by monoclonal antibodies or malaria-infected erythrocytes binding to the CD36 surface receptor in vitro. *J Clin Invest 84:468.*

152. Urban, B. C., D. J. Ferguson, A. Pain, N. Willcox, M. Plebanski, J. M. Austyn, and D. J. Roberts. 1999. Plasmodium falciparum-infected erythrocytes modulate the maturation of dendritic cells. *Nature 400:73.*

153. Denis, C. V., P. Andre, S. Saffaripour, and D. D. Wagner. 2001. Defect in regulated secretion of P-selectin affects leukocyte recruitment in von Willebrand factor-deficient mice. *Proc Natl Acad Sci U S A 98:4072.*

154. Hanke, J. H., J. P. Gardner, R. L. Dow, P. S. Changelian, W. H. Brissette, E. J. Weringer, B. A. Pollok, and P. A. Connelly. 1996. Discovery of a novel, potent, and Src family-selective tyrosine kinase inhibitor. Study of Lck- and FynT-dependent T cell activation. *J Biol Chem 271:695.*

155. Jung, U., and K. Ley. 1999. Mice lacking two or all three selectins demonstrate overlapping and distinct functions for each selectin. *J Immunol 162:6755.*

156. Jung, U., K. E. Norman, K. Scharffetter-Kochanek, A. L. Beaudet, and K. Ley. 1998. Transit time of leukocytes rolling through venules controls cytokine-induced inflammatory cell recruitment in vivo. *J Clin Invest 102:1526.*

157. Simoncini, T., A. Hafezi-Moghadam, D. P. Brazil, K. Ley, W. W. Chin, and J. K. Liao. 2000. Interaction of oestrogen receptor with the regulatory subunit of phosphatidylinositol-3-OH kinase. *Nature 407:538.*

158. Day, N. P., T. T. Hien, T. Schollaardt, P. P. Loc, L. V. Chuong, T. T. Chau, N. T. Mai, N. H. Phu, D. X. Sinh, N. J. White, and M. Ho. 1999. The prognostic and pathophysiologic role of pro- and antiinflammatory cytokines in severe malaria. *J Infect Dis 180:1288.*

159. Turner, G. D., V. C. Ly, T. H. Nguyen, T. H. Tran, H. P. Nguyen, D. Bethell, S. Wyllie, K. Louwrier, S. B. Fox, K. C. Gatter, N. P. Day, N. J. White, and A. R. Berendt. 1998. Systemic endothelial activation occurs in both mild and severe malaria. Correlating dermal microvascular endothelial cell phenotype and soluble cell adhesion molecules with disease severity. *Am J Pathol 152:1477.*

160. Miller, J., R. Knorr, M. Ferrone, R. Houdei, C. P. Carron, and M. L. Dustin. 1995. Intercellular adhesion molecule-1 dimerization and its consequences for adhesion mediated by lymphocyte function associated-1. *J Exp Med 182:1231.*

161. Jun, C. D., M. Shimaoka, C. V. Carman, J. Takagi, and T. A. Springer. 2001. Dimerization and the effectiveness of ICAM-1 in mediating LFA-1-dependent adhesion. *Proc Natl Acad Sci U S A 98:6830.*

162. Berendt, A. R., A. McDowall, A. G. Craig, P. A. Bates, M. J. Sternberg, K. Marsh, C. I. Newbold, and N. Hogg. 1992. The binding site on ICAM-1 for

Plasmodium falciparum-infected erythrocytes overlaps, but is distinct from, the LFA-1-binding site. *Cell 68:71.*

163. Ockenhouse, C. F., R. Betageri, T. A. Springer, and D. E. Staunton. 1992. Plasmodium falciparum-infected erythrocytes bind ICAM-1 at a site distinct from LFA-1, Mac-1, and human rhinovirus. *Cell 68:63.*

164. Casasnovas, J. M., T. Stehle, J. H. Liu, J. H. Wang, and T. A. Springer. 1998. A dimeric crystal structure for the N-terminal two domains of intercellular adhesion molecule-1. *Proc Natl Acad Sci U S A 95:4134.*

165. Swerlick, R. A., K. H. Lee, L. J. Li, N. T. Sepp, S. W. Caughman, and T. J. Lawley. 1992. Regulation of vascular cell adhesion molecule 1 on human dermal microvascular endothelial cells. *J Immunol 149:698.*

166. Petzelbauer, P., J. R. Bender, J. Wilson, and J. S. Pober. 1993. Heterogeneity of dermal microvascular endothelial cell antigen expression and cytokine responsiveness in situ and in cell culture. *J Immunol 151:5062.*

167. Alon, R., D. A. Hammer, and T. A. Springer. 1995. Lifetime of the P-selectin-carbohydrate bond and its response to tensile force in hydrodynamic flow. *Nature 374:539.*

168. Srichaikul, T., N. Archararit, T. Siriasawakul, and T. Viriyapanich. 1976. Histamine changes in Plasmodium falciparum malaria. *Trans R Soc Trop Med Hyg 70:36.*

169. MacDonald, S. M., J. Bhisutthibhan, T. A. Shapiro, S. J. Rogerson, T. E. Taylor, M. Tembo, J. M. Langdon, and S. R. Meshnick. 2001. Immune

mimicry in malaria: Plasmodium falciparum secretes a functional histamine-releasing factor homolog in vitro and in vivo. *Proc Natl Acad Sci U S A 98:10829.*

170. Looareesuwan, S., L. Sjostrom, S. Krudsood, P. Wilairatana, R. S. Porter, F. Hills, and D. A. Warrell. 1999. Polyclonal anti-tumor necrosis factor-alpha Fab used as an ancillary treatment for severe malaria. *Am J Trop Med Hyg 61:26.*

171. van Hensbroek, M. B., A. Palmer, E. Onyiorah, G. Schneider, S. Jaffar, G. Dolan, H. Memming, J. Frenkel, G. Enwere, S. Bennett, D. Kwiatkowski, and B. Greenwood. 1996. The effect of a monoclonal antibody to tumor necrosis factor on survival from childhood cerebral malaria. *J Infect Dis 174:1091.*

172. Looareesuwan, S., P. Wilairatana, S. Vannaphan, V. Wanaratana, C. Wenisch, M. Aikawa, G. Brittenham, W. Graninger, and W. H. Wernsdorfer. 1998. Pentoxifylline as an ancillary treatment for severe falciparum malaria in Thailand. *Am J Trop Med Hyg 58:348.*

173. Riddle, M. S., J. L. Jackson, J. W. Sanders, and D. L. Blazes. 2002. Exchange transfusion as an adjunct therapy in severe Plasmodium falciparum malaria: a meta-analysis. *Clin Infect Dis 34:1192.*

174. Jorgensen, C., I. Couret, F. Canovas, C. Bologna, J. Brochier, T. Reme, and J. Sany. 1996. In vivo migration of tonsil lymphocytes in rheumatoid synovial tissue engrafted in SCID mice: involvement of LFA-1. *Autoimmunity 24:179.*

175. Casasnovas, J. M., and T. A. Springer. 1994. Pathway of rhinovirus disruption by soluble intercellular adhesion molecule 1 (ICAM-1): an intermediate in which ICAM-1 is bound and RNA is released. *J Virol 68:5882.*

176. David, P. H., M. Hommel, L. H. Miller, I. J. Udeinya, and L. D. Oligino. 1983. Parasite sequestration in Plasmodium falciparum malaria: spleen and antibody modulation of cytoadherence of infected erythrocytes. *Proc Natl Acad Sci U S A 80:5075.*

177. Diggs, C. L., F. Hines, and B. T. Wellde. 1995. Plasmodium falciparum: passive immunization of Aotus lemurinus griseimembra with immune serum. *Exp Parasitol 80:291.*

178. Pouvelle, B., P. Meyer, C. Robert, L. Bardel, and J. Gysin. 1997. Chondroitin-4-sulfate impairs in vitro and in vivo cytoadherence of Plasmodium falciparum infected erythrocytes. *Mol Med 3:508.*

179. Paul, R., Z. G. Zhang, B. P. Eliceiri, Q. Jiang, A. D. Boccia, R. L. Zhang, M. Chopp, and D. A. Cheresh. 2001. Src deficiency or blockade of Src activity in mice provides cerebral protection following stroke. *Nat Med 7:222.*

180. Schlaepfer, D. D., K. C. Jones, and T. Hunter. 1998. Multiple Grb2-mediated integrin-stimulated signaling pathways to ERK2/mitogen-activated protein kinase: summation of both c-Src- and focal adhesion kinase-initiated tyrosine phosphorylation events. *Mol Cell Biol 18:2571.*

181. Rothberg, K. G., J. E. Heuser, W. C. Donzell, Y. S. Ying, J. R. Glenney, and R. G. Anderson. 1992. Caveolin, a protein component of caveolae membrane coats. *Cell 68:673.*

182. Abrami, L., M. Fivaz, T. Kobayashi, T. Kinoshita, R. G. Parton, and F. G. van der Goot. 2001. Cross-talk between caveolae and glycosylphosphatidylinositol-rich domains. *J Biol Chem 276:30729.*

183. Lee, H., S. E. Woodman, J. A. Engelman, D. Volonte, F. Galbiati, H. L. Kaufman, D. M. Lublin, and M. P. Lisanti. 2001. Palmitoylation of caveolin-1 at a single site (Cys-156) controls its coupling to the c-Src tyrosine kinase: targeting of dually acylated molecules (GPI-linked, transmembrane, or cytoplasmic) to caveolae effectively uncouples c-Src and caveolin-1 (TYR-14). *J Biol Chem 276:35150.*

184. Shenoy-Scaria, A. M., D. J. Dietzen, J. Kwong, D. C. Link, and D. M. Lublin. 1994. Cysteine3 of Src family protein tyrosine kinase determines palmitoylation and localization in caveolae. *J Cell Biol 126:353.*

185. Cao, H., W. E. Courchesne, and C. C. Mastick. 2002. A phosphotyrosine-dependent protein interaction screen reveals a role for phosphorylation of caveolin-1 on tyrosine 14: recruitment of C-terminal Src kinase. *J Biol Chem 277:8771.*

186. Mineo, C., G. N. Gill, and R. G. Anderson. 1999. Regulated migration of epidermal growth factor receptor from caveolae. *J Biol Chem 274:30636.*